4.1 Introduction

The research based on heterocyclic liquid crystals has attracted much more attention in recent years due to larger choices in the design and synthesis of novel heterocycles containing mesogenic compounds [1, 2]. It has been widely studied that the presence of heterocyclic moieties in core structures generates mesogenic materials [3, 4]. As the heterocyclic compounds having oxygen, nitrogen and sulphur atoms which are more polarisable than carbon, amalgamation of heterocyclic units as core moiety in liquid crystals results in variety of their mesogenic properties as well as physical properties. The presence of such electronegative atoms has often led to greater polar induction and reduced symmetry [5-7]. Polar induction by heteroatoms can be responsible for developing and enriching the mesogenic properties of heterocyclic liquid crystals [6-8]. Numerous compounds containing heterocyclic moiety such as furan, thiophene, pyrrole, benzothiazole, pyridine, pyrimidine, oxadiazole have been reported to possess a variety of mesogenic properties [9, 10]. Pyrrole and thiophene based conducting polymers have been widely studied for their mesomorphic behavior [11-13].

L. A. Karamysheva et al. [14] reported the thiophene -2-carboxelates and 2,2'-bithienyl derivative homologous series. Series-I compounds exhibited either monotropic or a narrow enantiotropic smectic phase with a mesophase thermal stability 30 ^{o}C, while series-II is not mesogenic **(Figure 1).**

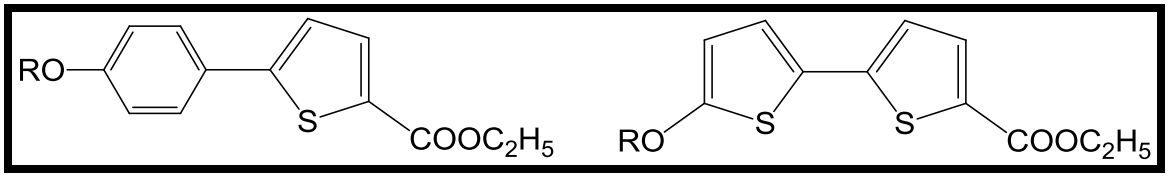

Series-I Series-II

Figure 1. Thiophene -2-carboxelates and 2,2'-bithienyl derivative

J. A. Nash and G. W. Gray [15] synthesized different thiophene derivatives and studied their mesomorphic behavior. Compounds II, IV and VI, which are $–CH_3$ substituted derivative, exhibited nematic phase with higher, thermal stability and phase range. Compounds I and V were not mesogenic, while Compound III was polymorphic with SmA, SmB and S3 phases **(Figure 2).**

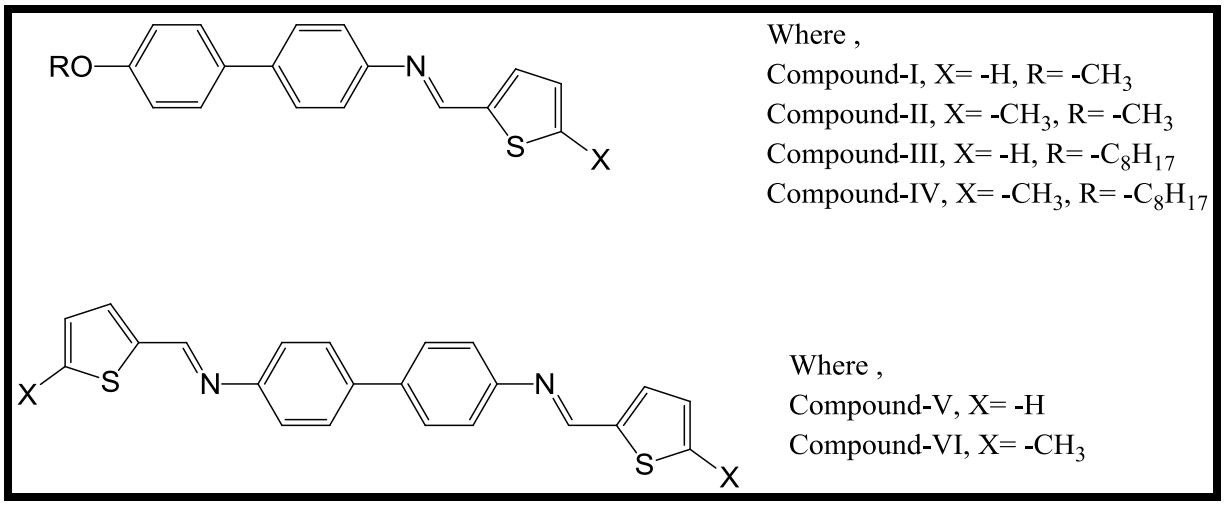

Figure 2. Thiophene based compounds

G. Koßmehl and D. Budwill [16] reported the homologous series-I and II of the liquid crystalline thiophene ester derivatives. In series-I, all homologous showed enantiotropic nematic phase while higher homologous from *n*- pentyl to *n*-octyl exhibited monotropic smectic phase along with nematic phase. In series-II, all the compounds exhibited cholesteric phase **(Figure 3).**

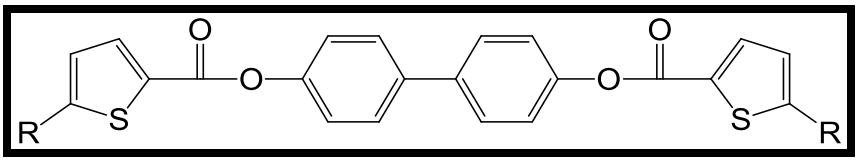

Series-I

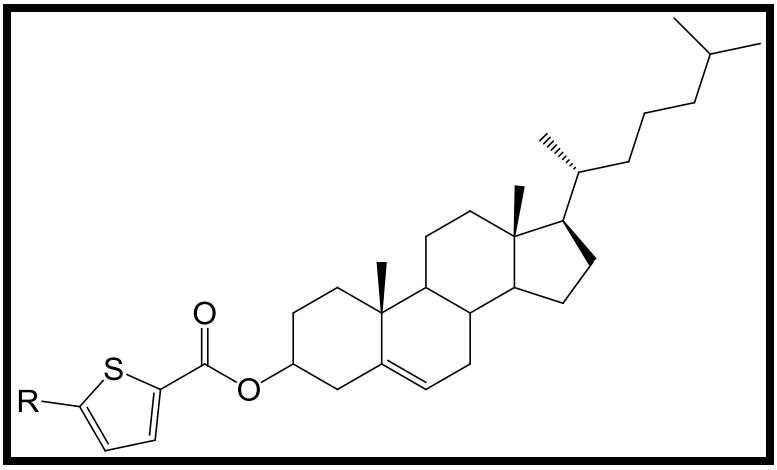

Series-II

Figure 3. Liquid crystalline thiophene ester derivatives

They have also synthesized and studied the mesomorphic behavior of azomethines, azines, vinylenes and hexatrienes containing thiophene and thieno[3,2-b]- thiophene systems [17] **(Figure 4).** Addition to this they have reported liquid crystalline compounds of azomethines and vinylenes derivatives based on thiophene [18] and thiophene based liquid crystalline compounds of azomethines and vinylenes with central azobenzene, stilbene and 1,2-di(2-thienyl)ethylene moieties [19].

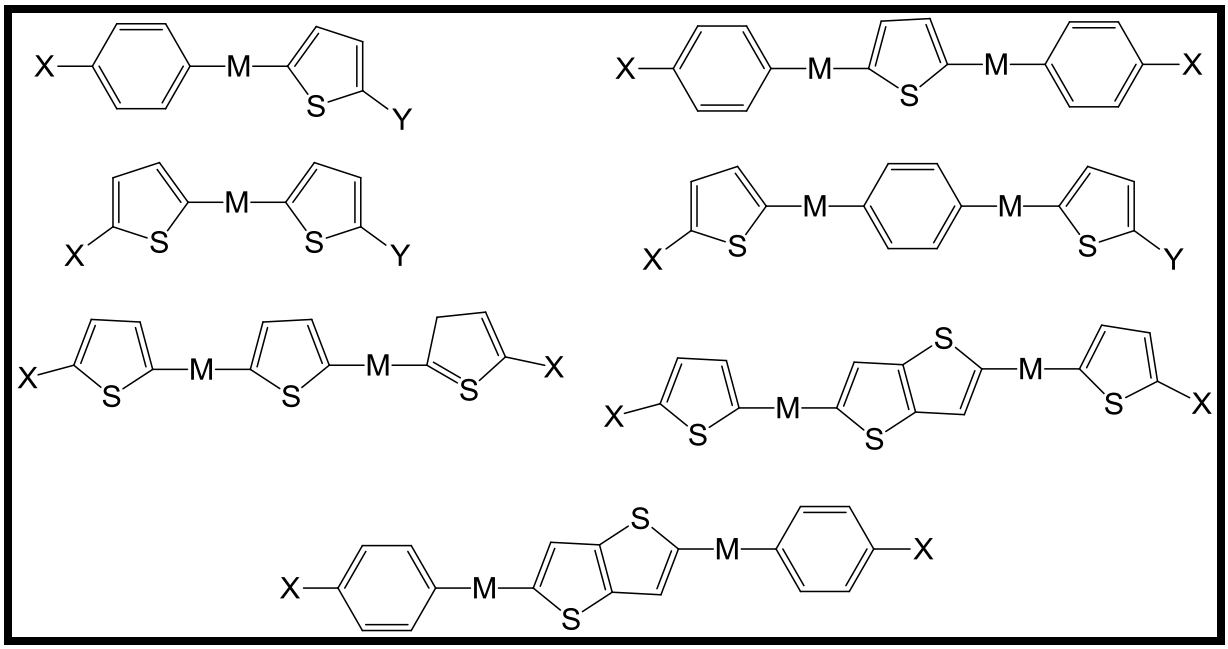

Figure 4. Thiophene based liquid crystalline compounds

In order to study the influence of heterocycles on mesogenic behavior, H. Gallardo and I. Favarin [4] synthesized a new type of hetero aromatic liquid-crystal compound with five membered furan and thiophene rings **(Figure 5).** In series-I, *n* = 4 homologue is not mesogenic, and *n*=6 and 7 homologues show the enantiotropic nematic phase; however, the homologues *n* = 5 and 8 exhibits the monotropic nematic mesophases. The homologue *n* = 9, shows monotropic nematic, smectic and crystalline polymorphism. The series-IIa and IIb are more nematogenic than the series-I, with a higher thermal stability.

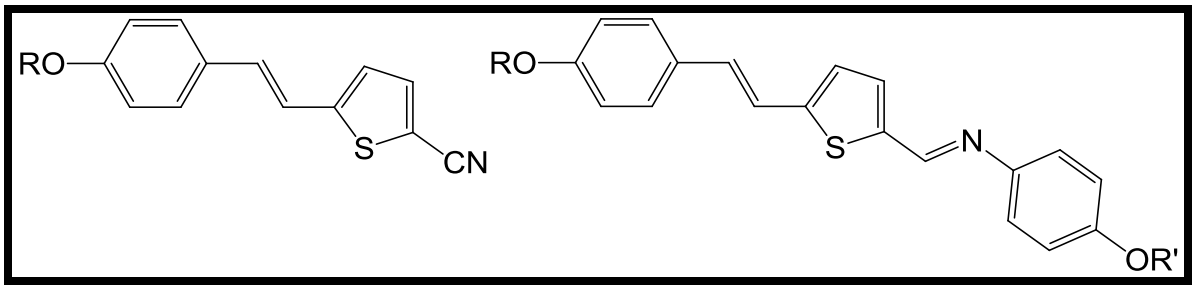

Series-I Series-II

Where R=R'= C_nH_{2n+1} R: n= 4 to 9; R': n= 2 Series-IIa, R': n= 7 Series-IIb

Figure 5. Hetero aromatic liquid-crystal compound with five membered thiophene ring

To investigate the effect of core linearity on the stability of mesophase, R. Cai and E. T. Samulski [8] synthesized homologous series of compounds containing non-linear mesogenic cores 2, 5-thiophene and 2, 2'-bithiophene **(Figure 6).**

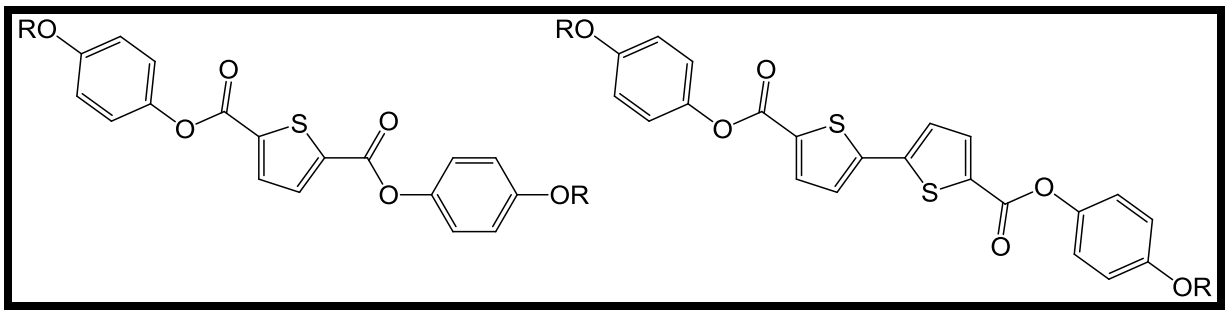

Series-I Series-II

Where R= C_nH_{2n+1} n= 1to 10 Where R= C_nH_{2n+1} n= 1to 7

Figure 6. Compounds containing non-linear mesogenic cores 2,5-thiophene and 2,2'-bithiophene

T. Narasimhaswamy et al. [20] reported the synthesis of a new thermotropic liquid crystal, which consists of a thiophene ring and 1,4 disubstituted benzene rings as the core, an ester and azomethine as the linking group, and an alkoxy unit as the end group **(Figure 7).** All the compounds show enantiotropic nematic phase. Compared to the Series I, Series II compounds showed an improved melting, clearing and phase stability temperature as a result of the addition of a third benzene ring.

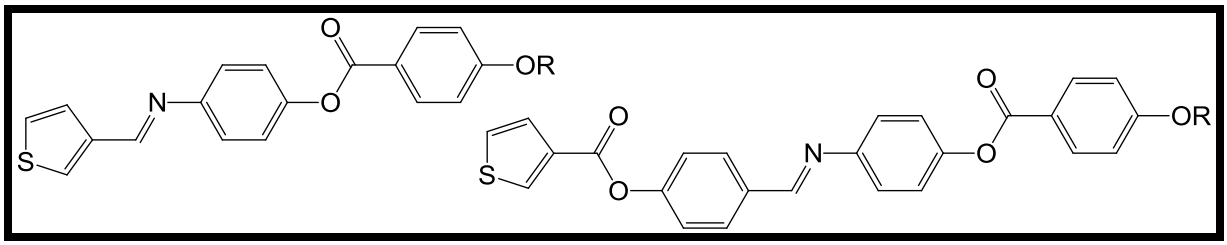

Series-I Series-II

Where R= C_nH_{2n+1} n= 4, 10, 12.

Figure 7. Thiophene based homologous series

Two homologous series based on thiophene are reported, with ester azomethine and cinnamate azomethine linkers by B. T. Thaker et al. [21] **(Figure 8).** All the compounds show nematic phases, while the higher homologues of series- I along with nematic phase show smectic C phase. The series containing the cinnamate azomethine linking unit has a higher thermal stability than ester-azomethine. For the mesomorphic property, the ester-azomethine linking unit is more favorable than cinnamate azomethine. In thiophene-based compounds, they lower the transition temperature.

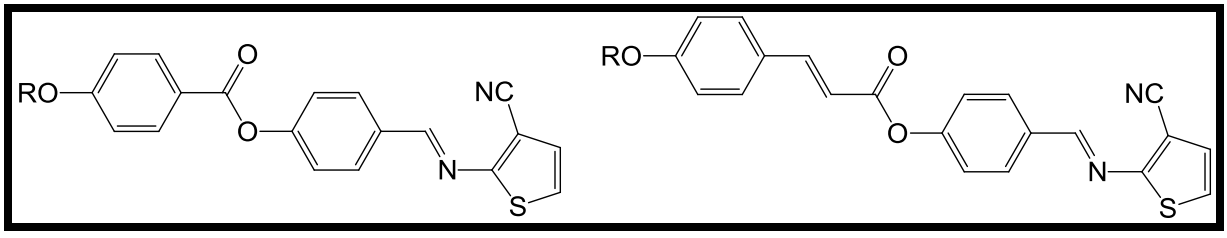

Series-I Series-II

Where R= C_nH_{2n+1} n= 1 to 8, 10, 12, 14, 16, 18.

Figure 8. Thiophene based homologous series with ester and cinnamate azomethine linkers.

In order to study the influence of the substitution position on the mesogenic behavior, M.K. Reddy et al. [7] synthesized two series **(Figure 9).** In series I, thiophene is connected to the benzene ring through an ester linkage at the 2-position, while in series II, through the 3-position. Both the series exhibited enantiotropic nematic phase with lower phase stabilities.

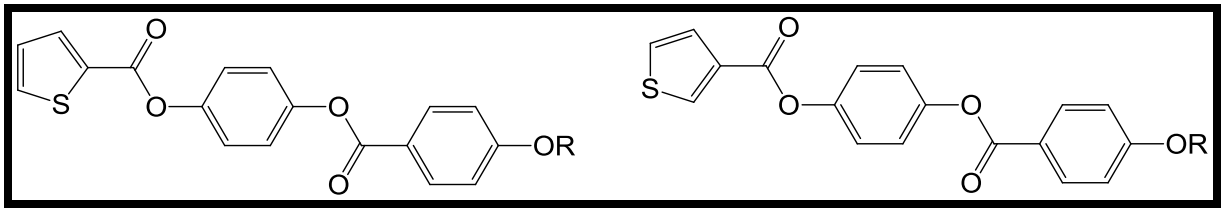

Series-I Series-II

Where R= C_nH_{2n+1} n = 2, 4, 8, 10, 12.

Figure 9. Thiophene ester based homologous series

Further to investigate the effect of the additional benzene ring on the mesomorphic behavior, they prepared series-III and a series-IV [22] **(Figure 10).** They conclude that the additional benzene ring in the core increases the anisotropic polarizability of the molecule, thereby increasing the stability of the mesophase.

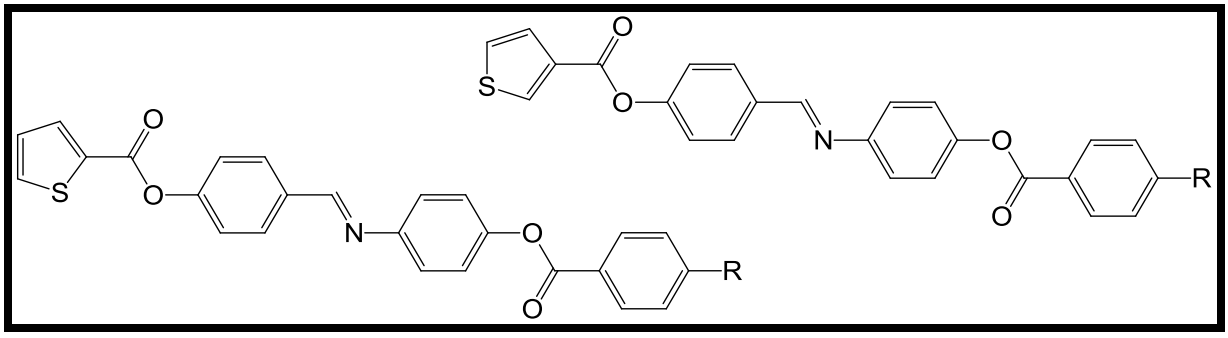

Series-III Series-IV

Where R= $C_{12}H_{25}$, $OC_{12}H_{25}$, OC_6H_{13}.

Figure 10. Thiophene ester based homologous series with additional phenyl ring

K.-L. Foo et al. [23] reported thiophene-imine-ester-based liquid crystals series-I and S. S. Nafee et al. [24] reported thiophene-imine-ester-based liquid crystals series-II, vary with the substitution position of thiophene **(Figure 11).** All the compounds in both series exhibited enantiotropic nematic phase, except *n*-octadecyloxy derivative of the series-I.

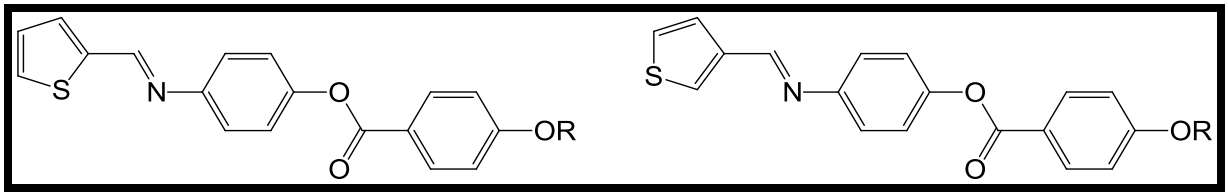

Series-I Series-II

Where R= C_nH_{2n+1} n= 6, 8, 10, 12, 14, 16, 18. Where R= C_nH_{2n+1} n= 6, 8, 10, 12, 14, 16.

Figure 11. Thiophene-imine-ester-based liquid crystals

Chalcone consists of two aromatic rings with various substitutes, connected by an unsaturated *α*, *β*-ketone. The different homologous series based on chalcone derivatives are reported by various research groups [25-36]. Chudgar and Shah [25] have prepared two homologous series, 4-*n*-alkoxy-4′-hydroxy chalcone (series-I) and 4-*n*-alkoxy-4′(4″-*n*-octyloxybenzoyloxy) chalcone (series-II). All derivatives of 4-*n*-alkoxy-4-hydroxy chalcone were not mesomorphic. Whereas *n*-hexyloxy onwards, all the derivatives of 4-*n*-alkoxy-4′(4″-*n*-octyloxybenzoyloxy)chalcone, exhibited a monotropic nematic phase **(Figure 12).**

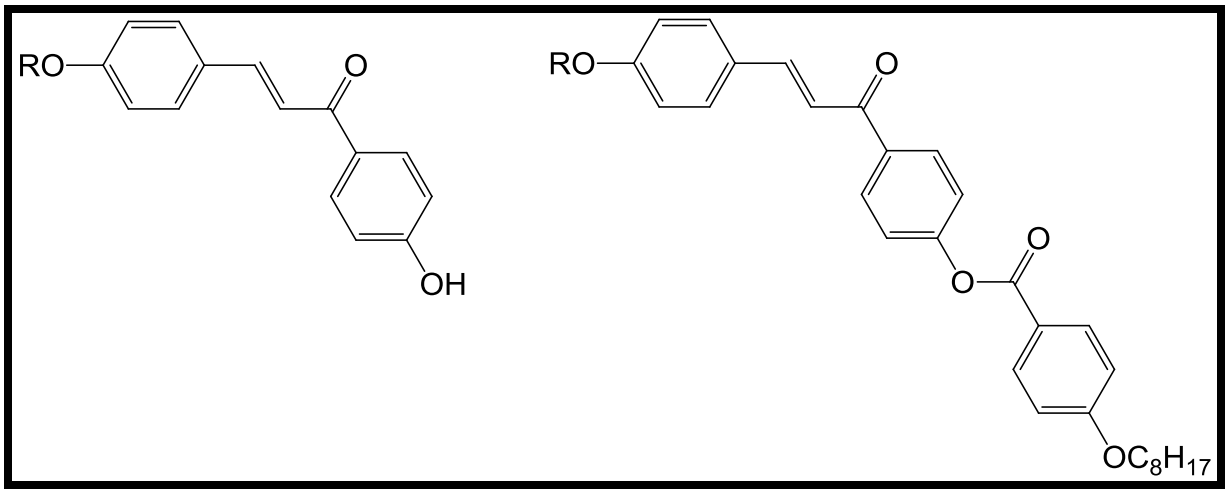

Series-I Series-II

Where R= C_nH_{2n+1} n= 1to10, 12, 14, 16.

Figure 12. 4-*n*-alkoxy-4′-hydroxy and 4-*n*-alkoxy-4′(4″-*n*-octyloxybenzoyloxy) chalcones

R. P. Chaudhari et al. synthesized two homologous series α-3-[-4’-*n*-alkoxy benzoyloxy] phenyl-β-4’’-methoxy benzoyl ethylene [26] and α-4-[4’-*n*-Alkoxy benzoyloxy] benzoyl β-4’’-methoxy phenyl ethylenes [27] **(Figure 13).** Their mesomorphic behavior checked and correlated with structurally similar compounds. In the first series, derivatives of

n-pentyl, *n*-tetradecyl, and *n*-hexadecyl show an enantiotropic nematic; while *n*-hexyl, *n*-octyl, *n*-decyl, and *n*-dodecyl exhibited smectic and nematic mesophase, the remaining homologues are not mesogenic. In the second homologues series, the *n*-heptyl to *n*-tetradecyl has a smectic phase and a nematic phase. The *n*-pentyl, *n*-hexyl, and *n*-hexadecyl homologues only show a nematic phase, while the remaining homologues are non-mesogenic.

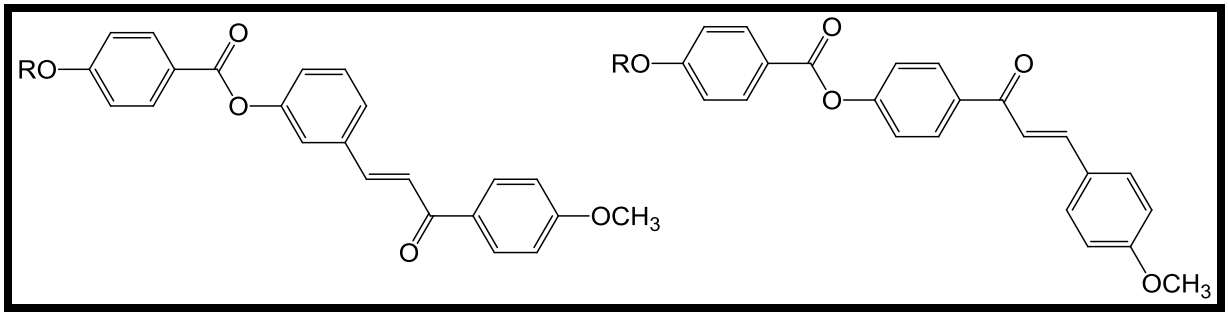

Series-I Series-II

Where R= C_nH_{2n+1} n= 1to 8, 10, 12, 14, 16.

Figure 13. Chalcone based homologous series

Three homologous series of chalcone derivatives with variation in the molecular structure of each series have been reported by H. N. Chauhan et al. [28-30] **(Figure 14).** Their mesogenic behavior was examined and compared with similar structural compounds. Of the three homologous series, I and II are partially smectogenic and partially nematogenic, and series III is nematogenic.

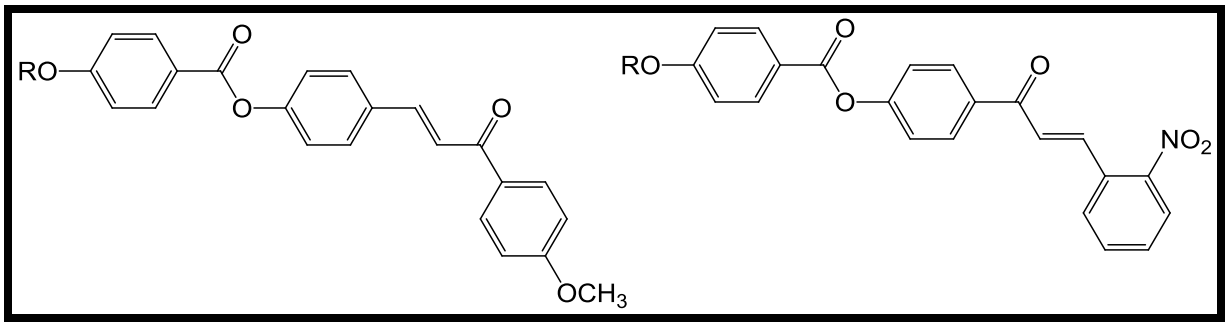

Series-I Series-II

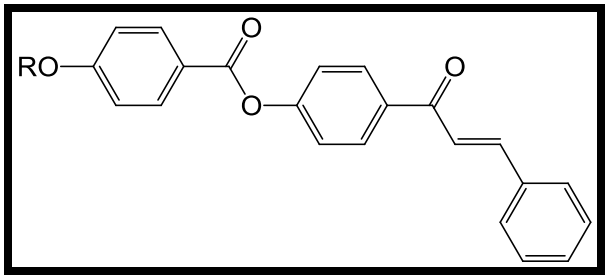

Series-III

Where R= C_nH_{2n+1} n= 1to 8, 10, 12, 14, 16.

Figure 14. Chalcone derivatives with variation in the molecular structure

V. C. Kotadiya et al. [31] synthesized a homologous series of symmetrical dimmers, namely bis (4-*n*-alkoxy benzoyloxy) α-phenyl β-benzoyl-ethylenes and studied their mesomorphic behavior **(Figure 15).** The homologs *n*-methoxy to *n*-butyloxy are not mesogenic; although *n*-pentyl to *n*-heptyl exhibits nematogenic behaviour, the higher homologs exhibit a smectic phase and a nematic phase.

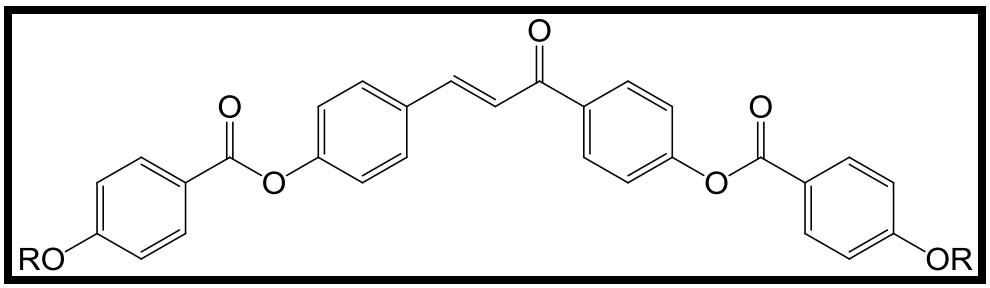

Where R= C_nH_{2n+1} n= 1to 8, 10, 12, 14, 16.

Figure 15. Bis (4-*n*-alkoxy benzoyloxy) α-phenyl β-benzoyl-ethylenes

R. L. Coelho et al. [32] reported bent-shaped compounds derived from chalcone and studied their mesomorphic and optical properties **(Figure 16).** The bent-shaped compounds derived from the chalcone, only compound c shows monotropic hexagonal columnar phase, and the other two are not mesogenic.

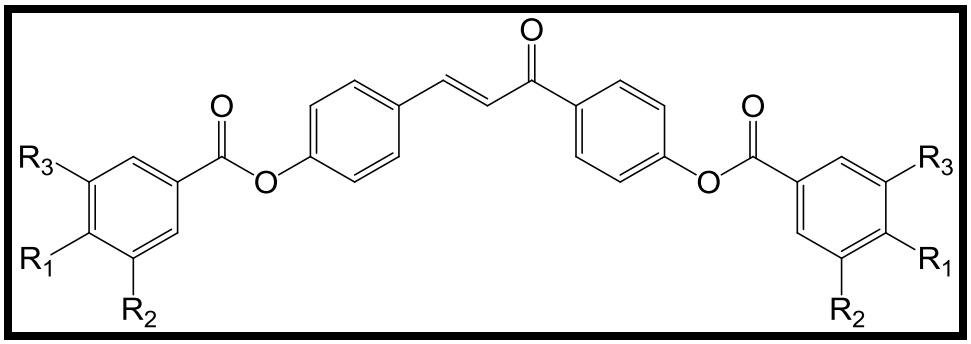

Where a. R_1= R_2=$OC_{12}H_{25}$, b. R_3=H; R_1=H, R_2=R_3=$OC_{12}H_{25}$; c. R_1= R_2=R_3=$OC_{12}H_{25}$

Figure 16. Bent-shaped compounds derived from chalcone

S.D. Durgapal et al. [33] prepared homologous series of coumarin derivatives consisting of chalcone central linkage along with terminal *n*-alkoxy chain and examined their mesomorphic behavior **(Figure 17).** In the series up to *n*-pentyloxy derivatives, they are not mesogenic; while *n*-hexyloxy and *n*-heptyloxy derivatives exhibits only the nematic phase. In the series *n*-octyloxy derivative showed smectic-A and nematic phases, and then higher homologous showed smectic-A phase.

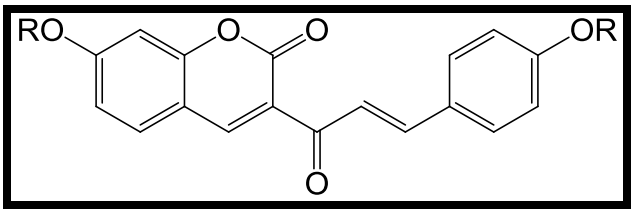

Where R= C_nH_{2n+1} n= 2, 4, 5, 6, 7, 8, 10, 12, 14, 16, 18.

Figure 17. Coumarin derivatives consisting of chalcone central linkage

K. N. Patel et al. [34] synthesized and studied mesomorphic properties of unsymmetrical bischalcones obtained from cyclohexanone **(Figure18).** The homologues *n*-butyloxy and *n*-hexyloxy in this series are non-mesogenic, while *n*-heptyloxy to *n*-hedadecyloxy exhibited only monotropic nematic phase

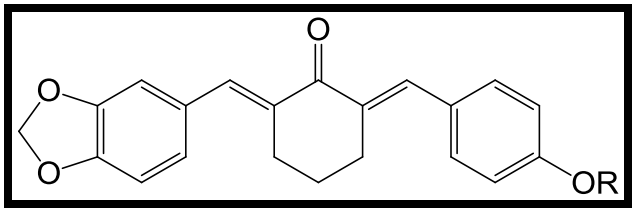

Where R= C_nH_{2n+1} n= 4, 6, 7, 8, 10, 12, 14, 16.

Figure 18. Unsymmetrical cyclohexanone-derived bischalcones

P. K. Rakhasia et al. [35] synthesized homologous series of thiophene based chalcone derivatives, studied their mesomorphic behavior and compared with structural isomer reported by R. H. Maheta and U. C. Bhoya [36] **(Figure 19).** The series-I derivatives exhibited both smectic and nematic phases, whereas series-II studied in comparison showed only smectic phase.

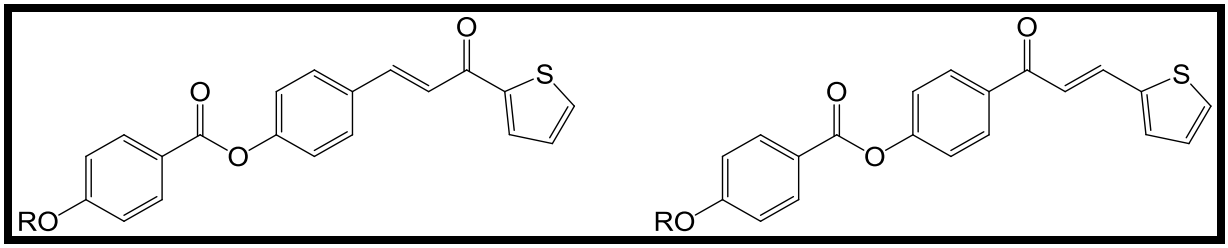

Series-I Series-II

Where R= C_nH_{2n+1} n= 1to 8, 10, 12, 14, 16.

Figure 19. Thiophene based chalcone derivatives

To study the effect of intramolecular hydrogen bonding on the mesophase behavior we have synthesized two homologous series, Schiff base of 4-*n*-alkoxy-2-hydroxy benzaldehyde and 4-*n*-alkoxy benzaldehyde with thiophene derivative **(Figure 20).**

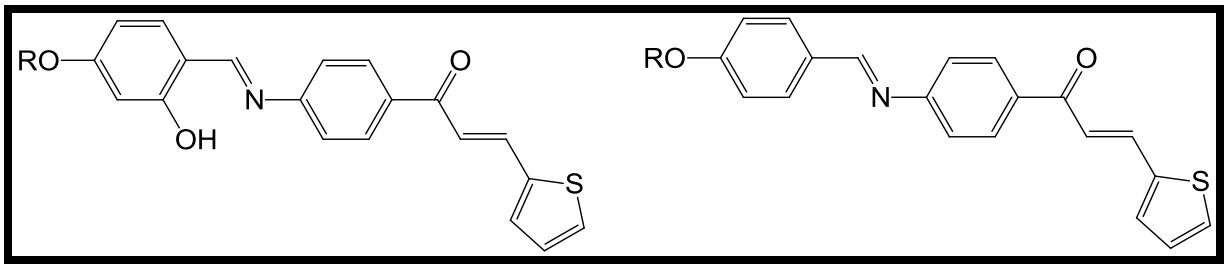

Series-I Series-II

Where R= C_nH_{2n+1} n= 2 to 8, 10, 12, 14, 16, 18.

Figure 20. Schiff base of 4-*n*-alkoxy-2-hydroxy benzaldehyde and 4-*n*-alkoxy benzaldehyde with thiophene derivative

Based on the literature review, thiophen ring, as well as chalcone linkage, was observed to be conducive to a nematic phase in molecular structure. The effect of molecular flexibility on the mesomorphic behavior of the two homologous series was investigated.

4.2 Experimental

4.2.1. Material

All reagents were purchased from commercial sources and used as received. 4-hydroxybenzaldehyde from SRL; alkyl bromides from SRL and Spectrochem;4-aminoacetophenone from Lobachem; 2-thiophene carboxaldehyde and 2,4 dihydroxybenzaldehyde from TCL. The purity of the synthesized compounds was checked by using Silica Gel TLC Plate from Merck.

4.2.2. Characterization

The ^{1}H NMR spectra and ^{13}C NMR spectra were recorded on an AV 400MHz Bruker FT-NMR spectrometer in $CDCl_3$ solution with tetramethylsilane (TMS) as an internal standard. IR spectra were recorded on Bruker spectrometer as KBr pellets. TG-DTA measurements were carried out on an SII EXSTAR6000TG-DTA instrument. The Experiments were performed in N_2 at a heating rate of 10 $^{o}C\ min^{-1}$ in the temperature range 30–550 ^{o}C using an aluminum pan. The transition temperatures and enthalpies were investigated by differential scanning calorimeter (DSC) using a PerkinElmer Thermal Analyzer with heating and cooling rate 10 $^{o}C\ min^{-1}$. The Leica DM 2500P polarizing optical microscope (POM) provided with a Linkam heating stage was used to study thermal behavior and optical texture of different compounds. Mass spectra of the compounds were recorded on Trace GC ultra DSQ II. X-ray intensity data were collected on a Bruker CCD area detector diffractometer with graphite-monochromatised MoKα radiation (λ = 0.71073 Å).

4.3 Synthesis

4.3.1 Synthesis of series E

4.3.1.1 Synthesis of 2-hydroxy-4-n-alkoxybenzyldehyde

2-Hydroxy- 4-n-alkoxy benzaldehye were prepared by following the method described in chapter 2, section 2.3.1.

4.3.1.2. Synthesis of (E)-1-(4-aminophenyl)-3-(thiophen-2-yl)prop-2-en-1-one.[37]

Equimolar quantities of 4-aminoacetophenone (0.05 moles) and thiophene-2-carboxaldehyde (0.05 moles) were dissolved in a minimum amount of alcohol. Sodium hydroxide solution (10 mL, 0.1 moles) was added slowly, and the mixture was stirred for 8 hr at room temperature. Then was poured slowly into 400 ml of ice water with constant stirring and kept in the refrigerator for 24 h. The precipitate obtained was filtered, washed and recrystallised from ethanol.

(E)-1-(4-aminophenyl)-3-(thiophen-2-yl)prop-2-en-1-one.

Yellowish solid ; Yield: 82%; ^{1}H NMR (400 MHz, $CDCl_3$, TMS) δ_H 7.95-7.91(m, 3H), 7.40-7.33 (m, 3H), 7.10-7.07 (dd, 1H, *J*=4.8, *J*=4.0), 6.71 (d, 2H, *J*=8.8 Hz), 4.24 (s, 2H); IR (υ_{max}, cm^{-1}, KBr) : 3469-3202 (υNH_2 asy., sy.), 1619 (υC=O ketone), 1575, 1511 (υ aromatic C=C); Mass (ESI): m/z $[M + H]^+$ 230.07

4.3.1.3. Synthesis of (E)-1-(4-((E)-(2-hydroxy-4-*n*-alkoxy benzylidene)amino)phenyl) -3-(thiophen-2-yl)prop-2-en-1-one.

2-Hydroxy-4-n-alkoxybenzaldehyde (n = 2 to 8, 10, 12, 14, 16, 18; 2 mmol) and (E)-1-(4-aminophenyl)-3-(thiophen-2-yl)prop-2-en-1-one (2 mmol) were dissolved in a minimum amount of absolute ethanol. To this solution, a few drops of glacial acetic acid were added and the reaction mixture was refluxed for 4 h. After cooling a crystalline yellow compound

was separated. The compound was filtered and washed with cool ethanol and dried in vacuum **(Scheme 1).**

(E)-1-(4-((E)-(2-hydroxy-4-ethoxybenzylidene)amino)phenyl) -3-(thiophen-2-yl)prop-2-en-1-one (E2)

Yellowish solid; Yield: 68%; ^{1}H NMR (400 MHz, $CDCl_3$, TMS) δ_H 13.50 (s, 1H), 8.58 (s, 1H),8.10(d, 2H, *J*=8.0 Hz), 7.97(d, 1H, *J*=15.6 Hz), 7.45(d, 1H, *J*=4.8 Hz), 7.40-7.35 (m, 4H), 7.32(d, 1H, *J*=9.2 Hz), 7.12 (dd, 1H, *J*=4.8 Hz, *J*=4.0 Hz), 6.52 (d, 2H, *J*=6.4 Hz), 4.13-4.08 (q, 2H), 1.47-1.44 (t, 3H); ^{13}C NMR (100 MHz , $CDCl_3$, TMS) δ_C 188.6, 164.0, 162.8, 152.4, 140.4, 137.2, 135.8, 134.0, 132.2, 130.0, 128.9, 128.4, 121.3, 120.5, 108.1, 101.5, 63.8, 14.7; IR (υ_{max}, cm^{-1}, KBr): 3447 (υOH), 2921, 2852(υ aliphatic C-H), 1650 (υC=O), 1591 (υC=N), 1558, 1511 (υ aromatic C=C), 1189 (υ PhO), 1112 (υ aliphatic C-O).

(E)-1-(4-((E)-(2-hydroxy-4-propoxybenzylidene)amino)phenyl) -3-(thiophen-2-yl)prop-2-en-1-one (E3)

Yellowish solid; Yield: 74%; ^{1}H NMR (400 MHz, $CDCl_3$, TMS) δ_H 13.50 (s, 1H), 8.58 (s, 1H), 8.10 (d, 2H, *J*=8.0 Hz), 7.99 (d, 1H, *J*=15.2 Hz), 7.45 (d, 1H, *J*=4.8 Hz), 7.40-7.35 (m, 4H), 7.31 (d, 1H, *J*=8.4 Hz), 7.12 (dd, 1H, *J*=4.4 Hz, *J*=4.0 Hz), 6.53 (d, 2H, *J*=6.8 Hz), 3.99 (t, 2H, *J*=6.4 Hz), 1.90-1.67 (m, 2H), 1.09-1.05 (t, 3H); ^{13}C NMR (100 MHz , $CDCl_3$, TMS) δ_C 188.6, 164.2, 164.1, 162.8, 152.5, 140.4, 137.2, 135.8, 134.0, 132.2, 130.0, 128.9, 128.4, 121.3, 120.5, 112.8, 108.1, 101.5, 69.8, 22.4, 10.5; IR (υ_{max}, cm^{-1}, KBr): 3447 (υOH), 2921, 2852(υ aliphatic C-H), 1650 (υC=O), 1591 (υC=N), 1558, 1511 (υ aromatic C=C), 1189 (υ PhO), 1112 (υ aliphatic C-O).

(E)-1-(4-((E)-(2-hydroxy-4-butoxybenzylidene)amino)phenyl) -3-(thiophen-2-yl)prop-2-en-1-one (E4)

Yellowish solid; Yield: 76%; ^{1}H NMR (400 MHz, $CDCl_3$, TMS) δ_H 13.50 (s, 1H), 8.59 (s, 1H), 8.10 (d, 2H, *J*=8.4 Hz), 7.99 (d, 1H, *J*=15.6 Hz), 7.46 (d, 1H, *J*=4.8 Hz), 7.40-7.36 (m, 4H), 7.32 (d, 1H, *J*=8.8 Hz), 7.13 (dd, 1H, *J*=4.4 Hz, *J*=4.0 Hz), 6.53 (d, 2H, *J*=5.2 Hz), 4.03(t, 2H, *J*=6.4 Hz), 1.85-1.28 (m, 4H), 1.03-0.99 (t, 3H); ^{13}C NMR (100 MHz , $CDCl_3$, TMS) δ_C 188.6, 164.2, 162.8, 140.4, 137.2, 134.0, 132.2, 130.0, 128.9, 128.4, 121.3, 120.5, 108.1, 101.5, 68.0, 31.1, 19.2, 13.9; IR (υ_{max}, cm^{-1}, KBr): 3447 (υOH), 2921, 2852(υ aliphatic C-H), 1650 (υC=O), 1591 (υC=N), 1558, 1511 (υ aromatic C=C), 1189 (υ PhO), 1112 (υ aliphatic C-O).

(E)-1-(4-((E)-(2-hydroxy-4-butoxybenzylidene)amino)phenyl) -3-(thiophen-2-yl)prop-2-en-1-one (E5)

Yellowish solid; Yield: 76%; ^{1}H NMR (400 MHz, $CDCl_3$, TMS) δ_H 13.50 (s, 1H), 8.58 (s, 1H), 8.09 (d, 2H, *J*=8.4 Hz), 7.99 (d, 1H, *J*=15.6 Hz), 7.45 (d, 1H, *J*=5.2 Hz), 7.40-7.36 (m, 4H), 7.33 (d, 1H, *J*=9.6 Hz), 7.13 (dd, 1H, *J*=4.0 Hz, *J*=3.6 Hz), 6.53 (d, 2H, *J*=6.8 Hz), 4.03(t, 2H, *J*=6.4 Hz), 1.85-1.28 (m, 6H), 1.03-0.99 (t, 3H); ^{13}C NMR (100 MHz , $CDCl_3$, TMS) δ_C 188.6, 164.2, 164.1, 162.8, 152.4, 140.4, 137.2, 135.7, 134.0, 132.2, 130.0, 128.9, 128.4, 121.2, 120.4, 112.8,108.1, 101.5, 68.3, 28.7, 28.1, 22.5, 14.1; IR (υ_{max}, cm^{-1}, KBr): 3447 (υOH), 2921, 2852(υ aliphatic C-H), 1650 (υC=O), 1591 (υC=N), 1558, 1511 (υ aromatic C=C), 1189 (υ PhO), 1112 (υ aliphatic C-O)

(E)-1-(4-((E)-(2-hydroxy-4-hexyloxybenzylidene)amino)phenyl) -3-(thiophen-2-yl)prop-2-en-1-one (E6)

Yellowish solid; Yield: 64%; Mass (ES): m/z $[M + H]^+$ 434.19 ^{1}H NMR (400 MHz, $CDCl_3$, TMS) δ_H 13.50 (s, 1H), 8.59 (s, 1H), 8.11 (d, 2H, *J*=8.4 Hz), 8.00 (d, 1H, *J*=15.2 Hz), 7.46 (d,

1H, *J*=4.8 Hz), 7.41-7.36 (m, 4H), 7.32 (d, 1H, *J*=9.2 Hz), 7.13 (dd, 1H, *J*=4.8 Hz, *J*=3.6 Hz), 6.53 (d, 2H, *J*=6.8 Hz), 4.05-4.01 (t, 2H, *J*=6.4 Hz), 1.86-1.37 (m, 8H), 0.96-0.92 (t, 3H); ^{13}C NMR (100 MHz , $CDCl_3$, TMS) δ_C 188.9, 164.5, 162.9, 152.9, 140.6, 137.2, 136.0, 134.0, 132.2, 130.0, 128.9, 128.4, 121.3, 120.5, 112.8, 108.1, 101.5, 68.4, 31.6, 29.1, 25.7, 22.6, 14.1;IR (υ_{max}, cm^{-1}, KBr): 3447 (υOH), 2921, 2852(υ aliphatic C-H), 1650 (υC=O), 1591 (υC=N), 1558, 1511 (υ aromatic C=C), 1189 (υ PhO), 1112 (υ aliphatic C-O).

(E)-1-(4-((E)-(2-hydroxy-4-heptyloxybenzylidene)amino)phenyl) -3-(thiophen-2-yl)prop-2-en-1-one (E7)

Yellowish solid; Yield: 62%; ^{1}H NMR (400 MHz, $CDCl_3$, TMS) δ_H 13.50 (s, 1H), 8.58 (s, 1H),8.10(d, 2H, *J*=8.4 Hz), 7.99(d, 1H, *J*=15.2 Hz), 7.45(d, 1H, *J*=5.2 Hz), 7.40-7.35 (m, 4H), 7.31(d, 1H, *J*=5.2 Hz),7.09 (dd, 1H, *J*=4.8 Hz, *J*=3.6 Hz), 6.52 (d, 2H, *J*=6.8 Hz), 4.03 (t, 2H, *J*=6.4 Hz), 1.86-1.26 (m, 10H), 0.93-0.90 (t, 3H); ^{13}C NMR (100 MHz , $CDCl_3$, TMS) δ_C 188.6, 164.2, 164.1, 162.8, 152.5, 140.4, 137.2, 135.8, 134.0, 132.2, 130.0, 128.9, 128.4, 121.3, 120.5, 112.8, 108.1, 101.5, 68.4, 31.8, 29.1, 26.0, 22.6, 14.1; IR (υ_{max}, cm^{-1}, KBr): 3447 (υOH), 2921, 2852(υ aliphatic C-H), 1650 (υC=O), 1591 (υC=N), 1558, 1511 (υ aromatic C=C), 1189 (υ PhO), 1112 (υ aliphatic C-O).

(E)-1-(4-((E)-(2-hydroxy-4-octyloxybenzylidene)amino)phenyl) -3-(thiophen-2-yl)prop-2-en-1-one (E8)

Yellowish solid; Yield: 68%; ^{1}H NMR (400 MHz, $CDCl_3$, TMS) δ_H 13.50 (s, 1H), 8.58 (s, 1H),8.10(d, 2H, *J*=8.4 Hz), 7.99(d, 1H, *J*=15.2 Hz), 7.45(d, 1H, *J*=5.2 Hz), 7.40-7.35 (m, 4H), 7.31(d, 1H, *J*=5.2 Hz),7.09 (dd, 1H, *J*=4.8 Hz, *J*=3.6 Hz), 6.52 (d, 2H, *J*=6.8 Hz), 4.03 (t, 2H, *J*=6.4 Hz), 1.86-1.26 (m, 10H), 0.93-0.90 (t, 3H); ^{13}C NMR (100 MHz , $CDCl_3$, TMS) δ_C 188.6, 164.3, 164.2, 162.9, 152.5, 140.5, 137.2, 134.1, 132.3, 130.1, 128.9, 128.5, 121.4, 120.5, 112.9, 108.2, 101.6, 68.4, 31.9, 29.4, 29.3, 29.1, 26.1, 14.2 IR (υ_{max}, cm^{-1}, KBr): 3421

(υOH), 2947, 2921, 2851(υ aliphatic C-H), 1649 (υC=O), 1593 (υC=N), 1557, 1514 (υ aromatic C=C), 1172 (υ PhO), 1115 (υ aliphatic C-O).

(E)-1-(4-((E)-(2-hydroxy-4-decyloxybenzylidene)amino)phenyl) -3-(thiophen-2-yl)prop-2-en-1-one (E10)

Yellowish solid; Yield: 70%; Mass (ES): m/z $[M + H]^+$ 490.26 ^{1}H NMR (400 MHz, $CDCl_3$, TMS) δ_H 13.50 (s, 1H), 8.59 (s, 1H),8.10(d, 2H, *J*=8.4 Hz), 8.00(d, 1H, *J*=15.2 Hz), 7.46(d, 1H, *J*=5.2 Hz), 7.40-7.36 (m, 4H), 7.32(d, 1H, *J*=9.2 Hz),7.13 (dd, 1H, *J*=4.8 Hz, *J*=4.0 Hz), 6.53 (d, 2H, *J*=6.4 Hz), 4.03 (t, 2H, *J*=6.4 Hz), 1.86-1.30 (m, 16H), 0.92-0.89 (t, 3H); ^{13}C NMR (100 MHz , $CDCl_3$, TMS) δ_C 188.6, 164.2, 164.1, 162.8, 152.5, 140.4, 137.2, 135.8, 134.0, 132.2, 130.0, 128.4, 120.5, 112.8, 108.1, 101.5, 68.4, 31.9, 29.6, 29.4, 29.3, 14.2; IR (υ_{max}, cm^{-1}, KBr): 3447 (υOH), 2921, 2852(υ aliphatic C-H), 1650 (υC=O), 1591 (υC=N), 1558, 1511 (υ aromatic C=C), 1189 (υ PhO), 1112 (υ aliphatic C-O).

(E)-1-(4-((E)-(2-hydroxy-4-dodecyloxybenzylidene)amino)phenyl)-3-(thiophen-2-yl)prop-2-en-1-one (E12)

Yellowish solid; Yield: 68%; ^{1}H NMR (400 MHz, $CDCl_3$, TMS) δ_H 13.50 (s, 1H), 8.59 (s, -1H),8.11(d, 2H, *J*=8.4 Hz), 8.00(d, *J*=15.4 Hz), 7.46(d, 1H, *J*=4.8 Hz), 7.41-7.36 (m, Ar**H**, 4H), 7.32(d, 1H, *J*=9.2 Hz),7.13 (dd, 1H, *J*=4.8 Hz, *J*=3.6 Hz), 6.53 (d, 2H, *J*=6.4 Hz), 4.03 (t, 2H, *J*=6.4 Hz), 1.86-1.29 (m, 20H), 0.92-0.89 (t, 3H); ^{13}C NMR (100 MHz , $CDCl_3$, TMS) δ_C 188.6, 164.3, 164.2, 162.9, 152.5, 137.2, 134.0, 132.3, 130.1, 128.9, 128.5, 121.4, 120.6, 112.9, 108.2, 101.6, 68.4, 29.8, 29.7, 29.6, 29.6, 29.5, 14.2. IR (υ_{max}, cm^{-1}, KBr): 3447 (υOH), 2921, 2852(υ aliphatic C-H), 1650 (υC=O), 1591 (υC=N), 1558, 1511 (υ aromatic C=C), 1189 (υ PhO), 1112 (υ aliphatic C-O).

(E)-1-(4-((E)-(2-hydroxy-4-tetradecyloxybenzylidene)amino)phenyl)-3-(thiophen-2-yl) prop-2-en-1-one (E14)

Yellowish solid; Yield: 68%; ^{1}H NMR (400 MHz, $CDCl_3$, TMS) δ_H 13.50 (s, 1H), 8.59 (s, 1H),8.10(d, 2H, *J*=8.0 Hz), 8.00(d, 1H, *J*=15.6 Hz), 7.46(d, 1H, *J*=4.8 Hz), 7.41-7.36 (m, 4H), 7.32(d, 1H, *J*=9.2 Hz),7.13 (dd, 1H, *J*=4.4 Hz, *J*=4.0 Hz), 6.53 (d, 2H, *J*=6.4 Hz), 4.03 (t, 2H, *J*=6.4 Hz), 1.84-1.28 (m, 24H), 0.91-0.88 (t, 3H); ^{13}C NMR (100 MHz , $CDCl_3$, TMS) δ_C 188.6, 164.2, 162.8, 152.5, ,140.4, 137.2, 135.8, 134.0, 132.2, 130.0, 128.9, 128.4, 121.3, 120.5, 112.9, 108.1, 101.5, 68.4, 32.0, 29.7, 29.6, 29.4, 22.7, 14.2; IR (υ_{max}, cm^{-1}, KBr): 3436 (υOH), 2919, 2850(υ aliphatic C-H), 1652 (υC=O), 1627 (υC=N), 1600, 1516 (υ aromatic C=C), 1197 (υ PhO), 1119 (υ aliphatic C-O).

(E)-1-(4-((E)-(2-hydroxy-4-hexadecyloxybenzylidene)amino)phenyl)-3-(thiophen-2-yl) prop-2-en-1-one (E16)

Yellowish solid; Yield: 68%; ^{1}H NMR (400 MHz, $CDCl_3$, TMS) δ_H 13.50 (s, 1H), 8.59 (s, 1H),8.10(d, 2H, *J*=8.4 Hz), 8.00(d, 1H, *J*=15.2 Hz), 7.46(d, 1H, *J*=5.2 Hz), 7.40-7.35 (m, 4H), 7.32(d, 1H, *J*=9.6 Hz), 7.12 (dd, 1H, *J*=4.8 Hz, *J*=3.6 Hz), 6.53 (d, 2H, *J*=6.8 Hz), 4.03 (t, 2H, *J*=6.4 Hz), 1.85-1.28 (m, 28H), 0.91-0.88 (t, 3H); ^{13}C NMR (100 MHz , $CDCl_3$, TMS) δ_C 188.7, 164.3, 164.2, 162.9, 152.5, 137.2, 134.0, 132.3, 130.1, 128.9, 128.5, 121.4, 120.6, 112.9, 108.2, 101.6, 68.4, 29.8, 29.8, 29.7, 29.6, 29.5, 14.2. IR (υ_{max}, cm^{-1}, KBr): 3428 (υOH), 2919, 2850(υ aliphatic C-H), 1652(υC=O), 1627 (υC=N), 1600, 1516 (υ aromatic C=C), 1197 (υ PhO), 1119 (υ aliphatic C-O).

(E)-1-(4-((E)-(2-hydroxy-4-octadecyloxybenzylidene)amino)phenyl)-3-(thiophen-2-yl) prop-2-en-1-one (E18)

Yellowish solid; Yield: 70%; ^{1}H NMR (400 MHz, $CDCl_3$, TMS) δ_H 13.49 (s, 1H), 8.59 (s, 1H),8.10(d, 2H, *J*=8.4 Hz), 8.00(d, 1H, *J*=15.2 Hz), 7.46(d, 1H, *J*=5.2 Hz), 7.41-7.36 (m, 4H), 7.32(d, 1H, *J*=9.2 Hz),7.13 (dd, 1H, *J*=4.8 Hz, *J*=4.0 Hz), 6.53 (d, 2H, *J*=6.8 Hz), 4.03 (t, 2H, *J*=6.4 Hz), 1.86-1.28 (m, 32H), 0.91-0.88 (t, 3H). ^{13}C NMR (100 MHz , $CDCl_3$,

TMS) δ_C 188.7, 162.3, 161.0,156.6, 140.5, 136.9, 135.0, 132.0, 130.9, 129.9, 128.7,128.5, 128.3, 121.1, 120.6, 114.8, 68.2, 31.9, 29.7, 29.7, 29.6, 29.6, 29.4, 29.2, 26.0, 22.7, 14.2. IR (υ_{max}, cm^{-1}, KBr): 3447 (υOH), 2921, 2852(υ aliphatic C-H), 1650 (υC=O), 1591 (υC=N), 1558, 1511 (υ aromatic C=C), 1189 (υ PhO), 1112 (υ aliphatic C-O).

4.3.2 Synthesis of series E

4.3.2.1 Synthesis of 4-n-alkoxy benzaldehyde

4-n-alkoxy benzaldehydes were synthesized by following the reported method [38, 39]

4-hydroxy benzaldehyde (0.1 moles, 12.2 gm), anhydrous K_2CO_3 (0.15 mols, 20.85 gm) , and corresponding n-alkyl bromides (0.12 mols) was added to dry acetone (60.00 ml) in a round-bottom flask fitted with a reflux condenser. The reaction mixture was refluxed for 8-12 hr. The whole mass was then added to cold water and the aldehyde thus separated in an oily layer for the lower member. It was extracted twice with Pet-ether. The pet-ether extract was washed with dilute NaOH solution to remove un-reacted 4- hydroxy benzaldehyde, followed by water and dried. Pet-ether was evaporated, and the 4-n-alkoxy benzaldehyde was thus obtained.

4.3.2.2 Synthesis of (E)-1-(4-aminophenyl)-3-(thiophen-2-yl)prop-2-en-1-one

The method is described in section 4.3.1.2.

4.3.2.3 Synthesis of (E)-1-(4-((E)-(4-n-alkoxybenzylidene) amino) phenyl)-3-(thiophen-2-yl) prop-2-en-1-one

4-n-alkoxybenzaldehyde (n=2 to 8, 10, 12, 14, 16, 18, 2 mmol) and (E)-1-(4-aminophenyl)-3-(thiophen-2-yl)prop-2-en-1-one (2 mmol) were dissolved in a minimum amount of absolute ethanol. To this solution, a few drops of glacial acetic acid were added and the reaction mixture was refluxed for 4 h. After cooling, a crystalline yellow compound was separated.

The compound was filtered and washed with cool ethanol and dried in a vacuum. The synthesis route of the series is given in **Scheme 1.**

(E)-1-(4-((E)-(4-ethoxybenzylidene) amino) phenyl)-3-(thiophen-2-yl) prop-2-en-1-one (F2)

Yellowish solid; Yield: 60%; ^{1}H NMR (400 MHz, $CDCl_3$, TMS) δ_H 8.39 (s, 1H), 8.08 (d, 2H, *J*=8.0 Hz), 7.98 (d, 1H, *J*=15.2 Hz), 7.87 (d, 2H, *J*=8.4 Hz), 7.44-7.38(m,4H), 7.27 (d,2H, *J*=7.2 Hz), 7.12 (dd, 1H, *J*=4.8 Hz, *J*=3.6 Hz), 7.01 (d, 2H, *J*=8.8 Hz), 7.11 (dd, , 1H, *J*=4.8 Hz, *J*=3.6 Hz), 7.00 (d, 2H, *J*=8.0 Hz), 4.13-4.10 (q, 2H), 1.48-1.46 (t, 3H); ^{13}C NMR (100 MHz , $CDCl_3$, TMS) δ_C 188.7, 162.1, 161.0, 156.5, 140.5, 136.9, 135.1, 132.1, 131.0, 129.9, 128.8, 128.4, 121.1, 120.6, 114.8, 63.7, 14.8. IR (υ_{max}, cm^{-1}, KBr): 2917, 2849 (υ aliphatic C-H), 1653 (υC=O), 1596 (υC=N), 1512 (υ aromatic C=C), 1170 (υ PhO), 1108 (υ aliphatic C-O).

(E)-1-(4-((E)-(4-propyloxybenzylidene) amino) phenyl)-3-(thiophen-2-yl) prop-2-en-1-one (F3)

Yellowish solid; Yield: 62%; ^{1}H NMR (400 MHz, $CDCl_3$, TMS) δ_H 8.40 (s, 1H), 8.09 (d, 2H, *J*=8.4 Hz), 7.99 (d, 1H, *J*=15.2 Hz), 7.87 (d, 2H, *J*=8.8 Hz), 7.45-7.38(m,4H), 7.27 (d,2H, *J*=8.4 Hz), 7.11 (dd, , 1H, *J*=4.8 Hz, *J*=4.0 Hz), 7.01 (d, 2H, *J*=8.4 Hz), 4.02 (t, 2H, *J*=6.4 Hz), 1.89-1.71 (m, 2H), 1.10-1.06 (t, 3H); ^{13}C NMR (100 MHz , $CDCl_3$, TMS) δ_C 188.7, 162.3, 161.0, 156.5, 140.5, 136.8, 135.0, 132.0, 131.0, 129.8, 128.7, 128.5, 128.3, 128.4, 121.0, 120.6, 114.7, 113.9, 69.7, 22.5,10.5. IR (υ_{max}, cm^{-1}, KBr): 2920, 2849 (υ aliphatic C-H), 1649 (υC=O), 1585 (υC=N), 1511 (υ aromatic C=C), 1167 (υ PhO), 1109 (υ aliphatic C-O).

(E)-1-(4-((E)-(4-butyloxybenzylidene) amino) phenyl)-3-(thiophen-2-yl) prop-2-en-1-one (F4)

Yellowish solid; Yield: 65%; ^{1}H NMR (400 MHz, $CDCl_3$, TMS) δ_H 8.39 (s, 1H), 8.08 (d, 2H, *J*=8.4 Hz), 7.99 (d, , 1H, *J*=15.6 Hz), 7.87 (d, 2H, *J*=8.8 Hz), 7.45-7.38(m,4H), 7.27 (d,2H, *J*=8.4 Hz), 7.11 (dd, , 1H, *J*=4.8 Hz, *J*=4.0 Hz), 7.00 (d, 2H, *J*=8.8 Hz), 4.05 (t, 2H, *J*=6.4 Hz), 1.85-1.50 (m, 4H), 1.03-0.99 (t, 3H); ^{13}C NMR (100 MHz , $CDCl_3$, TMS) δ_C 188.7, 162.3, 161.0, 156.5,140.5, 136.8, 135.6, 135.0, 132.0, 130.9, 129.8, 128.7, 128.5, 128.3, 121.0,114.7,67.9, 31.2, 19.2, 13.9. IR (υ_{max}, cm^{-1}, KBr): 2917, 2849 (υ aliphatic C-H), 1653 (υC=O), 1596 (υC=N), 1512 (υ aromatic C=C), 1170 (υ PhO), 1108 (υ aliphatic C-O), 720(υ long alkyl chain) cm^{-1}.

(E)-1-(4-((E)-(4-pentyloxybenzylidene) amino) phenyl)-3-(thiophen-2-yl) prop-2-en-1-one (F5)

Yellowish solid; Yield: 68%; ^{1}H NMR (400 MHz, $CDCl_3$, TMS) δ_H 8.39 (s, 1H), 8.08 (d, 2H, *J*=6.4 Hz), 7.99 (d, , 1H, *J*=15.6 Hz), 7.87 (d, 2H, *J*=7.2 Hz), 7.42-7.38 (m, 4H), 7.27 (d, 2H), 7.11 (dd, , 1H, *J*=4.8 Hz, *J*=3.6 Hz), 7.00 (d, 2H, *J*=6.8 Hz), 4.04 (t, 2H, *J*=6.4 Hz), 1.83-1.44 (m, 8H), 0.96-0.92 (t, 3H); ^{13}C NMR (100 MHz , $CDCl_3$, TMS) δ_C 188.7, 162.4, 161.1, 156.6, 140.5, 136.9, 135.1, 132.1, 130.9, 129.9, 128.8, 128.7, 128.6, 121.1, 120.6, 114.8, 68.3, 28.9, 28.2, 22.5, 14.08. IR (υ_{max}, cm^{-1}, KBr): 2933, 2865(υ aliphatic C-H), 1650 (υC=O), 1588 (υC=N), 1588, 1510 (υ aromatic C=C), 1163 (υ PhO), 1109 (υ aliphatic C-O), 720(υ long alkyl chain).

(E)-1-(4-((E)-(4-hexyloxybenzylidene) amino) phenyl)-3-(thiophen-2-yl) prop-2-en-1-one (F6)

Yellowish solid; Yield: 61%; ^{1}H NMR (400 MHz, $CDCl_3$, TMS) δ_H 8.40 (s, 1H), 8.09 (d,

2H, *J*=8.4 Hz), 7.98 (d, 1H, *J*=15.2 Hz), 7.87 (d, 2H, *J*=8.4 Hz), 7.45-7.38(m,4H), 7.27 (d,2H, *J*=8.8 Hz), 7.12 (dd, 1H, *J*=4.8 Hz, *J*=3.6 Hz), 7.01 (d, 2H, *J*=8.8 Hz), 4.05 (t, *J*=6.4, 2H), 1.87-1.36 (m, 8H), 0.95-0.92 (t, 3H); ^{13}C NMR (100 MHz , $CDCl_3$, TMS) δ_C 188.8, 162.4, 161.1, 156.7, 140.6, 136.9, 132.1, 131.0, 129.9, 128.8, 128.7, 128.4, 121.1, 120.7, 114.9, 68.3, 31.6, 29.2, 25.8, 14.2. IR (υ_{max}, cm^{-1}, KBr): 2939, 2866(υ aliphatic C-H), 1646 (υC=O), 1571 (υC=N), 1509 (υ aromatic C=C), 1165 (υ PhO), 1110 (υ aliphatic C-O), 718(υ long alkyl chain).

(E)-1-(4-((E)-(4-heptyloxybenzylidene) amino) phenyl)-3-(thiophen-2-yl) prop-2-en-1-one (F7)

Yellowish solid; Yield: 64%; Mass (ES): m/z $[M + H]^+$ 431.31; ^{1}H NMR (400 MHz, $CDCl_3$, TMS) δ_H 8.40 (s, 1H), 8.08 (d, 2H, *J*=8.4 Hz), 7.99 (d, 1H, *J*=15.2 Hz), 7.87 (d, 2H, *J*=8.8 Hz), 7.43-7.37 (m, 4H), 7.27 (d, 2H, *J*=8.0 Hz), 7.12 (dd,1H, *J*=4.8 Hz, *J*=3.6 Hz), 7.00 (d, 2H, *J*=8.4 Hz), 4.05 (t, *J*=6.4 Hz, 2H), 1.85-1.33 (m, 10H), 0.92-0.91 (t, 3H); ^{13}C NMR (100 MHz , $CDCl_3$, TMS) δ_C 188.7, 162.4, 161.1, 156.6, 140.5, 136.9, 135.7, 135.1, 132.1, 130.9, 129.9, 128.7, 128.6, 128.4, 121.1, 114.8, 68.3, 31.8, 29.2, 29.1, 25.6, 22.7, 14.2. IR (υ_{max}, cm^{-1}, KBr): 2929, 2850 (υ aliphatic C-H), 1650 (υC=O), 1584 (υC=N), 1510 (υ aromatic C=C), 1160 (υ PhO), 1109 (υ aliphatic C-O), 710(υ long alkyl chain).

(E)-1-(4-((E)-(4-octyloxybenzylidene) amino) phenyl)-3-(thiophen-2-yl) prop-2-en-1-one (F8)

Yellowish solid; Yield: 72%;; ^{1}H NMR (400 MHz, $CDCl_3$, TMS) δ_H 8.38 (s, 1H), 8.08 (d, 2H, *J*=8.4 Hz), 7.99 (d, 1H, *J*=15.6 Hz), 7.87 (d, 2H, *J*=8.8 Hz), 7.43-7.37 (m, 4H), 7.27 (d, 2H, *J*=8.8 Hz), 7.11 (dd, , 1H, *J*=5.6 Hz, *J*=4.0 Hz), 7.00 (d, 2H, *J*=8.8 Hz), 4.03 (t, 2H, *J*=6.4 Hz), 1.86-1.31 (m, 12H), 0.91-0.89 (t, 3H); ^{13}C NMR (100 MHz , $CDCl_3$, TMS) δ_C 188.6, 162.3, 161.0, 156.5, 140.5, 136.8, 135.6, 135.0, 132.0, 130.9, 129.8, 128.7, 128.5,

128.3, 121.0, 114.8, 114.7, 113.9, 68.3, 31.8, 29.3, 29.2, 29.1, 25.9, 22.7, 14.2. IR (υ_{max}, cm^{-1}, KBr): 2983, 2932 (υ aliphatic C-H), 1651 (υC=O), 1589 (υC=N), 1510 (υ aromatic C=C), 1168 (υ PhO), 1112 (υ aliphatic C-O), 720(υ long alkyl chain).

(E)-1-(4-((E)-(4-decyloxybenzylidene) amino) phenyl)-3-(thiophen-2-yl) prop-2-en-1-one (F10)

Yellowish solid; Yield: 70%; ^{1}H NMR (400 MHz, $CDCl_3$, TMS) δ_H 8.41 (s, 1H), 8.09 (d, 2H, *J*=8.8 Hz), 7.99 (d,1H, *J*=15.6 Hz), 7.88 (d, 2H, *J*=8.8 Hz), 7.45-7.38 (m, 4H), 7.28 (d, 2H, *J*=8.8 Hz), 7.12 (dd, , 1H, *J*=4.4 Hz, *J*=3.6 Hz), 7.01 (d, 2H, *J*=8.8 Hz), 4.05 (t, 2H, *J*=6.4 Hz), 1.87-1.30 (m, 16H), 0.92-0.89 (t, 3H); ^{13}C NMR (100 MHz , $CDCl_3$, TMS) δ_C 188.7, 162.4, 161.0, 156.6, 140.5, 136.9, 135.1, 132.1, 131.0, 130.9, 129.9, 128.7, 128.6, 128.4, 121.1, 120.7, 114.8, 68.3, 31.9, 29.6, 29.4, 29.4, 29.2, 26.0, 22.7, 14.2. IR (υ_{max}, cm^{-1}, KBr): 2921, 2851 (υ aliphatic C-H), 1648 (υC=O), 1586 (υC=N), 1511 (υ aromatic C=C), 1167 (υ PhO), 1111 (υ aliphatic C-O), 703(υ long alkyl chain).

(E)-1-(4-((E)-(4-dodecyloxybenzylidene) amino) phenyl)-3-(thiophen-2-yl) prop-2-en-1-one (F12)

Yellowish solid; Yield: 68%; ^{1}H NMR (400 MHz, $CDCl_3$, TMS) δ_H 8.40 (s, 1H), 8.09 (d, 2H, *J*=8.4 Hz), 7.99 (d,1H, *J*=15.2 Hz), 7.87 (d, 2H, *J*=8.8 Hz), 7.45-7.38 (m, 4H), 7.27 (d, 2H, *J*=8.4 Hz), 7.12 (dd, , 1H, *J*=4.8 Hz, *J*=3.6 Hz), 7.01 (d, 2H, *J*=8.8 Hz), 4.05 (t, 2H, *J*=6.4 Hz), 1.87-1.29 (m, 20H), 0.92-0.89 (t, 3H). ^{13}C NMR (100 MHz , $CDCl_3$, TMS) δ_C 188.8, 162.4, 161.1, 156.7, 140.6, 136.9, 132.1, 131.0, 129.9, 128.8, 128.6, 128.4, 121.1, 120.7, 114.9, 68.3, 32.0, 29.7, 29.6,29.6, 29.5, 14.2. IR (υ_{max}, cm^{-1}, KBr): 2920, 2849 (υ aliphatic C-H), 1649 (υC=O), 1585 (υC=N), 1511 (υ aromatic C=C), 1167 (υ PhO), 1109 (υ aliphatic C-O), 716(υ long alkyl chain).

(E)-1-(4-((E)-(4-tetradecyloybenzylidene) amino) phenyl)-3-(thiophen-2-yl) prop-2-en-1-one(F14)

Yellowish solid; Yield: 62%; ^{1}H NMR (400 MHz, $CDCl_3$, TMS) δ_H 8.40 (s, 1H), 8.09 (d, 2H, *J*=8.4 Hz), 7.99 (d, , 1H, *J*=15.6 Hz), 7.87 (d, 2H, *J*=8.4 Hz), 7.45-7.38 (m, 4H),7.28 (d, 2H, *J*=8.4 Hz), 7.12 (dd, , 1H, *J*=4.8 Hz, *J*=3.6 Hz), 7.01 (d, 2H, *J*=8.8 Hz), 4.05 (t, 2H, *J*=6.4 Hz), 1.87-1.28 (m, 24H), 0.92-0.88 (t, 3H); ^{13}C NMR (100 MHz , $CDCl_3$, TMS) δ_C 188.7, 162.4, 161.0, 156.6, 140.8, 136.9, 135.1, 132.1, 130.9, 129.9, 128.7, 128.6, 128.4, 121.1, 120.7, 114.8, 68.3, 32.0, 29.7, 29.6,29.6, 29.4, 29.2, 26.0, 22.7, 14.2. IR (υ_{max}, cm^{-1}, KBr): 2918, 2850 (υ aliphatic C-H), 1653 (υC=O), 1595 (υC=N), 1512 (υ aromatic C=C), 1170 (υ PhO), 1108 (υ aliphatic C-O), 720(υ long alkyl chain).

(E)-1-(4-((E)-(4-hexadecyloxybenzylidene) amino) phenyl)-3-(thiophen-2-yl) prop-2-en-1-one (F16)

Yellowish solid; Yield: 70%; ^{1}H NMR (400 MHz, $CDCl_3$, TMS) δ_H 8.40 (s, 1H), 8.09 (d, 2H, *J*=8.4 Hz), 7.99 (d, 1H, *J*=15.6 Hz), 7.87 (d, 2H, *J*=8.4 Hz), 7.45-7.38 (m, 4H),7.28 (d, 2H, *J*=8.4 Hz), 7.12 (dd, 1H, *J*=4.8 Hz, *J*=4.0 Hz), 7.01 (d, 2H, *J*=8.8 Hz), 4.05 (t, 2H, *J*=6.4 Hz), 1.87-1.28 (m, 28H), 0.92-0.88 (t, 3H); ^{13}C NMR (100 MHz , $CDCl_3$, TMS) δ_C 188.8, 162.4, 161.1, 156.7, 140.5, 140.4, 136.9, 135.4, 135.1, 132.1, 130.9, 129.9, 128.7, 128.6, 128.4, 121.1, 120.7, 114.8, 68.3, 32.0, 29.7, 29.7, 29.6,29.6, 29.4, 29.2, 26.0, 22.7, 14.2. IR (υ_{max}, cm^{-1}, KBr): 2917, 2849 (υ aliphatic C-H), 1653 (υC=O), 1596 (υC=N), 1512 (υ aromatic C=C), 1170 (υ PhO), 1108 (υ aliphatic C-O), 720(υ long alkyl chain).

(E)-1-(4-((E)-(4-octadecyloxybenzylidene) amino) phenyl)-3-(thiophen-2-yl) prop-2-en-1-one (F18)

Yellowish solid; Yield: 72%; ^{1}H NMR (400 MHz, $CDCl_3$, TMS) δ_H 8.40 (s, 1H), 8.09 (d, 2H, *J*=8.0 Hz), 7.99 (d, 1H, *J*=15.2 Hz), 7.87 (d, 2H, *J*=8.4 Hz), 7.45-7.38 (m, 4H),7.28 (d, 2H,

J=8.0 Hz), 7.12 (dd, , 1H, *J*=4.8 Hz, *J*=3.6 Hz), 7.01 (d, 2H, *J*=8.8 Hz), 4.05 (t, 2H, *J*=6.4 Hz), 1.85-1.28 (m, 32H), 0.91-0.88 (t, 3H); ^{13}C NMR (100 MHz , $CDCl_3$, TMS) δ_C 188.6, 162.4, 161.0, 156.6, 140.5, 136.9, 135.1, 132.1, 130.9, 129.9, 128.7, 128.6, 128.4, 121.1, 120.7, 114.8, 68.3, 32.0, 29.7, 29.7, 29.6,29.6, 29.4, 29.2, 26.0, 22.7, 14.2. IR (υ_{max}, cm^{-1}, KBr): 2917, 2849 (υ aliphatic C-H), 1653 (υC=O), 1596 (υC=N), 1512 (υ aromatic C=C), 1170 (υ PhO), 1108 (υ aliphatic C-O), 720(υ long alkyl chain).

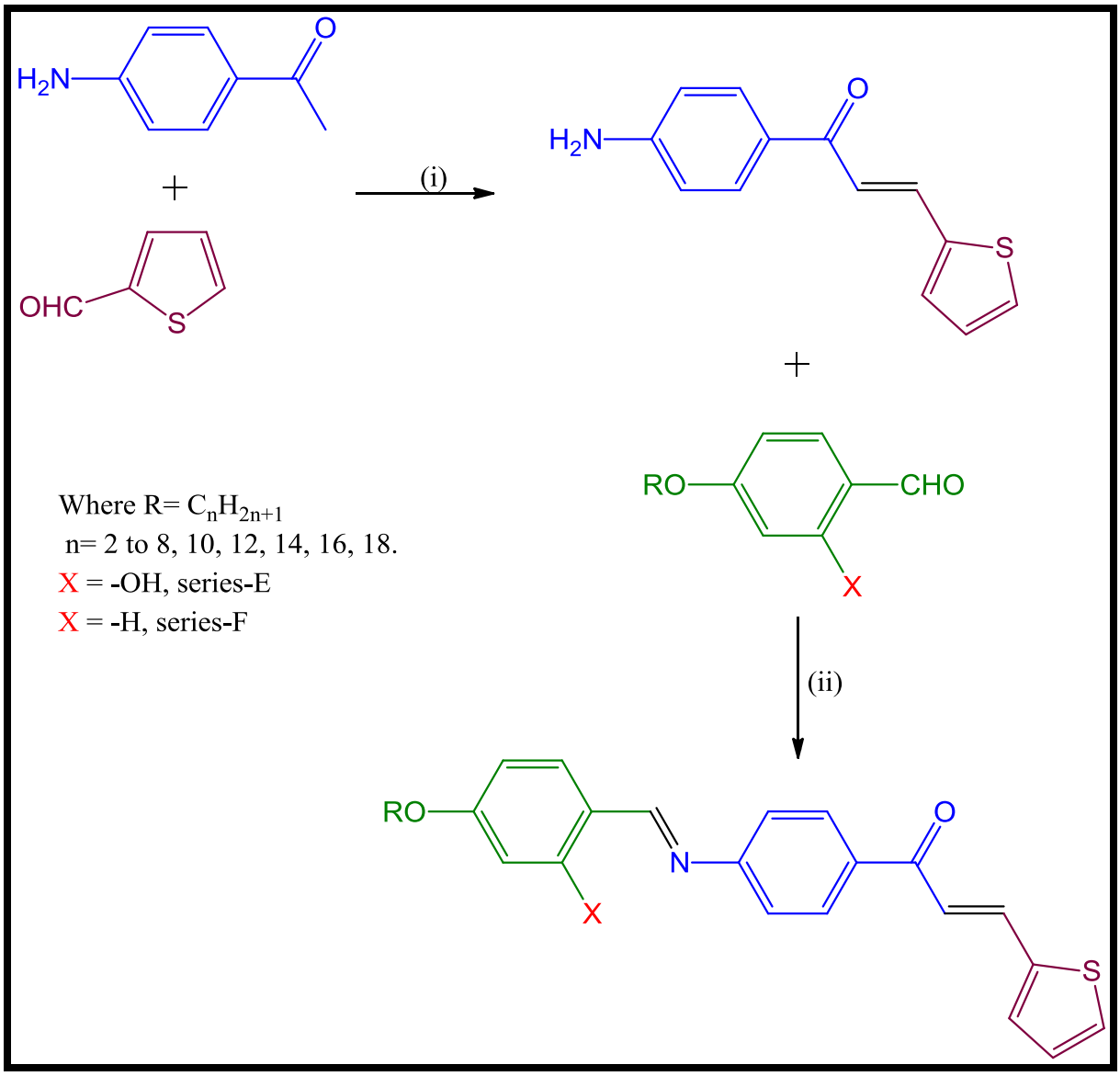

i) Aq. NaOH, alcohol, stir 4 hr, ii) Few drops of glacial AcOH, absolute EtOH, reflux 4 hr

Scheme 1. Synthetic protocol of thiophene based homologous series E and F

4.4 Results and Discussion

4.4.1 Series E

In this series, twelve homologous Schiff base derivatives of 2-hydroxy-4-n-alkoxybenzaldehyde with (E)-1-(4-aminophenyl)-3-(thiophen-2-yl)prop-2-en-1-one were prepared by varying the terminal alkoxy groups from n=2 to 8, 10, 12, 14, 16, 18. The compounds were characterized by ^{1}H and ^{13}C–NMR, ESI-MS, and IR.

In the ^{1}H-NMR of (E)-1-(4-aminophenyl)-3-(thiophen-2-yl)prop-2-en-1-one, the -NH_2 protons appeared at δ 4.23 as a singlet. Further chalcon -COCH = CH, protons merge with aromatic protons and are observed between δ 7.95-7.91 and 7.40-7.33. One of the protons of the thiophene ring has a double doublet at 7.09, and the *J* values are 4.8 and 3.6 *Hz* These data are in good agreement with the structure of the synthesized compound. In addition, the peak $[M + H]^+$ obtained at m/z 230.07 in ESI Mass confirmed the structure of the compound. In the ^{1}H-NMR spectrum of the series E compounds, the hydroxyl proton (–OH) of the Schiff base is observed as a singlet at about δ 13.50. As there is an intra-molecular hydrogen bond between the hydroxyl group and the imine group, the proton is observed to be deshielded. The imine proton (CH = N) is observed as a singlet at δ 8.59. One of the chalcon protons is observed as a doublet at δ 8.00 with a *J* value of 15.2 *Hz,* and the other is merged with the aromatic protons between δ 7.41-7.36. The remaining aromatic protons are observed between δ 8.10-6.53. The hydrogens on the carbon atom attached to oxygen, the alkoxy protons (-OCH_2-) are highly deshielded and appeared at δ 4.03 as a triplet, with a *J* value of 6.4 *Hz*. The other methylene protons of the alkoxy chain (-CH_2) are found between δ 1.86-1.28 as a multiplet. The proton of the terminal methyl group is observed as a triplet at δ 0.90.

In the ^{13}C-NMR spectrum of the compounds, ketone carbon was observed at δ 188.6. The peak at δ 162.4, corresponds to imine carbon (-CH=N), and aromatic carbons are

observed in between δ 164.0-108.5. A methylene carbon attached to alkoxy oxygen was observed at δ 68.3. The other methylene carbons of the alkoxy chain were found in between δ 32.0-22.6. The methyl carbon of the long alkoxy chain was observed at approximately δ 14.2. The ESI-Mass spectra of the homologues **E6 and E10**, $[M + H]^+$ peaks, are obtained at m/z 434.19 and 490.26 respectively, confirming the molecular structure.

In the FT-IR spectrum of (E)-1-(4-aminophenyl)-3-(thiophen-2-yl)prop-2-en-1-one , two absorption bands are observed near 3469 and 3202 cm^{-1}, corresponding to asymmetric stretching and symmetric stretching, which confirms the presence of primary amines. In the FT-IR spectrum of the series E compounds, the peak at 3447 cm^{-1} is attributed to –OH stretching. The characteristic peak of the carbonyl group appears at 1650 cm^{-1}. The compounds displayed bands of approximately 1591 cm^{-1} corresponding to (υC=N).

The thermal stability of the compound was measured by the TG-DTA analysis, and the results showed that the synthesized compound was thermally stable up to 300°C because there was no mass loss up to 300°C **(Figure 21).** In the 300 to 400 °C temperature range, mass loss is highest.

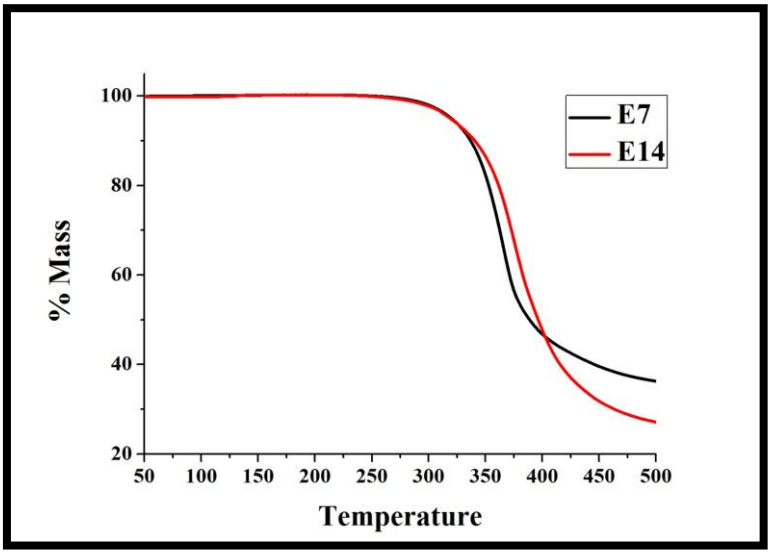

Figure 21. TGA thermograme of **E7** and **E14**

The mesomorphic behavior of all synthesized compounds was investigated by polarizing optical microscope (POM). The phase transition temperature achieved by POM was confirmed by a DSC trace of some compounds and the corresponding phase transition enthalpy was achieved by DSC analysis. The data are listed in **Table 1.**

Series-E		
En	Heating	Cooling
E2	Cr 166.7 (68.0) I	I 140.0 (61.8) Cr
E3	Cr 186.7 (52.0) I	I 149.0 (69.6) Cr
E4	Cr 164.7 (99.2) I	I 147.0 (83.5) Cr
E5	Cr 160.3 (97.4) I	I 131.4 (82.9) Cr
E6	Cr 147.4 (70.5) I	I 130.3 (0.5) N 117.0 (67.6) Cr
E7	Cr 140.7N (9.06) 149.1 (68.73) I	I 131.3 (0.5) N 123.8 (72.5) Cr
E8	Cr 120.0 (4.0) N 139.1 (72.3) I	I 131.1 (0.9) N 118.6 (68.7) Cr
E10	Cr 134.9 N 140.3 (89.5) I	I 128.2 (1.0) N 109.3 (79.9) Cr
E12	Cr 113.7 (18.3) N 130.1 (1.8) I	I 129.8 (1.0) N 103.0 (41.7) Cr
E14	Cr 118.9 (8.7) SmA 131.6 (69.2) I	I 127.9 (3.2) SmA 105.8 (92.2) Cr
E16	Cr 118. 0 (70.2) SmA 130.8 (1.8) I	I 127.7 (2.6) SmA 106.5 (69.1) Cr
E18	Cr 120.5 (119.7) SmA 132.8 (3.7) I	I 128.9 (4.4) SmA 110.6 (114.6) Cr

Table 1. Phase transition temperatures in ^{o}C, along with transition enthalpy values (ΔH Jg^{-1}).

The results of the compounds indicate that *n*-ethoxy **E2** to *n*-pentyloxy **E5** derivatives are not mesogenic. They melt directly from the crystalline phase in the isotropic liquid and cool down; from the isotropic liquid directly in the crystalline phase, no intermediate phase exists. As the compound heats up, the thermal motions of the molecules within the lattice increase, and finally the vibrations become so intense that the regular arrangement of

molecules is crashed with the loss of long-range orientational and positional order to give the disorganized isotropic liquid. In this process, as temperature increases, some compounds have one or more intermediate phase, referred to as mesophases [40]. Due to the unfavorable magnitudes of anisotropic forces of intermolecular attractions, they cannot withstand external thermal vibrations, they immediately destroy the crystal lattice and suddenly transform into an isotropic liquid that does not show an intermediate phase [41]. In the DSC thermogram of compound **E5**, the endothermic peak at 160.3°C is an enthalpy change of 97.4 J/g, which is attributed to crystal to isotropic transition and one peak observed on cooling at 131.4 ^{o}C with enthalpy changes 82.9 J/g due to isotropic liquid to crystal transition **(Figure 23a).** This confirms the POM observation that the compound **E5** is non-mesogenic. The derivative **E6** has the monotropic nematic phase. The *n*-heptyloxy **E7** to *n*-dodecyloxy **E12** derivatives are exhibited the enantiotropic smectic-A phase. **Figure 22a** shows the marble texture of the nematic phase of the compound **E7** on cooling at 130 ^{o}C and on further cooling at 123.8 ^{o}C, the nematic to crystal transition of compound **E7** is depicted in **Figure 22b.** The DSC thermogram of **E7** shows two endothermic peaks at 140.7 ^{o}C and 149.1 ^{o}C, and the corresponding transitions are crystal to nematic and nematic to isotropic. Enthalpy associated with these transitions are 9.0 and 68.7J/g, respectively. During the cooling process, two peaks were observed, corresponding to the transition from isotropic to nematics and from nematics to the crystals **(Figure 23b).** The higher member of the homologous series, *n*-tetradecyloxy **E14** to *n*-octadecyloxy **E18** derivatives are exhibiting an enantiotropic smectic-A phase. **Figure 22c** shows the Fan shaped texture of smectic-A of compound **E14** on cooling at 126.5 ^{o}C and **Figure 22d** shows the transition from the nematic phase to the crystalline phase when the compound **E18** is further cooled to 105.8°C. In the DSC thermogram of compound **E18**, two endoderm peaks observed at 120.5°C and 132.8 °C, represent crystal to SmA and SmA to isotropic liquid transitions. When cooled, it shows

exothermic peaks at 128.9°C and 110.6°C with associated enthalpies 4.4 J/g and 114.6 J/g, correspond to the isotropic to SmA and SmA to crystalline phase transitions. The DSC thermogram for **E18** is represented in **Figure 23c**.

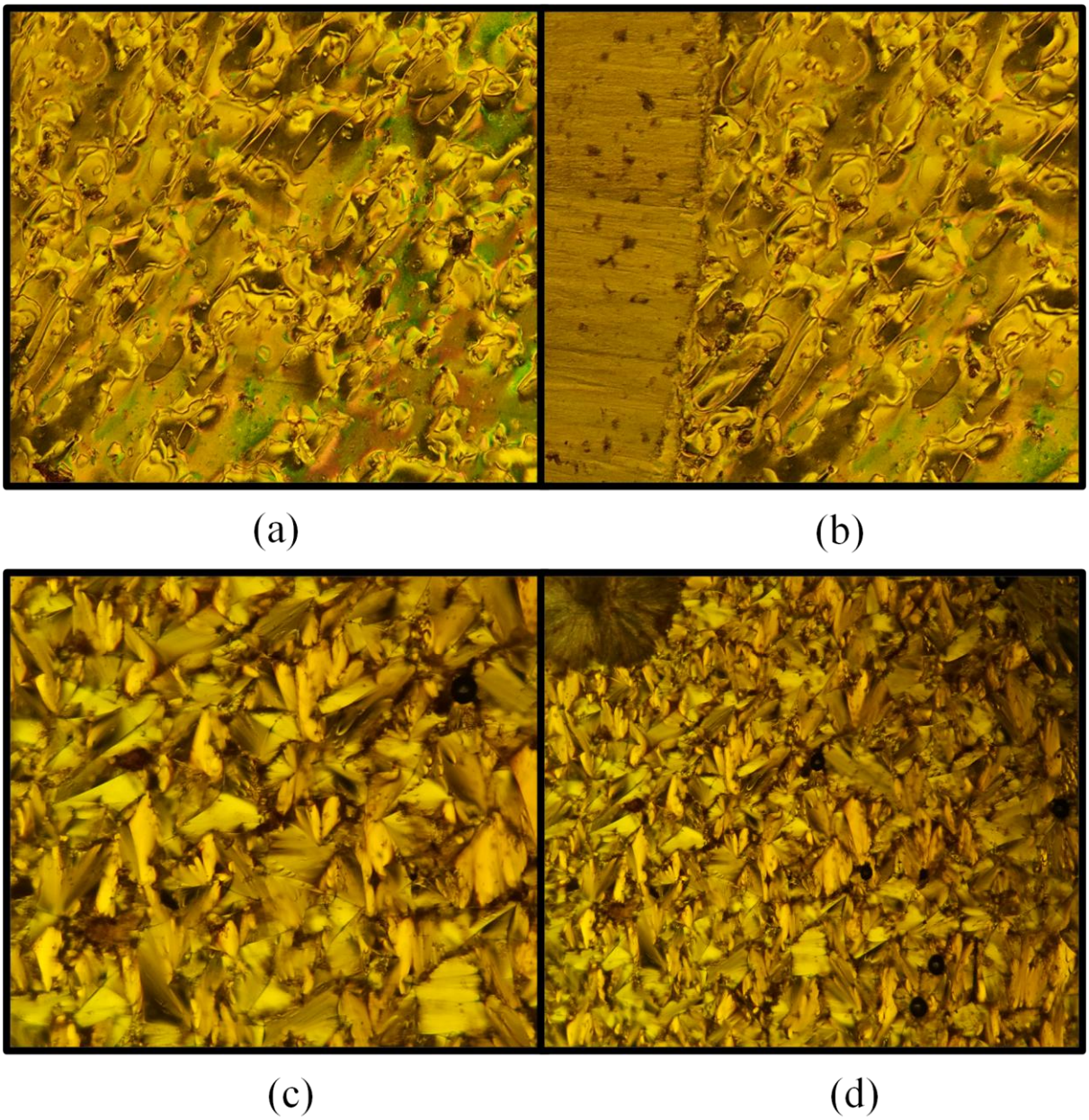

Figure 22a. Marble texture of nematic phase of compound **E7** on cooling at 130 ^{o}C ; **b.** Nematic to crystal transition of compound **E7** on cooling at 123.8 ^{o}C; **c**. Fan shaped texture of Smectic-A of compound **E14** on cooling at 126.5 ^{o}C; **d.** Smectic-A to crystal transition of compound **E14** on cooling at 105.8 ^{o}C

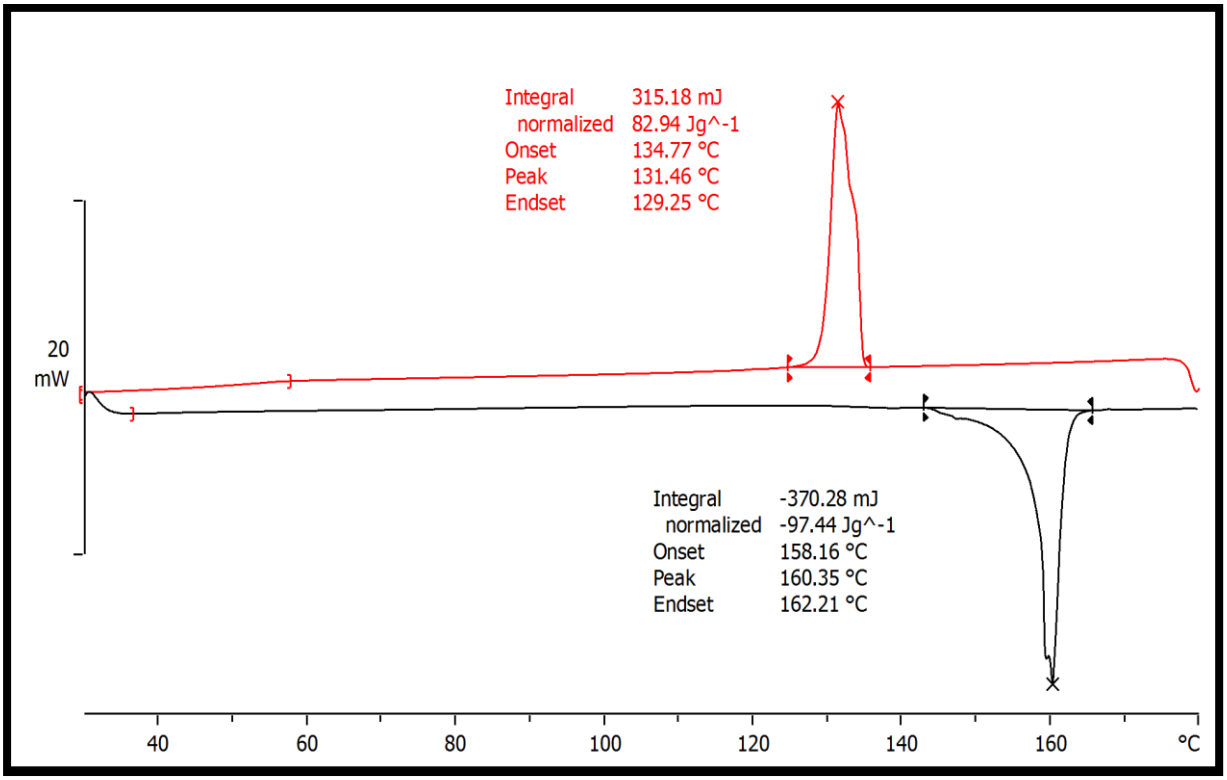

Figure 23a. DSC thermograme of E5

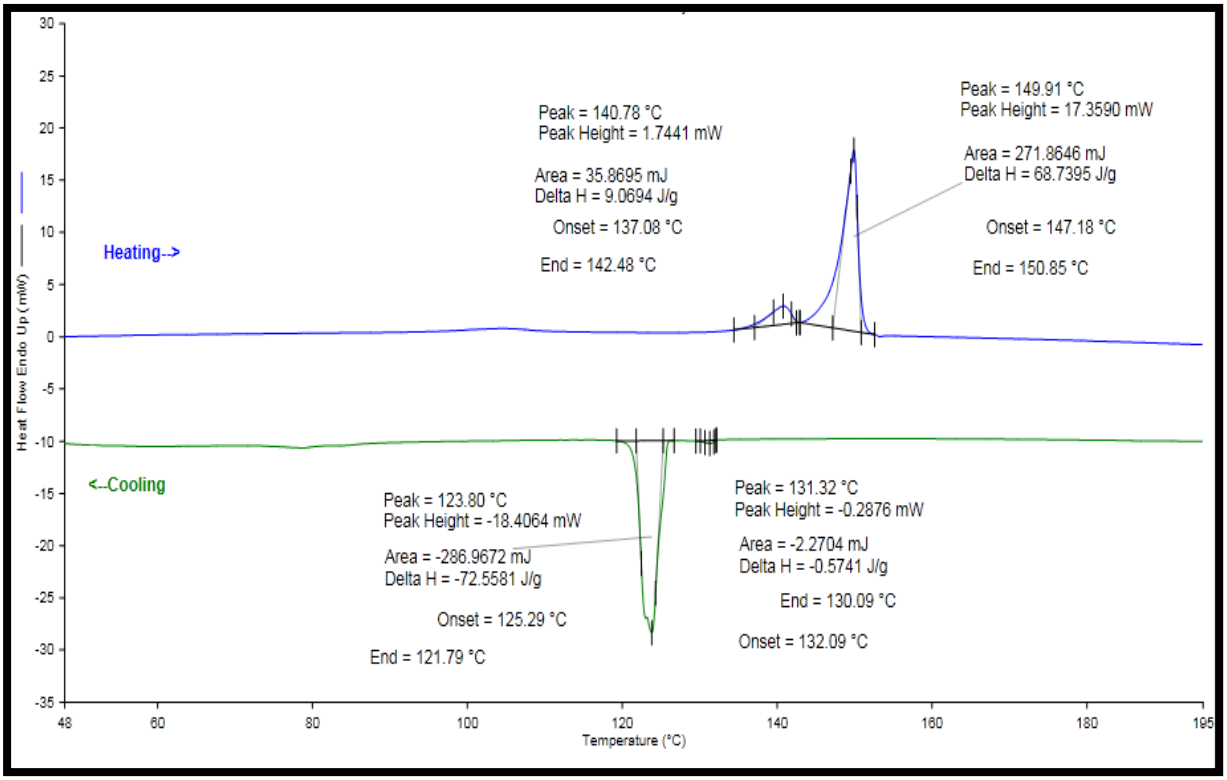

Figure23b. DSC thermograme of E7

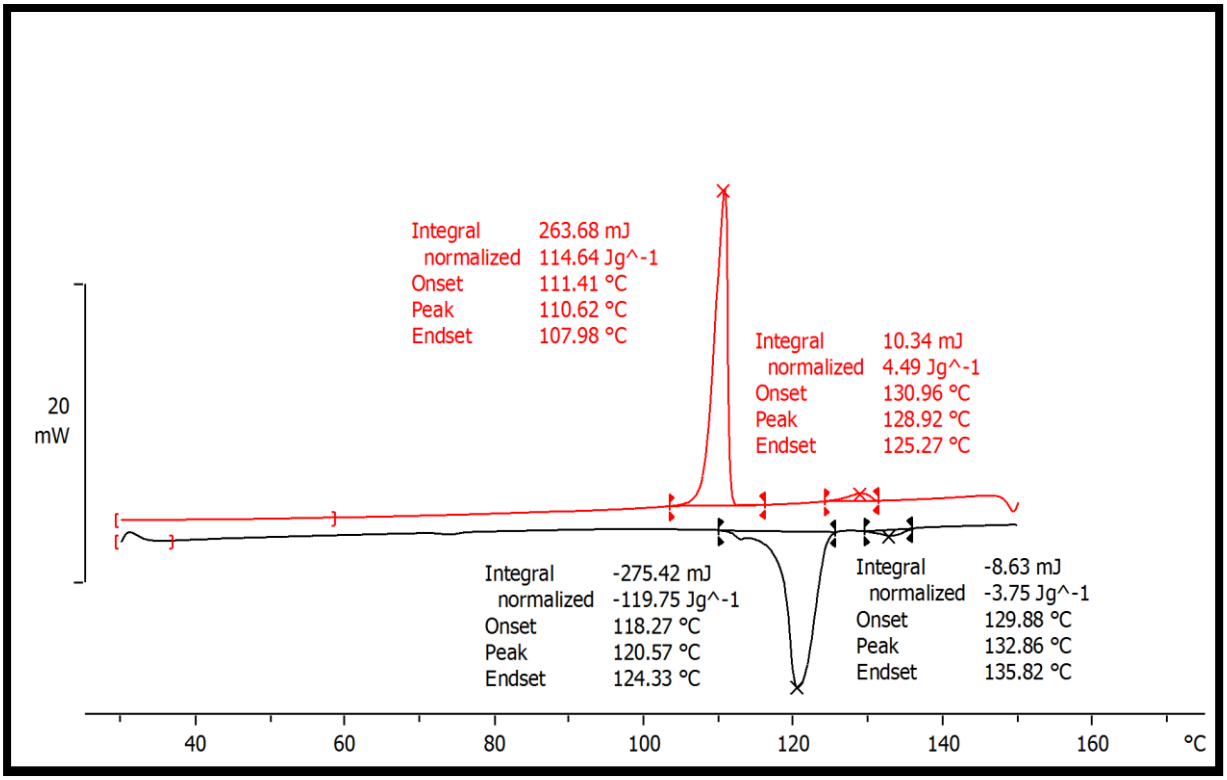

Figure 23c. DSC thermograme of E18

The influence of molecular flexibility on the transition temperature and phase sequence of the corresponding compound is illustrated in **Figure 24.** The results show that the different types of mesophases appeared to depend on the flexibility of the molecule, the number of carbon atoms in the terminal alkoxy group. The enantiotropic nematic phase commences from *n*-heptyloxy derivative of the series **(E7)** and continues to *n*-tetradecyloxy derivative **(E12)**, while the smectic-A phase starts from *n*-tetradecyloxy derivative **(E14)** and continues until the last member of the series *n*-octadecyloxy **(E18)** derivative. This is because the long chains attract, entangle and stabilize the layered packaging necessary to form the smectic phase. This is consistent with earlier observations [42].

The *n*-hexyloxy derivative **(E6)** of this series shows monotropic behavior and, exhibits a nematic phase. It is also observed that the clearing point decreases significantly as the chain length increases because of the increased flexibility.

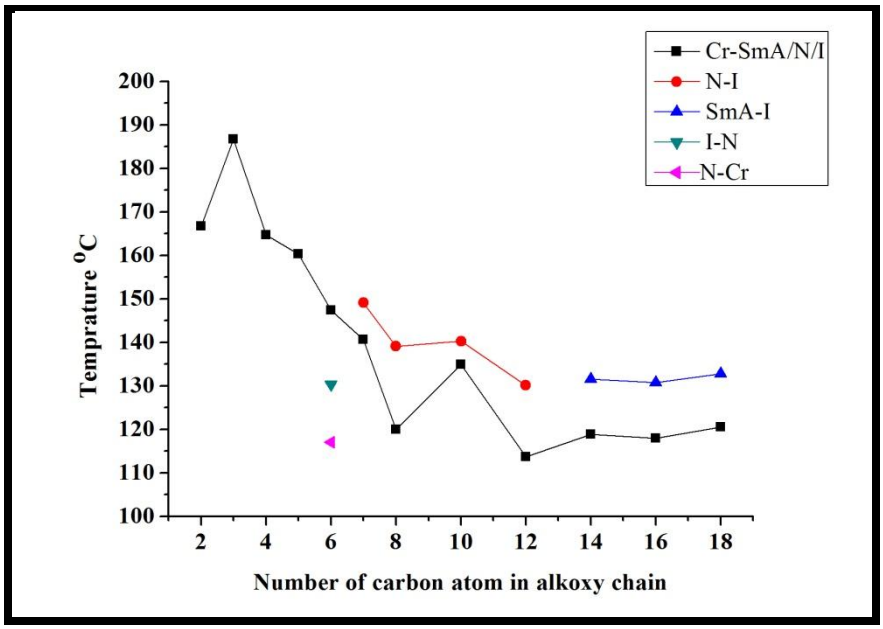

Figure24. Dependence of transition temperatures on the increasing terminal alkoxy chain length on heating

See **Figure 25** to understand the influence of alkoxy chain length in the smectic-A and nematic ranges of the heating and cooling cycles, respectively. According to these results, the compound **(E8)** shows a wider mesogenic temperature range than all the mesogens of the series during the heating cycle, while the compound **(E12)** is in the cooling cycle. The graph shows that the length of the alkoxy chain following *n*-dodecyloxy derivative nematic phase disappears. This is because the flexibility of the long chain tends to destroy the molecular packing necessary to form the nematics phase. Although the smectic-A behavior increases with the length of the alkoxy chain, and the trend towards the last homologous *n*-octadecyloxy derivative continues.

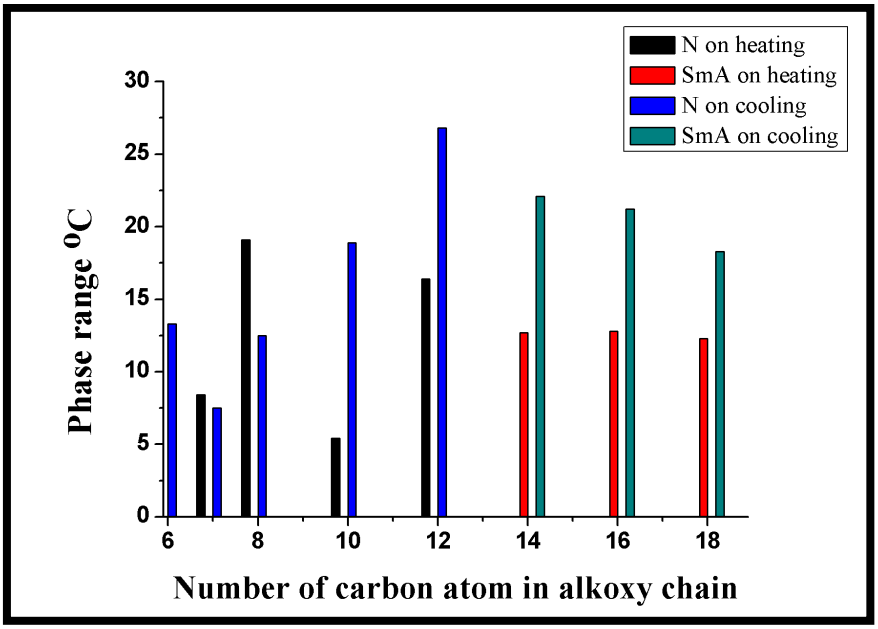

Figure 25. Temperature range of nematic and smectic phase, on heating and cooling

4.4.2 Series-F

In the ^{1}H-NMR spectrum of the series F compounds, the imine proton (CH = N) was observed as a singlet at δ 8.41. Of the two Chacon protons, one is observed as a doublet at δ 7.99 with a *J* value of 15.2 *Hz*, and the other merges with the aromatic proton between δ 7.45-7.38. The remaining aromatic protons were observed between δ 8.09-7.00. The hydrogens on the carbon atom attached to oxygen, (-OCH_2-) alkoxy protons are highly deshielded and appeared at δ 4.05 as a triplet, with a *J* value of 6.4 *Hz*. The other methylene protons of the alkoxy chain (-CH_2) were found between δ 1.87-1.30 as a multiplet. The protons terminal methyl group is observed at δ 0.91 ppm, as a triplet. In the ^{13}C-NMR spectrum of compounds of homologues series, α,β- unsaturated ketone carbon was observed at δ 188.7 ppm. The peak at δ 162.4 ppm corresponds to imine carbon (-CH=N). The aromatic carbons were observed in between δ 161.0-113.9 ppm. A methylene carbon attached to alkoxy oxygen was observed at δ 68.3 ppm. The other methylene carbons of the alkoxy chain were found in between δ 31.9-22.0 ppm. The methyl carbon of the long alkoxy chain

was observed at approximately δ 14.2 ppm. The ESI-Mass spectra of one of the homologue **F7** $[M + H]^+$ peak obtained at m/z 431.31 confirmed the structure of the molecule.

In the FT-IR spectrum of the series F compounds, the characteristic peak of the carbonyl carbon group appears at 1648 cm^{-1}. The compounds showed bands around 1586 cm^{-1} corresponding to (υC=N). Due to the asymmetric stretching of C-O-C, the aryl alkyl ether produces two strong absorption bands at about 1250 cm^{-1}, and one strong absorption band at about 1030 cm^{-1} due to symmetric stretching. The absorption band at about 720 cm^{-1} represents a long alkyl chain.

The thermal stability of the compound was measured by the TGDTA analysis, and the results showed that the synthesized compound was thermally stable up to 250°C because there was no mass loss up to 250°C **(Figure 26).** In the temperature range of 250 to 500 °C, the mass loss is greatest.

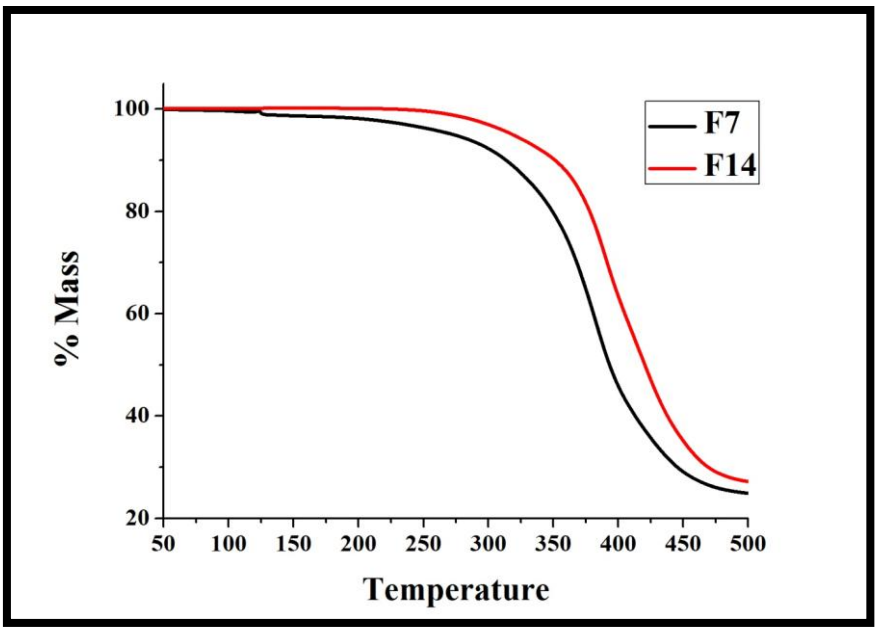

Figure 26. TG-DTA thermogram of compound **F7** and **F14**

Use a polarizing optical microscope (POM) to examine the mesogenic behavior of all synthesized compounds, and use DSC traces of the compounds to confirm the phase transition temperature achieved by POM. The transition enthalpy of the phase change is obtained from the DSC analysis. The transition temperature in ^{o}C and the corresponding transition enthalpy (ΔH Jg^{-1}) are given in **Table 2**.

Series-F		
Fn	Heating	Cooling
F2	Cr 194.2 (70.6) I	I 76.1 (52.7) Cr
F3	Cr 149.6 (60.8) I	I 104.6 (56.2) Cr
F4	Cr 125.7 (25.9) I	I 70.7 (40.7) Cr
F5	Cr 129.2 (53.4) I	I 91.8 (44.4) Cr
F6	Cr 141.4 (75.9) I	I 95.4 (75.2) Cr
F7	Cr 119.0 (57.4) I	I 95.7 (0.4) N 85.0 (44.8) Cr
F8	Cr 119.4 (84.8) I	I 87.3 (0.77) N 69.9 (96.5) Cr
F10	Cr 116.0 (93.3) I	I 104.2 (0.8) N 92.7 (81.5) Cr
F12	Cr 128.8 (67.7) I	I 101.3 (0.6) N 91.6 (62.1) Cr
F14	Cr 112.1 (113.8) I	I 101.4 (1.3) N 94.5 (96.9) Cr
F16	Cr 111.8 (99.0) I	I 99.6 (82.0) Cr
F18	Cr 113.2 (69.6) I	I 101.3 (66.2) Cr

Table 2. Phase transition temperatures in ^{o}C, along with transition enthalpy values (ΔH Jg^{-1}).

The polarizing optical microscope and DSC analysis of the compounds revealed that *n*-ethoxy **F2** to *n*-hexyloxy **F6** derivatives were not mesogenic. They melt directly from the crystalline phase into the isotropic liquid and cool down; from the isotropic liquid directly into the crystalline phase, an intermediate phase does not exist. In the DSC thermogram of

compound **F6**, the endothermic peak at 141.4°C is an enthalpy change of 75.9 J/g, which is attributed to crystal to isotropic transition and one peak observed on cooling at 95.4 ^{o}C with enthalpy changes 75.2 J/g due to isotropic liquid to crystal transition (**Figure 27**). This confirms the POM finding that the compound **F6** is non-mesogenic. The derivatives, *n*-heptyloxy **F7** to *n*-tetradecyloxy **F14** has a monotropic nematic phase; they are directly converted into an isotropic liquid when heated, but show a typical marbled optical texture of a nematic phase when cooled. This may be due to the fact that there is no position order, but the molecules have a preferred orientation order as they diffuse through the whole sample [43]. **Figure 28a** shows the nematic phase with a typical marble texture when the compound **F14** is cooled to 125.6 °C, and **Figure 28b** shows the transition from the nematic phase to the crystalline phase when the compound **F14** is further cooled to 94.5°C. The monotropic behavior of compound **F14** is confirmed by the DSC thermogram, which shows a single endothermic peak at 112.1°C when heated, and the enthalpy change corresponding to the melting point is 113.8 J/g. When cooled, it shows exothermic peaks at 101.4°C and 94.5°C with associated enthalpy changes 1.3 J/g and 96.9 J/g, correspond to the isotropic liquid to nematic and nematic to crystalline phase transitions **(Figure 29).** The value of change of enthalpy, for the transition from crystal to isotropy, and from nematic to crystal is much greater than that of isotropic liquid to the nematic phase. This is because of the low order presence in the nematics phase [40]. The higher member of the homologous series, *n*-hexadecyloxy **F16** and *n*-octadecyloxy **F18** derivatives are also not mesogenic. In the DSC thermogram of compound **F16**, only the heating and cooling peaks observed at 111.8 °C (Cr-I) and 99.6 °C (I-Cr) confirm the non-mesogenic nature (**Figure 27)**.

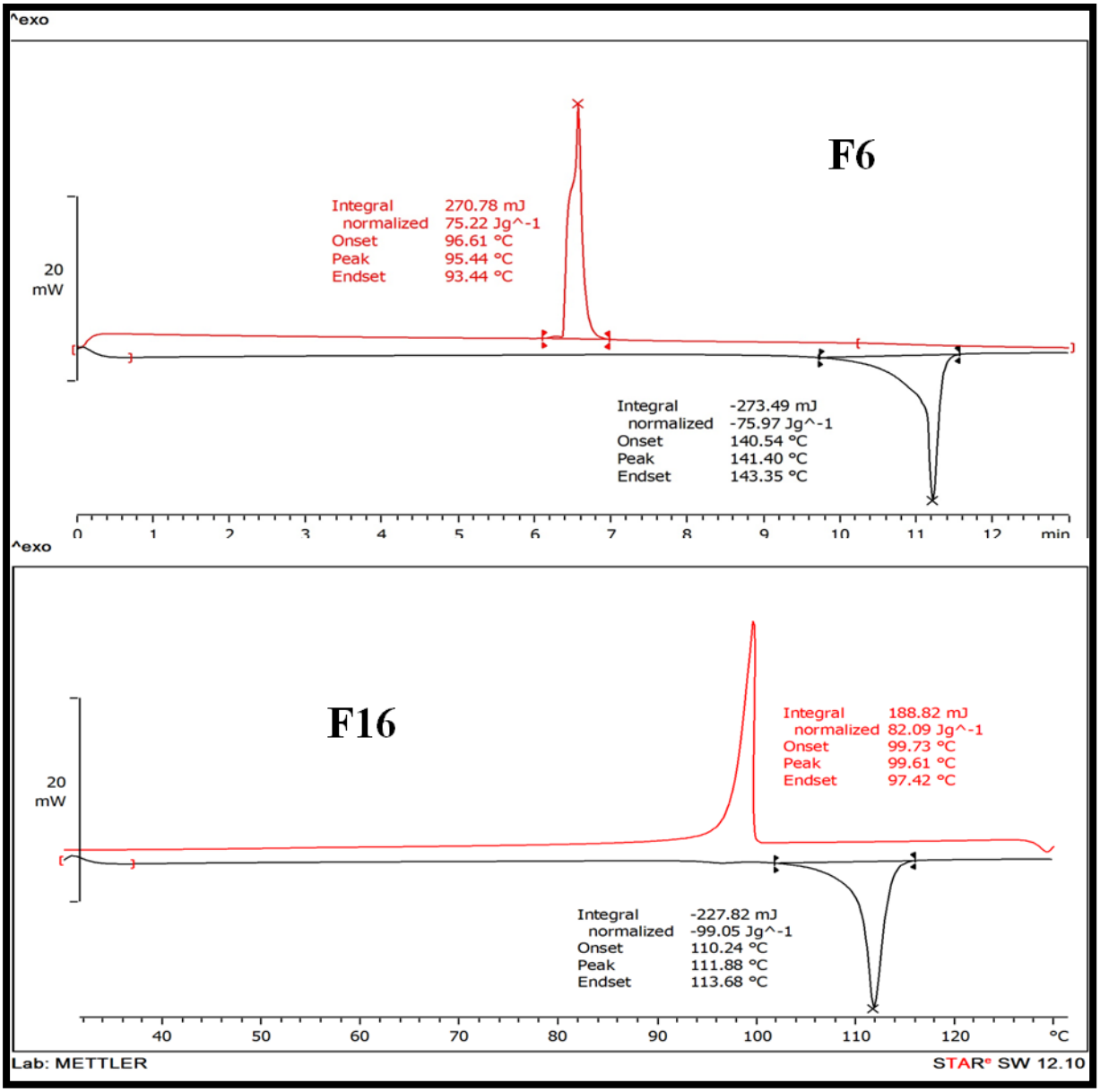

Figure 27. DSC thermograme of **F6** and **F16**

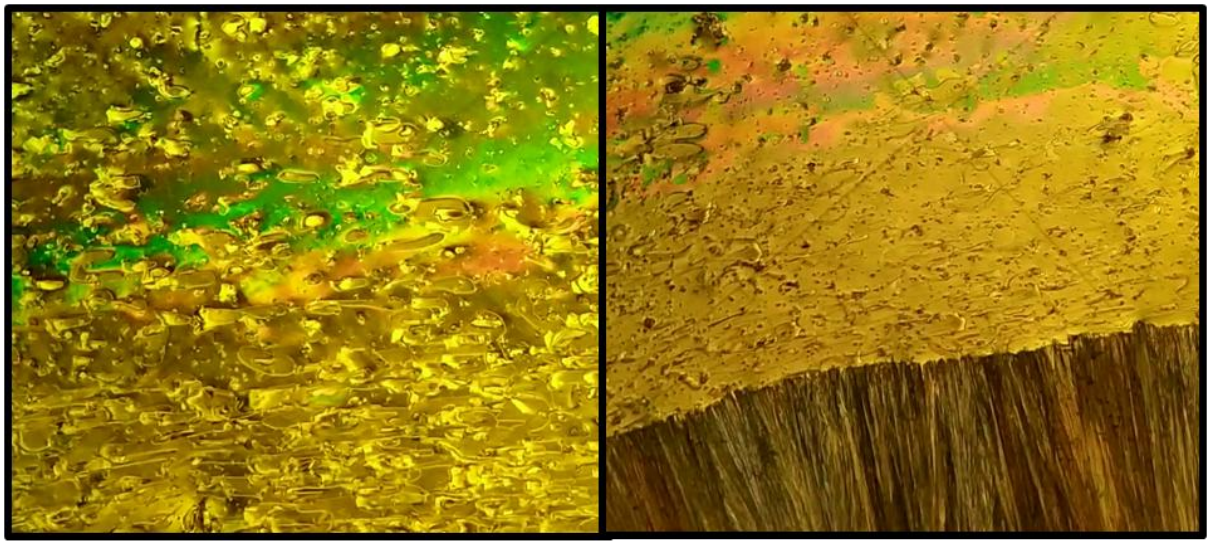

(a) (b)

Figure 28a. Marble texture of compound **F14** on cooling at 125.6 ^{o}C; **b.** Nematic to crystal transition of compound **F14** on cooling at 94.5 ^{o}C

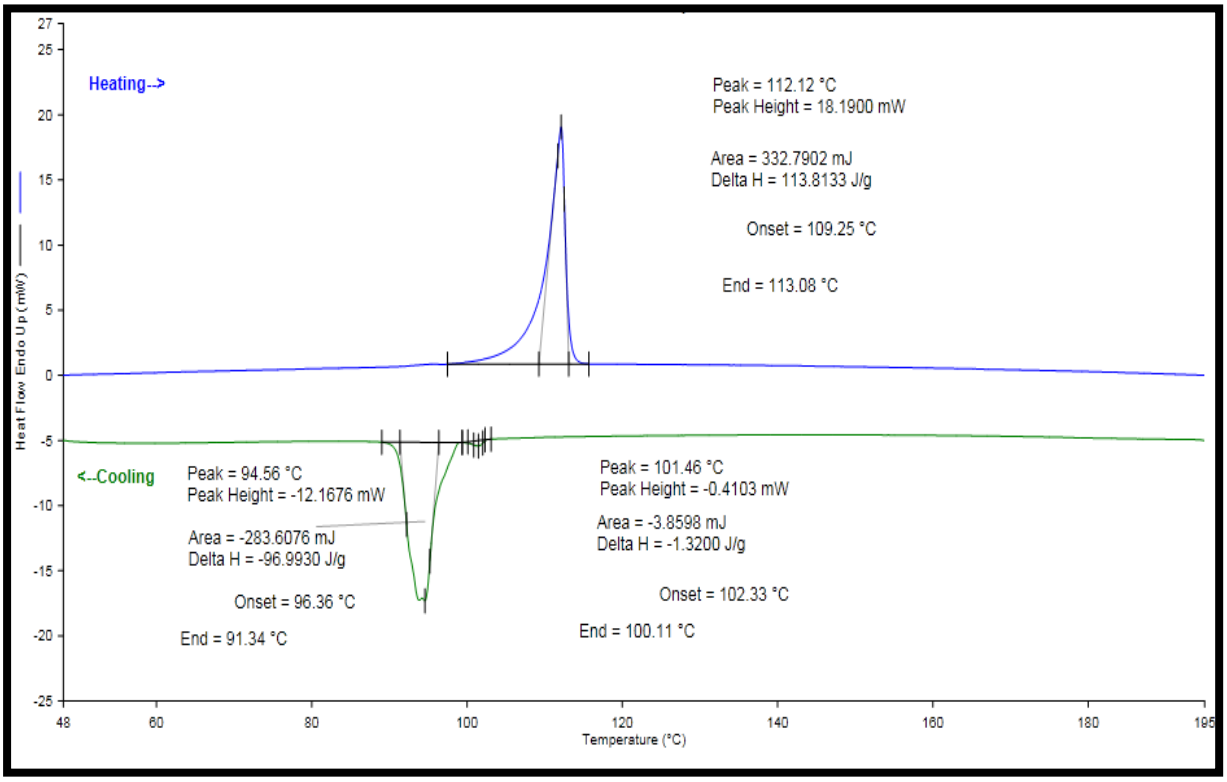

Figure 29. DSC thermograme of **F14**

Phase behavior diagram to understand the influence of molecular flexibility on the mesogenic behavior of the homologous series illustrated in **Figure 30**. In order to understand the effect of molecular flexibility on the monotropic nematic phase range, the temperature of °C is compared with the number of carbon atoms in the alkoxy chain in the cooling cycle, as shown in **Figure 31.** The figure illustrates that the F8 compound has the widest range of phases. As the number of carbon increases in the alkoxy chain, the phase range decreases and disappears in compound **F16**.

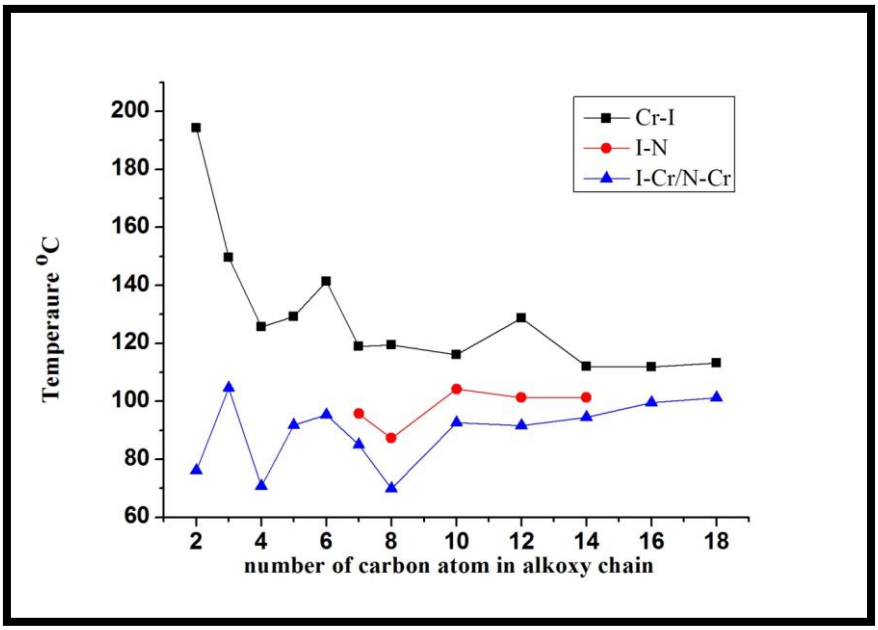

Figure 30. Dependence of transition temperatures on the increasing terminal alkoxy chain length

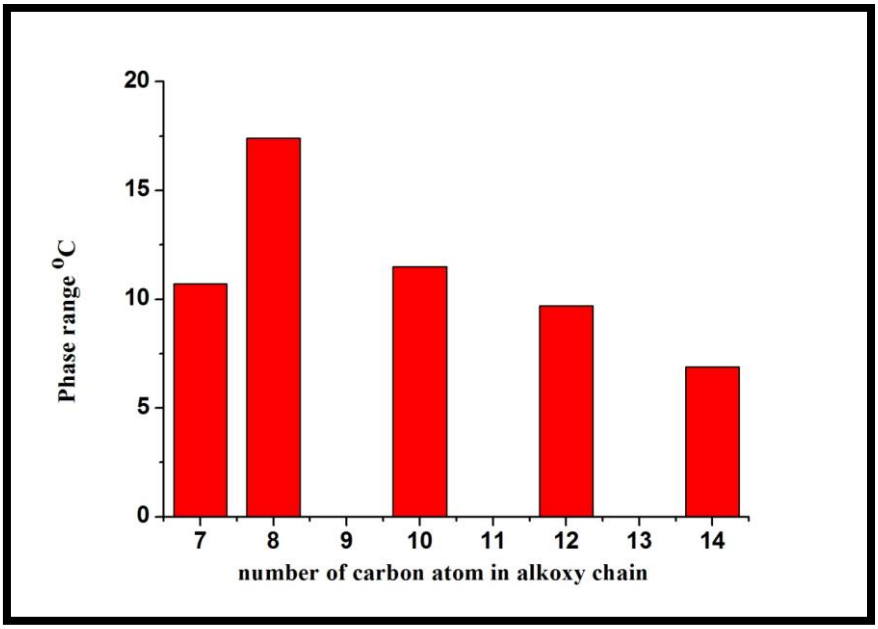

Figure 31. Temperature range of nematic phase on cooling

Single-crystal X-ray diffraction studies

A suitable single crystal of compound **F2** was selected, and X-ray intensity data were collected on a Bruker CCD area detector diffractometer with graphite-monochromatised MoKα radiation (λ = 0.71073 Å). The crystal was kept at 293 K during data collection. The structure was solved by direct methods through SHELXS-97 [44, 45]. All hydrogen-free atoms in the molecule have been located in the best difference map. Full-matrix least-squares refinement was carried out using SHELXL-97 [46, 47]. All hydrogen atoms were included as idealized atoms riding on the respective carbon atoms with C–H bond lengths appropriate to the carbon atom hybridization. Atomic scattering factors were taken from International Tables for X-ray Crystallography [48]. The crystallographic data of compound **F2** are summarized in **Table 3**. *ORTEP* view of the compound **F2** with displacement ellipsoids drawn at 40% probability level is given in **Figure 32**. The packing arrangement of molecules viewed down the b-axis is depicted in **Figure 33**. For clarity, the disordered components have been excluded during plotting.

Empirical formula	$C_{22}H_{19}NO_2S$
Formula weight	361.44
Temperature/K	293(2)
Crystal system	Monoclinic
Space group	$P2_1/c$
a/Å	19.343(4)
b/Å	5.8353(9)
c/Å	16.574(4)
α/°	90
β/°	98.78(2)
γ/°	90
Volume/$Å^3$	1848.8(7)
Z	4
ρcalcg/cm^3	1.299
μ/mm-1	0.191
F(000)	760.0
Crystal size/mm^3	0.3× 0.2× 0.2
Radiation	MoKα (λ = 0.71073)
Theta range for data collection/°	6.036 to 49.998
Index ranges	$-22 \leq h \leq 23$, $-6 \leq k \leq 6$, $-19 \leq l \leq 19$
Reflections collected	17826
Independent reflections	3233 [Rint = 0.1550, Rsigma = 0.1238]
Data/restraints/parameters	3233/391/302
Goodness-of-fit on F^2	1.003
Final R indexes [I>=2σ (I)]	R1 = 0.0782, wR2 =0.1170
Final R indexes [all data]	R1 = 0.2195, wR2 = 0.1639
Largest diff. peak/hole / e $Å^{-3}$	0.18/-0.15
CCDC number	2089178

Table 3. Crystal data and structure refinement of Compound **F2**

In the crystal structure of compound F2, the length of the N15-C16 bond is 1,270 (5) Å, which is expressed as an imine bond. The C8-O8 bond length is 1.220(5) Å, which is slightly shorter than the typical C-O double bond [49], and the double bond C6-C7 1.319(5) Å, confirming the formation of chalcone. The two benzene rings connected by the imine bond

are found to be not in the same plane. The dihedral angle of the C9-C10-C11-C12-C13-C14 benzene ring and the C17-C18-C19-C20-C21-C22 benzene ring is found 51.64 (2)°.

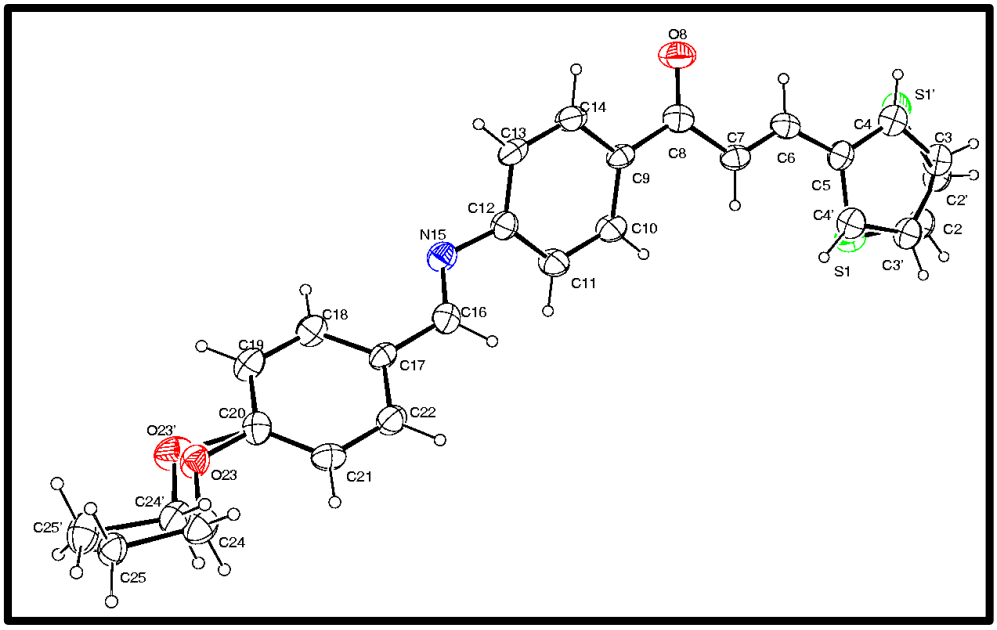

Figure 32. *ORTEP* view of the molecule with displacement ellipsoids drawn at 40% Probability level

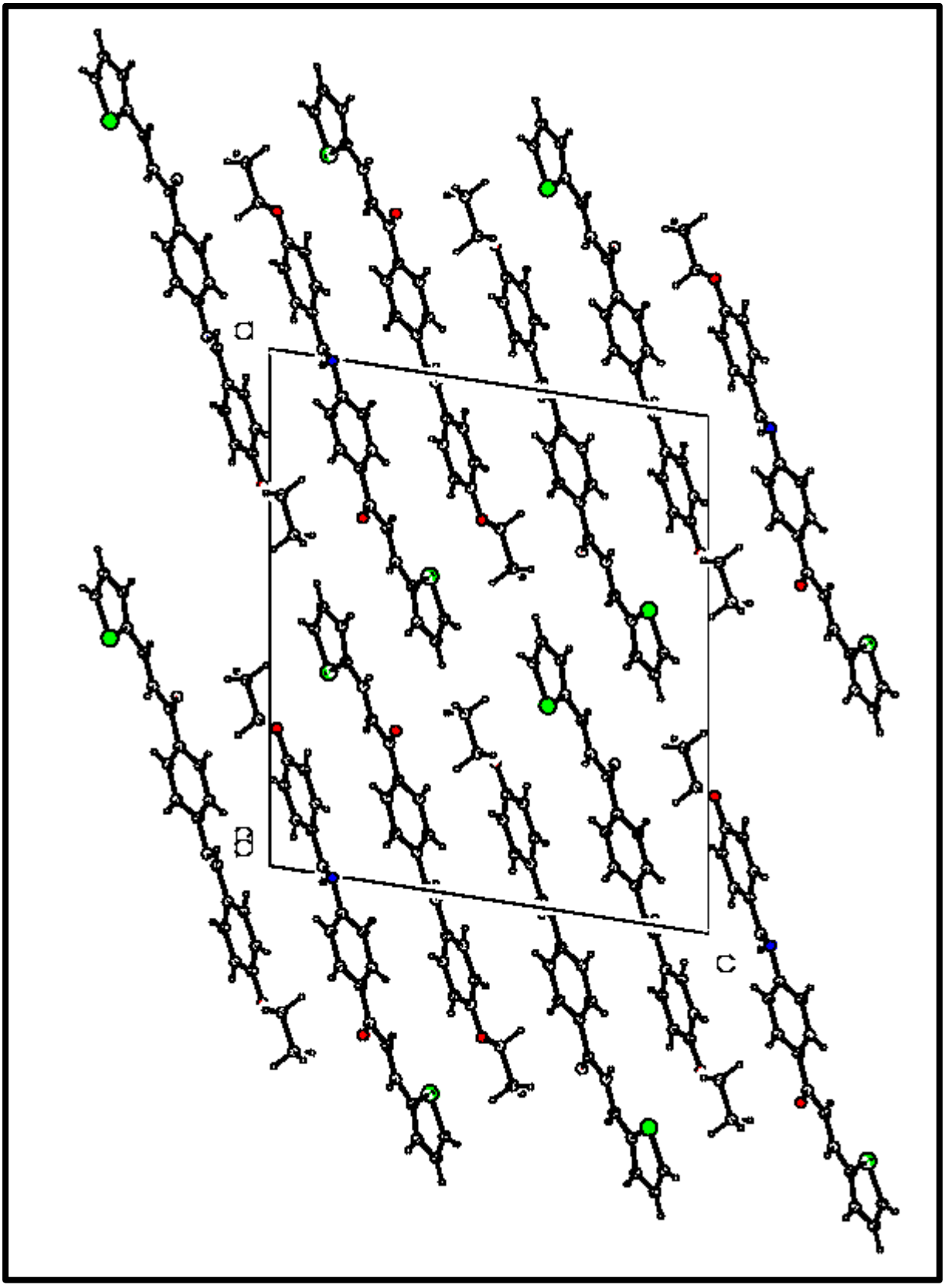

Figure 33. The packing arrangement of molecules viewed down the b-axis

4.5 Comparison of mesomorphic behavior of homologous series-E and series-F.

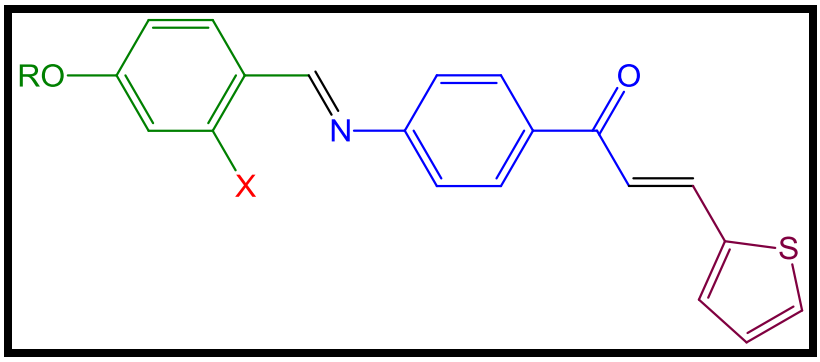

Series-E: X= OH and R= C_nH_{2n+1} n= 2 to 8, 10, 12, 14, 16, 18.

Series-F: X= H and R= C_nH_{2n+1} n= 2 to 8, 10, 12, 14, 16, 18.

Figure 34. Structure of series E and F

The similarity between the molecular structure of the series E, and series-F is that both series have the same linking groups imine and chalcone, both series have the same terminal groups thiophene and *n*-alkoxy group and both series have a common phenyl ring as the core unit **(Figure 34).** The difference is that series-F has a laterally unsubstituted phenyl ring as one of the core units, while series-E has a 2-hydroxy substituted phenyl ring as one of the core units.

The following points are observed by comparing the series E with the series F.

i) Series E exhibits nematic phase and smectic-A phase, while series F only shows the monotropic nematic phase.

ii) The phase thermal stability of the series E is higher than that of the series F

iii) Compared to Series F compounds, Series E compounds are thermally more stable. Series E compounds are thermally stable up to 300 ^{o}C, while Series F compounds are thermally stable up to 250 ^{o}C.

In the series F, one of the mesogenic cores is benzylideneaniline, but the series E contained 2-hydroxybilzylidenaniline, which has intramolecular hydrogen bonds, and hence the resulting compounds have higher mesophase stability. The presence of the lateral group in the phenyl ring of series E, increases the breadth of the molecule compared to a laterally unsubstituted molecule of series F. Lateral substituents are may also give rise to shielding effects due to intramolecular association. The intramolecular hydrogen bonding may increase the rigidity of the molecules, while significantly improving the chemical stability of the highly reactive unsubstituted Schiff's bases [50-61].

4.6 Comparison of mesomorphic behavior of homologous series-E and series-A.

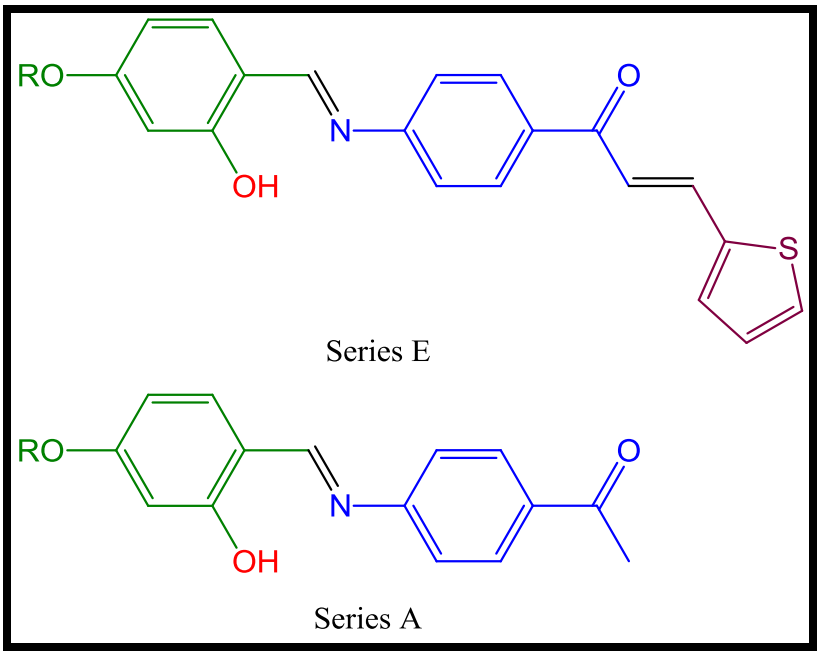

The difference between the molecular structure of Series E and Series A (chapter 2) are terminal groups **(Figure 35).** The comparison of these two series indicates the effect of the introduction of thiophene ring into the molecular structure of the series A.

The following points are observed by comparison of series E and A

i) Series E exhibits the nematic phase and the smectic-A phase, while series A shows only the smactic-A phase.

ii) An introduction of the thiophene ring at terminal end by chalcone linking group, makes the molecular structure conducive to the nematic phase.

iii) An introduction of the thiophene ring at terminal end by chalcone linking group in the molecular structure slightly decreases the smectic phase stability, and phase range.

4.7 Conclusion

Two homologous series of Schiff base derivatives of (E)-1-(4-aminophenyl)-3-(thiophen-2-yl)prop-2-en-1-one with 2-hydroxy-4-*n*-alkoxybenzaldehyde and 4-*n*-alkoxybenzaldehyde were prepared by varying the terminal alkoxy groups from n=2 to 8, 10, 12, 14, 16, 18. The compounds have been characterized by ^{1}H and ^{13}C–NMR, ESI-MS, and IR spectroscopy. Single crystal X-ray diffraction studies of compound (E)-1-(4-((E)-(4-ethoxybenzylidene) amino) phenyl)-3-(thiophen-2-yl) prop-2-en-1-one has been reported. A homologous series-F is nematogenic, while series-E is nematogenic and smectogenic. In series-E lower members **E7** to **E12** are nematogenic and higher members **E14** to **E18** are smectogenic. In series-F, the intermediate members **F7** to **F14** are mesomorphic while the remaining lower members **F2** to **F6** and upper members **F16**, **F18** of the series are non-mesogenic. The appearance of mesophase and the phase range depends on molecular flexibility. Intramolecular hydrogen bonding, significantly affects the mesomorphic behavior of studied homologous series.

4.8 References

[1] Wang H, Wang Y, Hu H, et al. Novel metallomesogens derived from heterocyclic benzoxazoles. Tetrahedron. 2008;64:4939–4948.

[2] Parra M, Vergara J, Alderete J, et al. Synthesis and mesomorphic properties of esters derived from Schiff's bases containing 1,3,4-thiadiazole. Liq. Cryst. 2004;31:1531–1537.

[3] Kaszyński P, Kapuściński S, Ciastek-Iskrzycka S. Chapter Four - Liquid crystalline derivatives of heterocyclic radicals. In: Scriven EF V, Ramsden CABT-A in HC, editors. Adv. Heterocycl. Chem. Academic Press; 2019. p. 263–331.

[4] Gallardo H, Favarin I. New mesogenic thiophene and furan derivatives. Liq. Cryst. 1993;13:115–125.

[5] Ha S-T, Koh T-M, Lin H-C, et al. Heterocyclic benzothiazole-based liquid crystals: synthesis and mesomorphic properties. Liq. Cryst. 2009;36:917–925.

[6] Chong YT, Muhamad Sarih N, Ha ST, et al. New homologues series of heterocyclic schiff base ester: synthesis and characterization. Adv. Phys. Chem. 2016;2016.

[7] Reddy MK, Reddy KS, Prakash M, et al. Synthesis and characterization of two phenyl ring core-based thiophene mesogens. Mol. Cryst. Liq. Cryst. 2013;582:1–14.

[8] Cai R, Samulski ET. New thermotropic liquid crystals derived from thiophenes. Liq. Cryst. 1991;9:617–634.

[9] Hariprasad S, Srinivasa HT. Symmetric 3 , 5-pyrazole and isoxazole heterocycles comprising a bent core unit : synthesis and mesomorphic characterisation. Liquid

Crystals .2015; 42(11): 1612-1620.

[10] Yeap G-Y, Mohammad A-T, Osman H. Synthesis, spectroscopic and mesomorphic studies on heterocyclic liquid crystals with 1,3-oxazepine-4,7-dione, 1,3-oxazepane-4,7-dione and 1,3-oxazepine-1,5-dione cores. J. Mol. Struct. 2010;982:33–44.

[11] Vicentini F, Barrouillet J, Laversanne R, et al. Side chain liquid crystalline polypyrrole Part I: synthesis and characterization. Liq. Cryst. 1995;19:235–240.

[12] Langley PJ, Davis FJ, Mitchell GR. Synthetic routes to polypyrroles with pendant mesogenic groups. Mol. Cryst. Liq. Cryst. Sci. Technol. Sect. A. Mol. Cryst. Liq. Cryst. 1993;236:225–230.

[13] Langley PJ, Davis FJ, Mitchell R. Synthesis , phase behaviour and polymerisation of mesogenic materials based on 3-substituted pyrroles. Journal of the Chemical Society, Perkin Transactions 2.1997;2229–2239.

[14] Karamysheva LA, Kovshev EI, Pavluchenko AI et.al. New heterocyclic liquid crystalline compounds. Mol. Cryst. Liq. Cryst. 1981 ; 67:241-251.

[15] Nash JA, Gray GW. Studies of some heterocyclic mesogens Mol. Cryst. Liq. Cryst.1974; 25: 299.

[16] Koßmehl G, Budwill D. Liquid crystalline compounds in the thiophene series 1, liquid crystalline thiophene carboxylic esters. Z. Naturforsch.1983; 38b: 1669-1677.

[17] Koßmehl G, Budwill D. Liquid crystalline compounds in the thiophene series 2, liquid crystalline azomethines, azines and vinylenes. Z. Naturforsch.1985; 40b: 1199—1213.

[18] Koßmehl G, Budwill D. Liquid crystalline compounds in the thiophene series- 3, azomethines and vinylenes. Z. N aturforsch.1986: 41b: 751-761.

[19] Koßmehl G, Budwill D. Liquid crystalline compounds in the thiophene series-4, azomethines and vinylenes with central azobenzene, stilbene and 1, 2-di(2-thienyl)ethylene moieties. Z. Naturforsch. 1987; 42b: 478-488.

[20] Narasimhaswamy T, Somanathan N, Lee DK, et al. Synthesis and ^{13}C CPMAS NMR characterization of novel thiophene-based nematogens. Chem. Mater. 2005;17:2013–2018.

[21] Thaker BT, Patel BS, Dhimmar YT, et al. Synthesis, characterization and mesomorphic properties of new rod-like thiophene based liquid crystals. Mol. Cryst. Liq. Cryst. 2012;562:98–113.

[22] Reddy MK, Reddy KS, Kumar BVNP, et al. Synthesis, structural and mesophase characterization of three ring based thiophene liquid crystals. Mol. Cryst. Liq. Cryst. 2014;593:1–24.

[23] Foo K-L, Ha S-T, Yeap GY, et al. Mesomorphic behaviors of a series of heterocyclic thiophene-imine-ester-based liquid crystals. Phase Transitions 2018;91:509–520.

[24] Nafee SS, Ahmed HA, Hagar M. Theoretical, experimental and optical study of new thiophene-based liquid crystals and their positional isomers. Liq. Cryst. 2020;1–12.

[25] Chudgar NK, Shah SN. New fluorescent mesogens with a chalcone central linkage. Liq. Cryst. 1989;4:661–668.

[26] Chaudhari RP, Chauhan ML, Doshi A V. Synthesis and mesogenic behavior of novel liquid crystals with a –CH=CH–CO– central bridge. Mol. Cryst. Liq. Cryst. 2013;575:88–95.

[27] Chaudhari RP, Doshi AA, Doshi A V. A Study of liquid crystalline properties and

their relation to the molecular structure of novel ethylene derivatives. Mol. Cryst. Liq. Cryst. 2013;582:63–71.

[28] Chauhan HN, Doshi A V. The Synthesis and mesomorphic properties of a novel homologous series: α-4-[4′-n-alkoxy benzoyloxy] benzoyl -β-2″-nitro phenyl ethylenes. Mol. Cryst. Liq. Cryst. 2013;570:92–100.

[29] Chauhan HN, Doshi A V. A Novel homologous series of thermotropic mesogens of ethylene derivatives: α-4-[4′-n-alkoxy benzoyloxy] phenyl β-4″methoxy benzoyl ethylenes. Mol. Cryst. Liq. Cryst. 2013;570:12–19.

[30] Chauhan HN, Patel VR, Doshi A V. Synthesis and evaluation of a novel homologous series of carbonylethylene-linked liquid crystals. Mol. Cryst. Liq. Cryst. 2013;574:67–74.

[31] Kotadiya VC, Bhoya UC. The mesomorphic properties of chalcone dimer derivatives. Mol. Cryst. Liq. Cryst. 2015;608:116–124.

[32] Coelho RL, Westphal E, Mezalira DZ, et al. Polycatenar liquid crystals based on bent-shaped chalcone and cyanopyridine molecules. Liq. Cryst. 2017;44:405–416.

[33] Durgapal SD, Soni R, Soman SS, et al. Synthesis and mesomorphic properties of coumarin derivatives with chalcone and imine linkages. J. Mol. Liq. 2020;297:111920.

[34] Patel KN, Prajapati AK, Kamath B V, et al. Synthesis and study of mesomorphic properties of unsymmetrical cyclohexanone-derived bis-chalcones. Liq. Cryst. 2016;43:729–734.

[35] Rakhasia PK, Bhola GN, Bhoya UC. Mesomorphism dependence of chalconyl derivatives on position of -CH=CH- unit. Mol. Cryst. Liq. Cryst. 2016;626:81–89.

[36] Maheta RH, Bhoya UC. Mesomorphic dependence on molecular rigidity by central bridge and homo–hetero ring systems. Mol. Cryst. Liq. Cryst. 2016;625:72–80.

[37] Tomma JH, Khazaal MS, Al-Dujaili AH. Synthesis and characterization of novel Schiff bases containing pyrimidine unit. Arab. J. Chem. 2014;7:157–163.

[38] C.Weygard and R.Gabler, J. Prakt Chem.1940;155:332.

[39] Gray GW, Jones B. Mesomorphism and chemical constitution. Part II. The trans-p-n-alkoxycinnamic acids. J. Chem. Soc. 1954;1467–1470.

[40] Collings, P.J., Hird M (1997). Introduction to Liquid Crystals: Chemistry and Physics. 1st ed. CRC Press, London.

[41] Nakum KJ, Katariya KD, Jadeja RN, et al. Schiff base of 4-n-alkoxy-2-hydroxy benzaldehyde with 4-amino acetophenone and their Cu (II) complexes : synthesis , characterization and mesomorphic behavior. Mol. Cryst. Liq. Cryst. 2019;690:1–13.

[42] Ahmed HA, Naoum MM, Saad GR. Effect of alkoxy-chain length proportionation on the mesophase behaviour of terminally di-substituted phenylazo phenyl benzoates. Liq. Cryst. 2013;40:914–921.

[43] Chandrasekhar S (1992). Statistical theories of nematic order. In Liquid Crystals (pp. 17-84). Cambridge: Cambridge University Press.

[44] G. M. Sheldrick, SHELXS-97. Quantitative Phase Analysis Based on Rietveld Structure Refinement for Carbonate Rocks. Progr. Solut. Cryst. Struct. Univ. Göttingen, Göttingen. 1997.

[45] Sheldrick GM. Phase annealing in SHELX-90: direct methods for larger structures. Acta Crystallogr. Sect. A 1990;46:467–473.

[46] G. M. Sheldrick S-97. Quantitative phase analysis based on rietveld structure refinement for carbonate rocks. Progr. Refinement Cryst. Struct. Univ. Göttingen, Göttingen ,. 1997

[47] Sheldrick GM. A short history of {\it SHELX}. Acta Crystallogr. Sect. A 2008;64:112–122.

[48] E. Prince (Ed.), International Tables for Crystallography, Vol. C, Kluver, Dordrecht 2004, Tables 4.2.6.8 and 6.1.1.4.

[49] Kumar B, Nakum KJ, Jadeja RN, et al. Crystal structure of [1-(3-chlorophenyl)- 5-hydroxy-3-methyl-1H-pyrazol-4-yl](p-tolyl) methanone. Acta Crystallogr. Sect. E Struct. Reports Online. 2015;71:o280–o281.

[50] Dixit S, Vora RA. Azomesogens having a lateral hydroxy substituent. Mol. Cryst. Liq. Cryst. 2009;501:43–52.

[51] Tian Y, Xu X, Zhao Y, et al. Synthesis of some chiral liquid crystals and study of the effect of intramolecular hydrogen bonding on the phase behaviour. Liq. Cryst. 1995;19:295–300.

[52] Yeap GY, Hng TC, Mahmood WAK, et al. Smectogenic properties of N, N′-bis[(2-hydroxy-4-alkoxyphenyl) methylene]benzene-1,4-diamine liquid crystals with double lateral H-bonds. Liq. Cryst. 2006;33:979–986.

[53] Vora RA, Gupta R. A mesogenic homologous series containing a phenolic end group. Mol. Cryst. Liq. Cryst. 1979; 56: 31-34

[54] Vora RA, Gupta R. In Liquid Crystals:Chandrashekhar S.(Ed),Heyden Verlag.1980;p 589-584.

[55] Berdagué P, Bayle JP, Ho MS et.al. New laterally aromatic branched liquid crystal materials with large nematic ranges. Liq. Cryst. 1993;14:667–674.

[56] Perez F, Berdagué P, Bayle JP et.al. Change of the lateral chain conformation in the solid and the nematic phase in laterally substituted nematogens. Liq. Cryst. 1993;14:667–674.

[57] Bayle JP, Perez F, Judeinstein P. New J Chem.1995;19:1015-1017.

[58] Prajapati AK, Vora RA, Pandya HM. Effect of lateral hydroxy/alkoxy group on mesomorphism of azobenzene derivatives. Mol. Cryst. Liq. Cryst. 2001, 369, 37–46.

[59] Vora RA.; Prajapati AK.; Kevat J.et.al. Mesogenic properties and the effect of 1,2,4-trisubstitution on the central benzene nucleus of a three-ring mesogen Liq. Cryst. 2001; 28: 983–989

[60] Prajapati AK, Varia MC. Azomesogens with polar chloro, nitro and phenolic –OH substituents, Liq. Cryst. 2008;35:1271-1277.

[61] Vander Veen J, Hegge TCJM. Low melting liquid crystalline *o*-hydroxy azo- and azoxybeuzenes. Angew Chem Int. Ed. 1974;13:344.

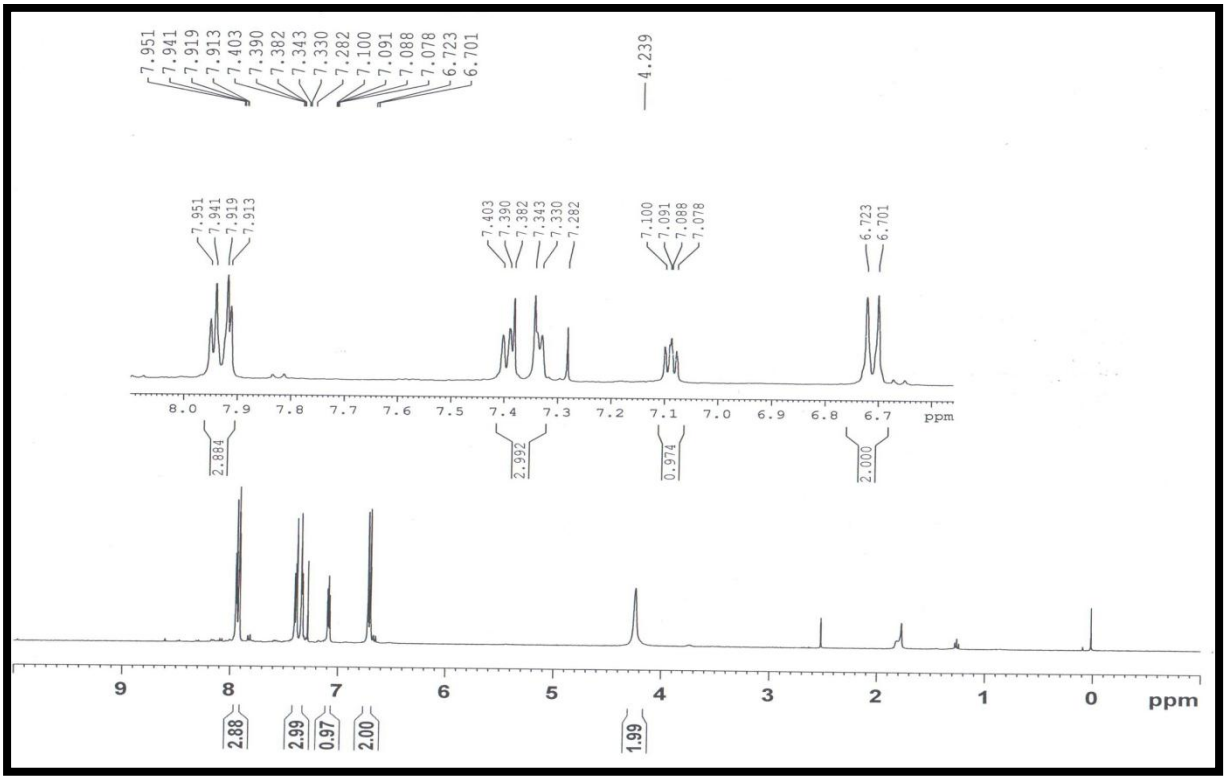

^{1}H-NMR of (E)-1-(4-aminophenyl)-3-(thiophen-2-yl)prop-2-en-1-one.

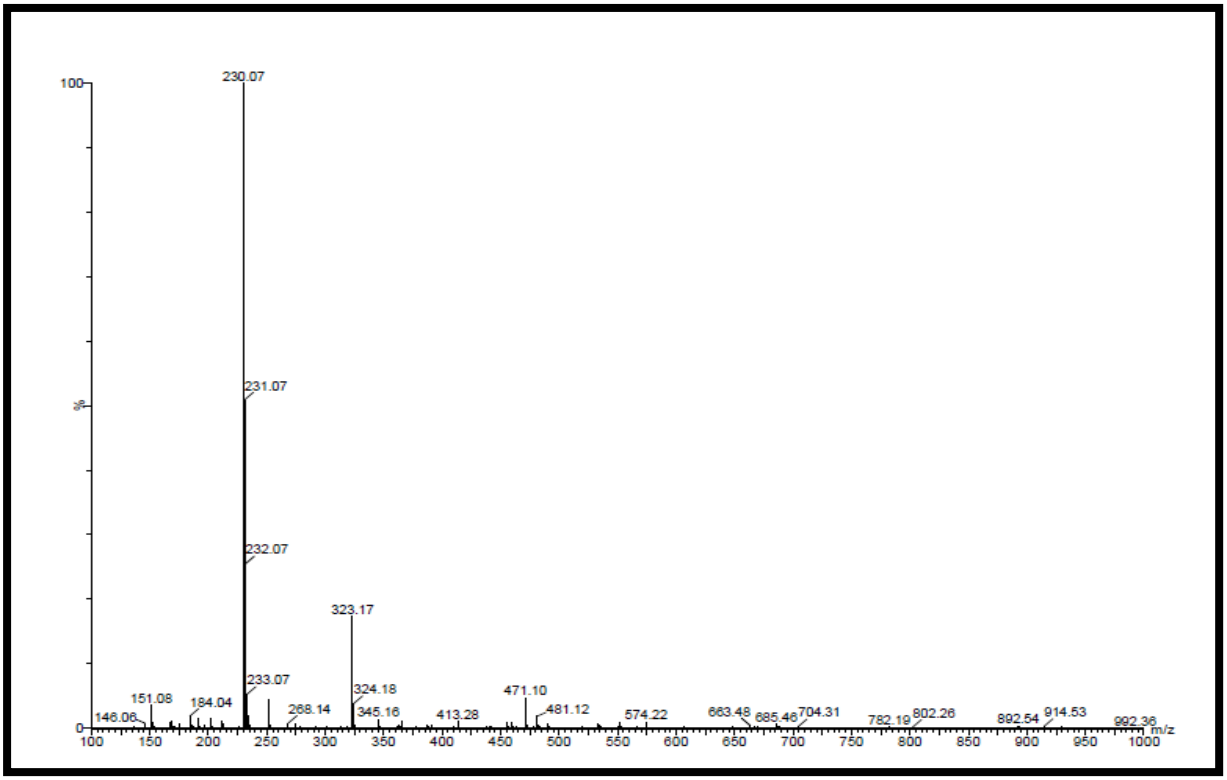

ESI-MS of (E)-1-(4-aminophenyl)-3-(thiophen-2-yl)prop-2-en-1-one.

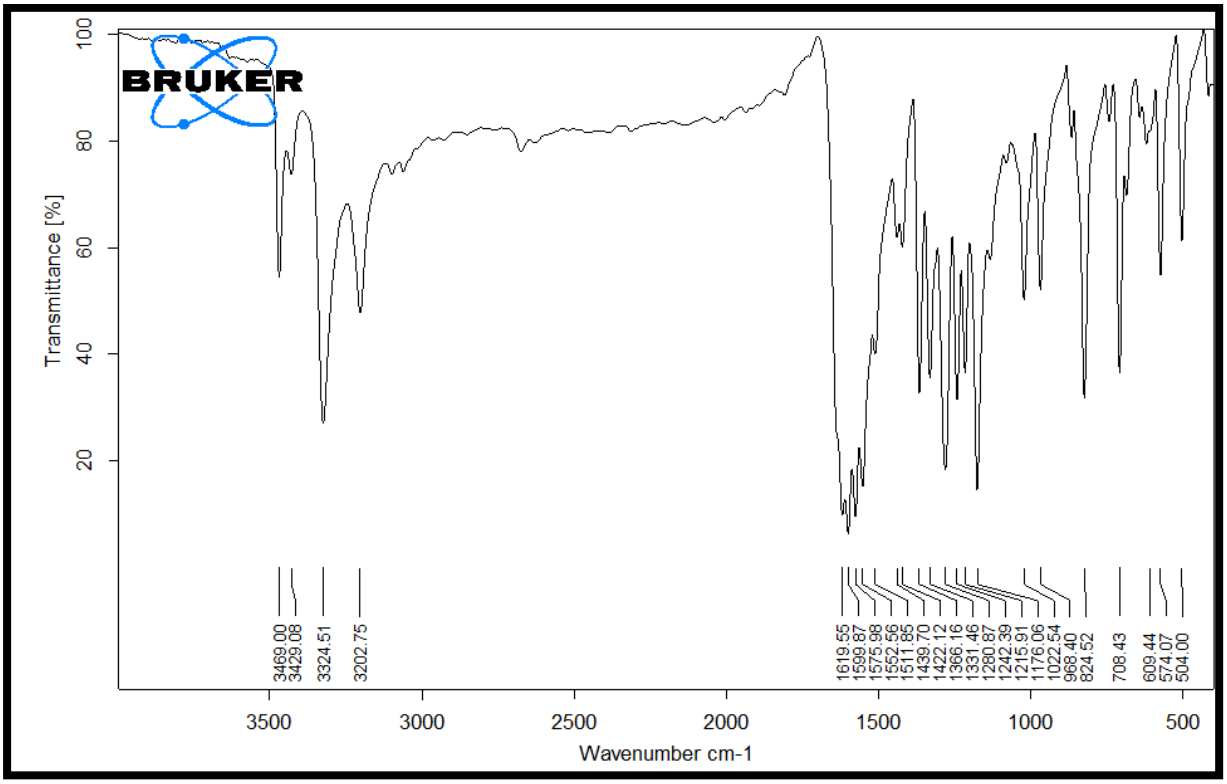

IR of (E)-1-(4-aminophenyl)-3-(thiophen-2-yl)prop-2-en-1-one.

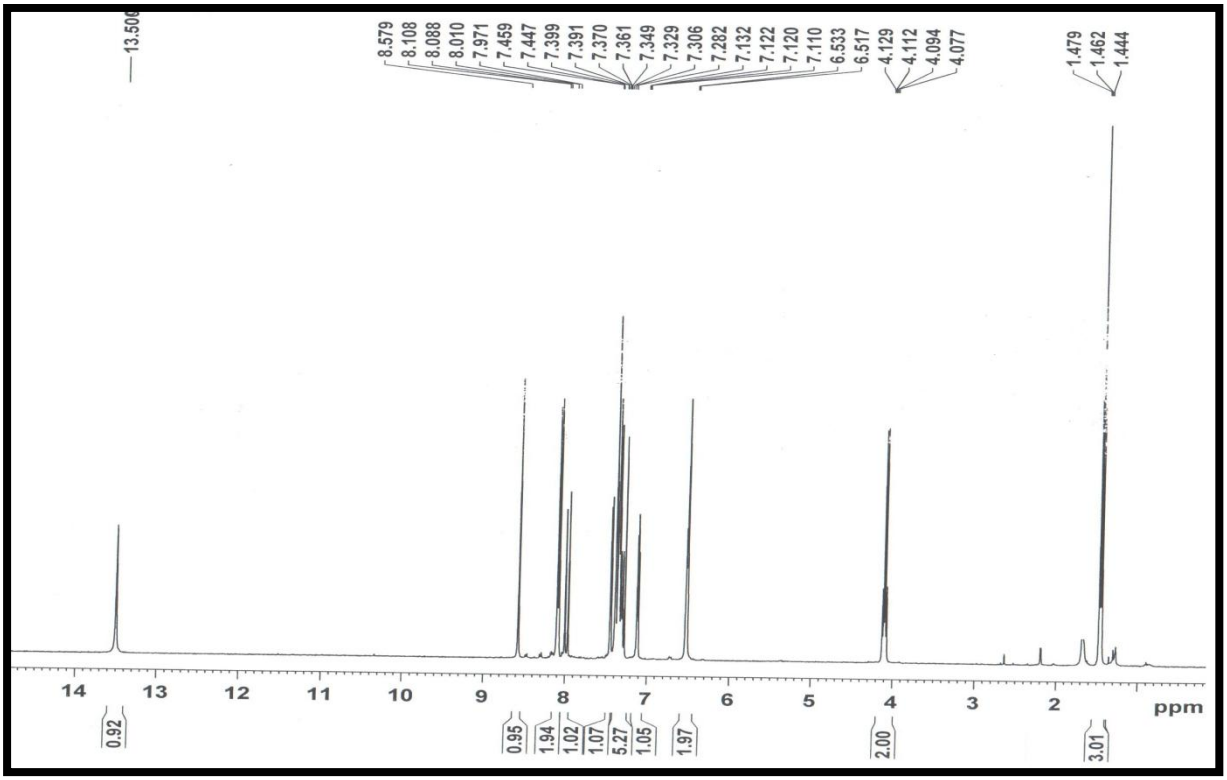

^{1}H-NMR of E2

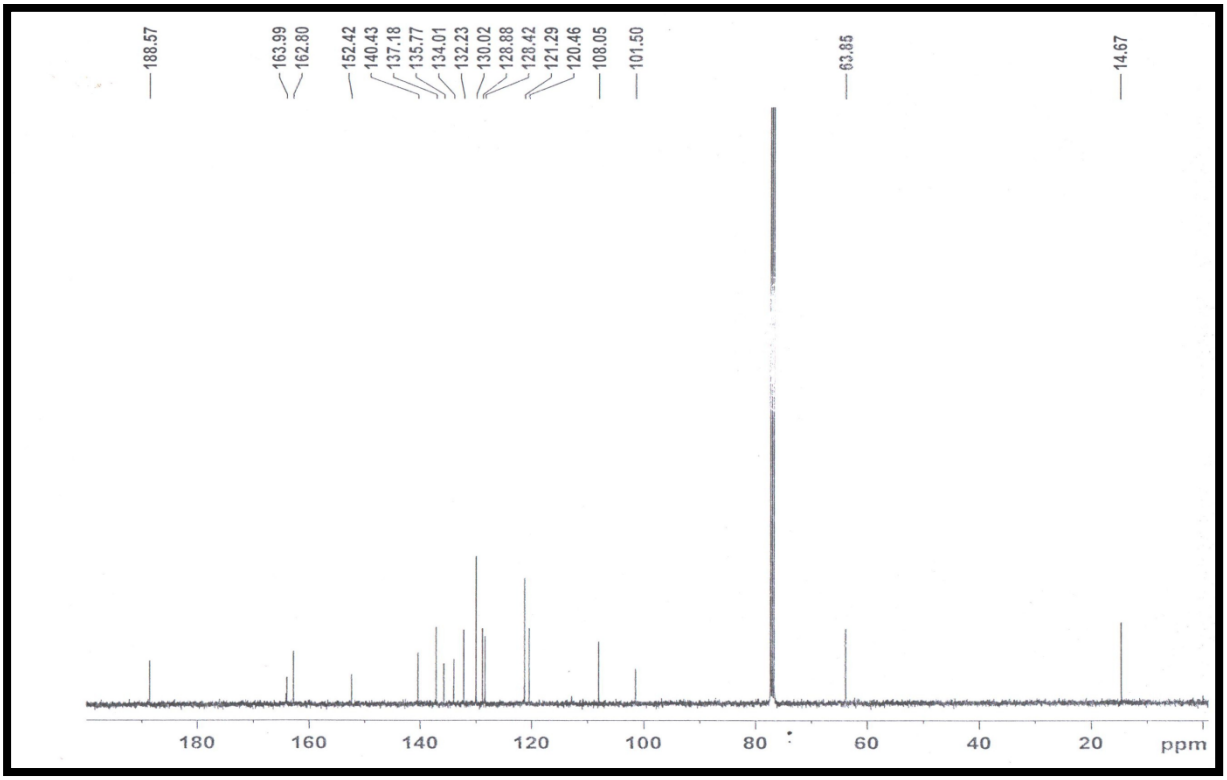

^{13}C-NMR of E2

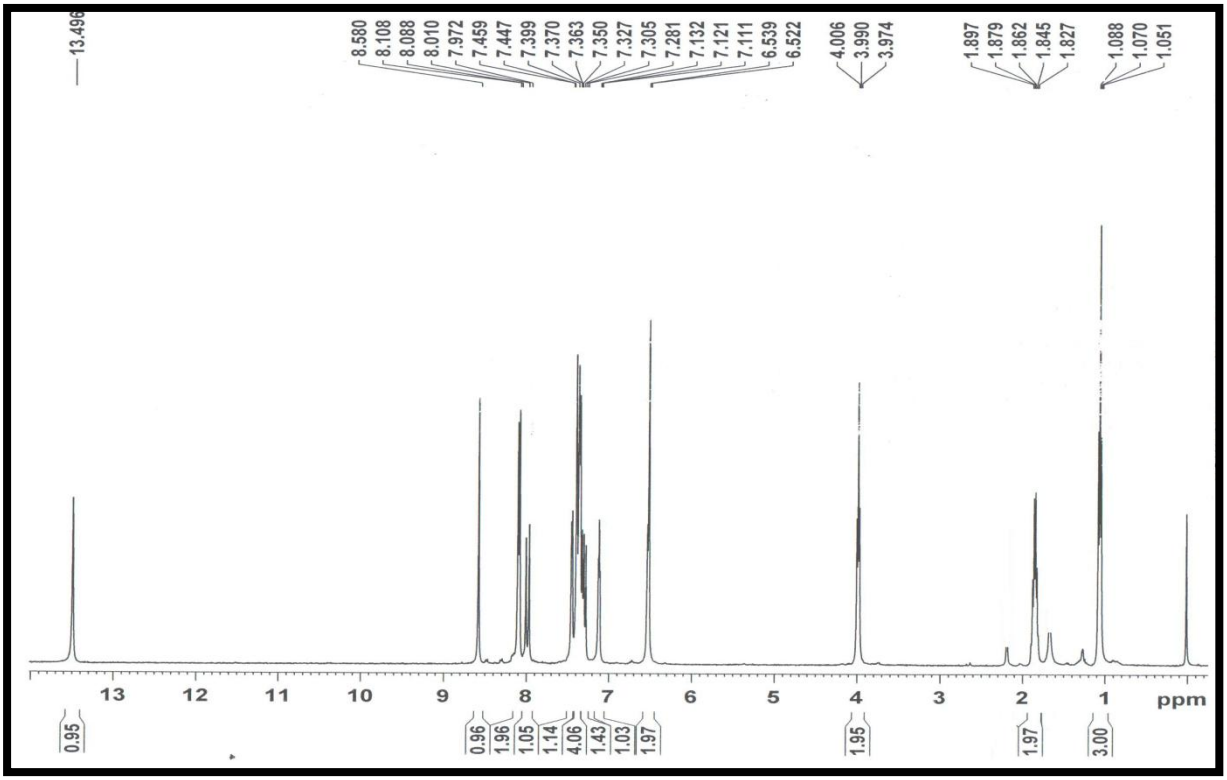

^{1}H-NMR of E3

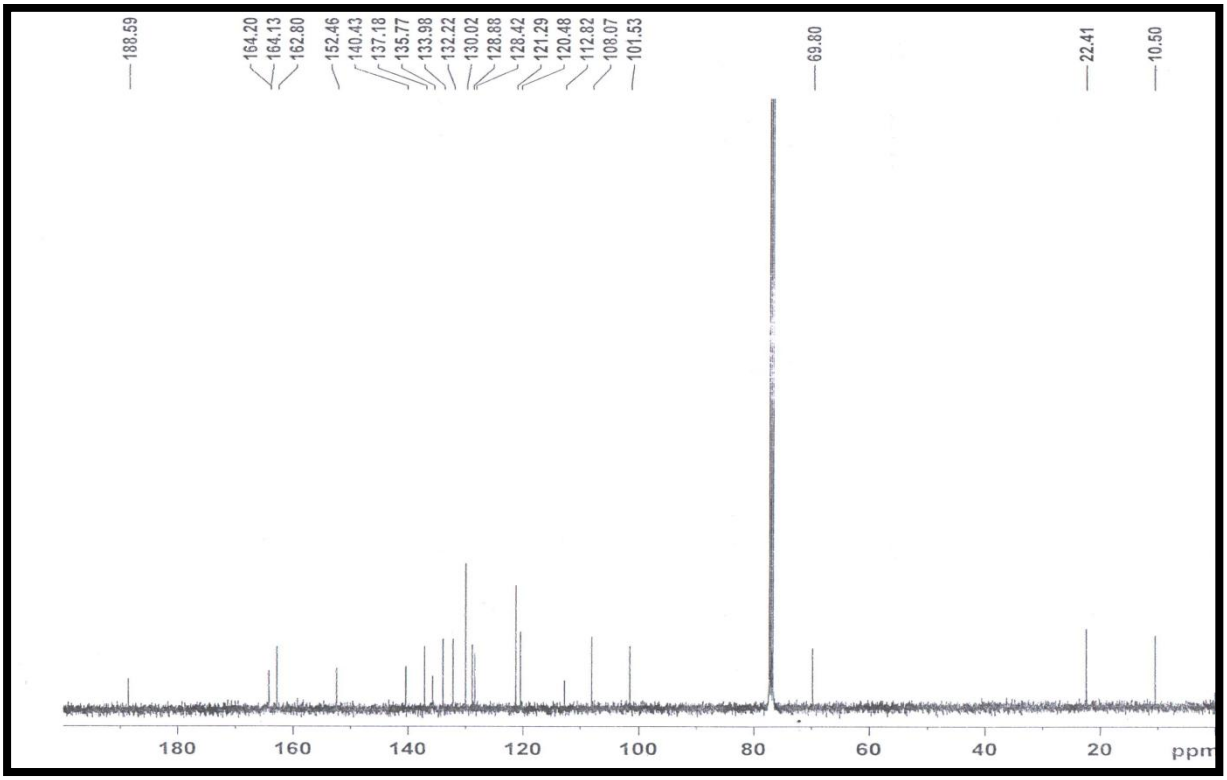

^{13}C-NMR of E3

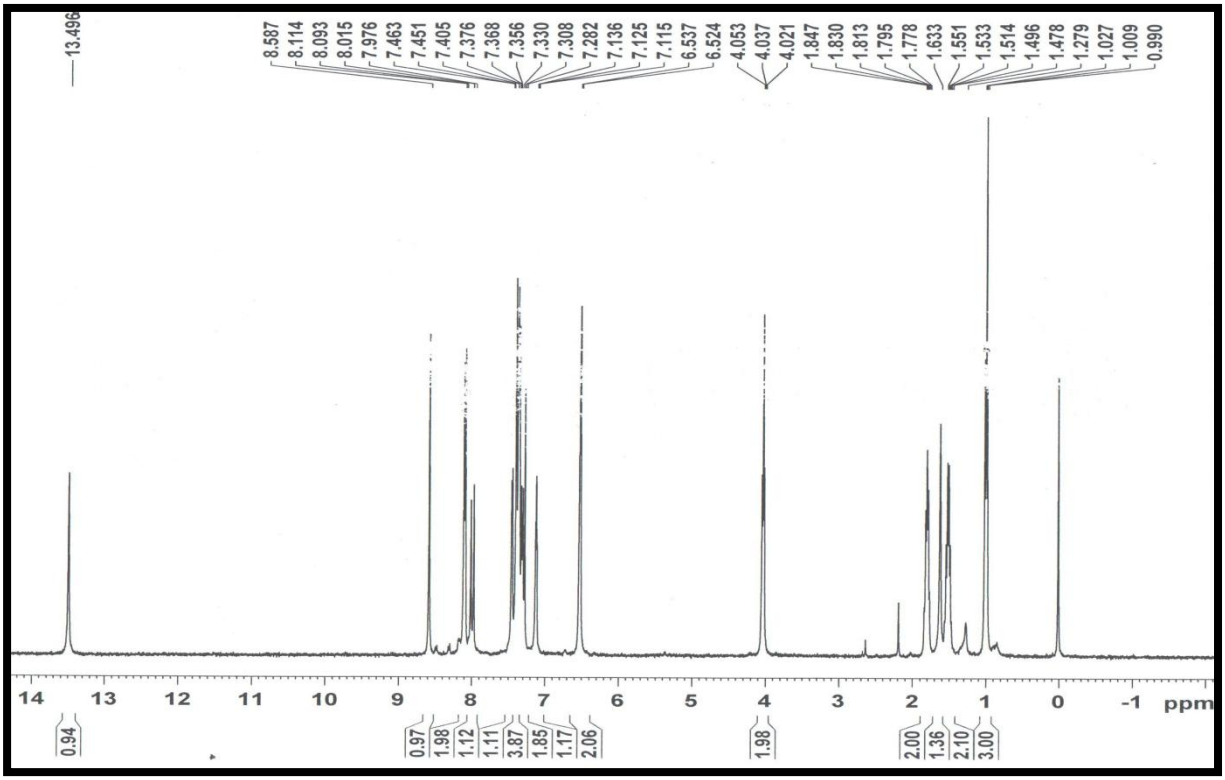

^{1}H-NMR of E4

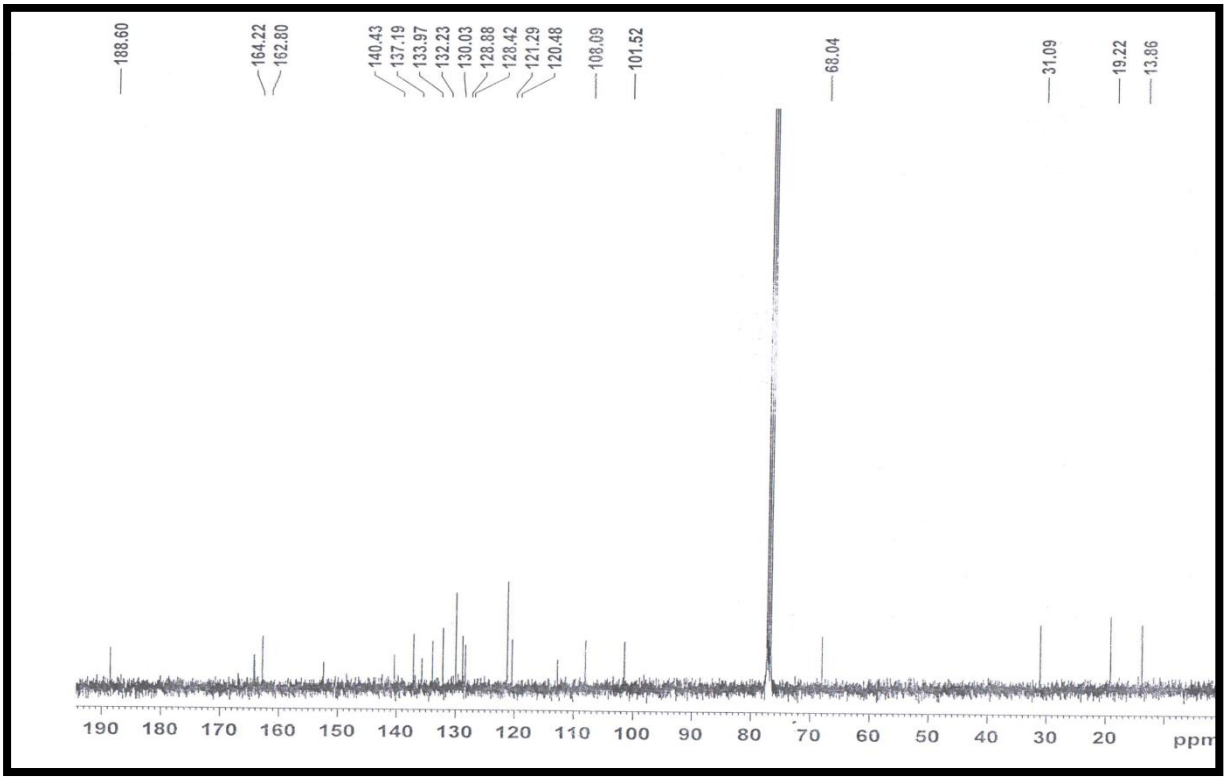

^{13}C-NMR of E4

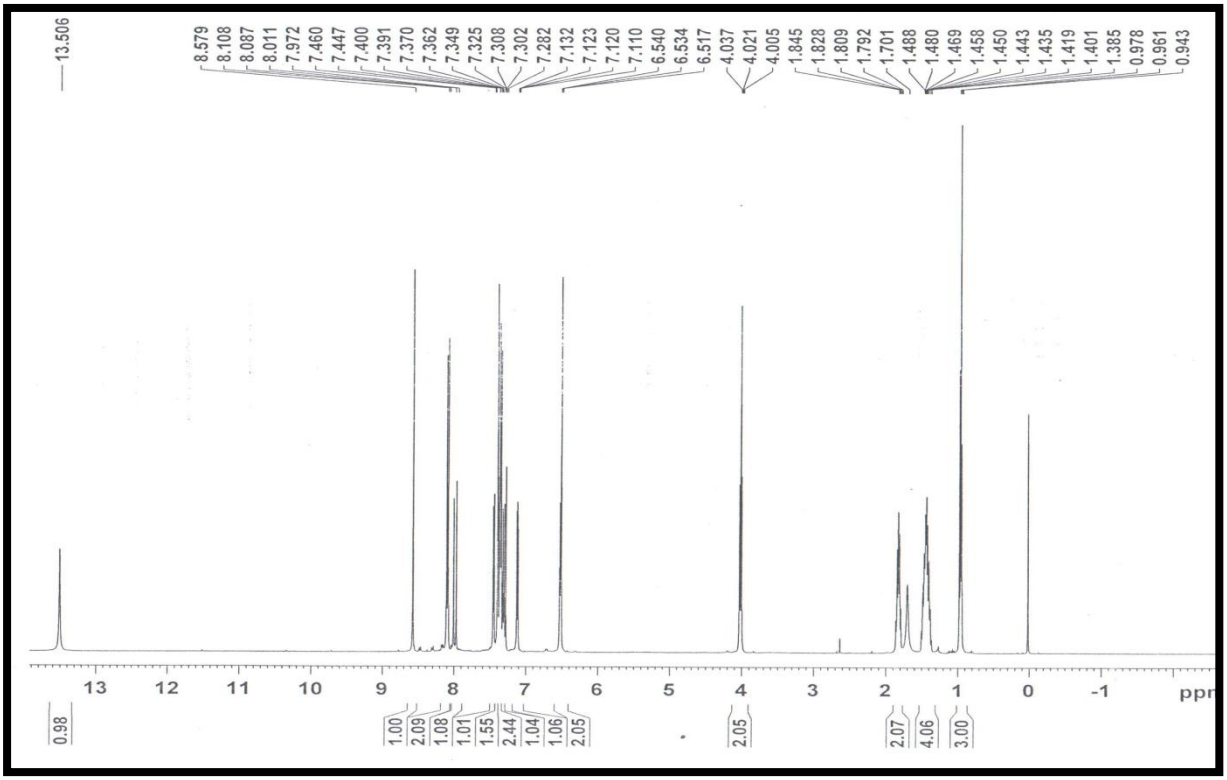

^{1}H-NMR of E5

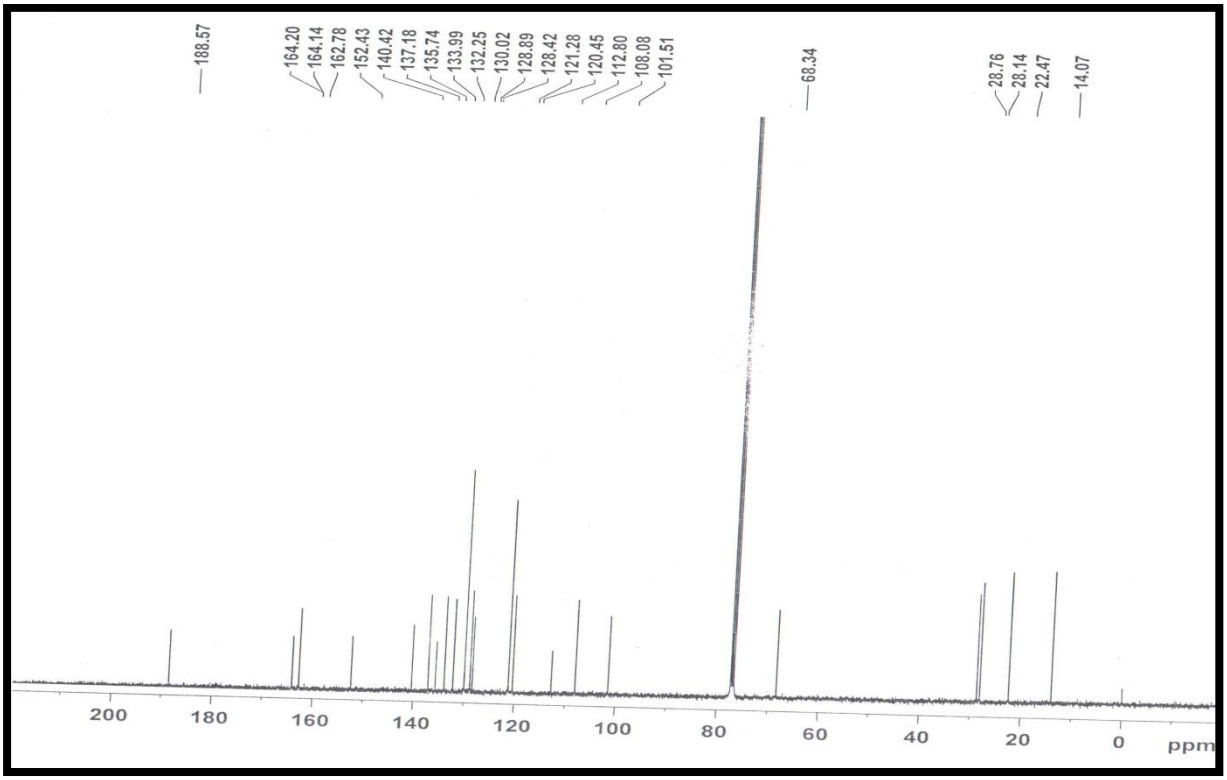

^{13}C-NMR of E5

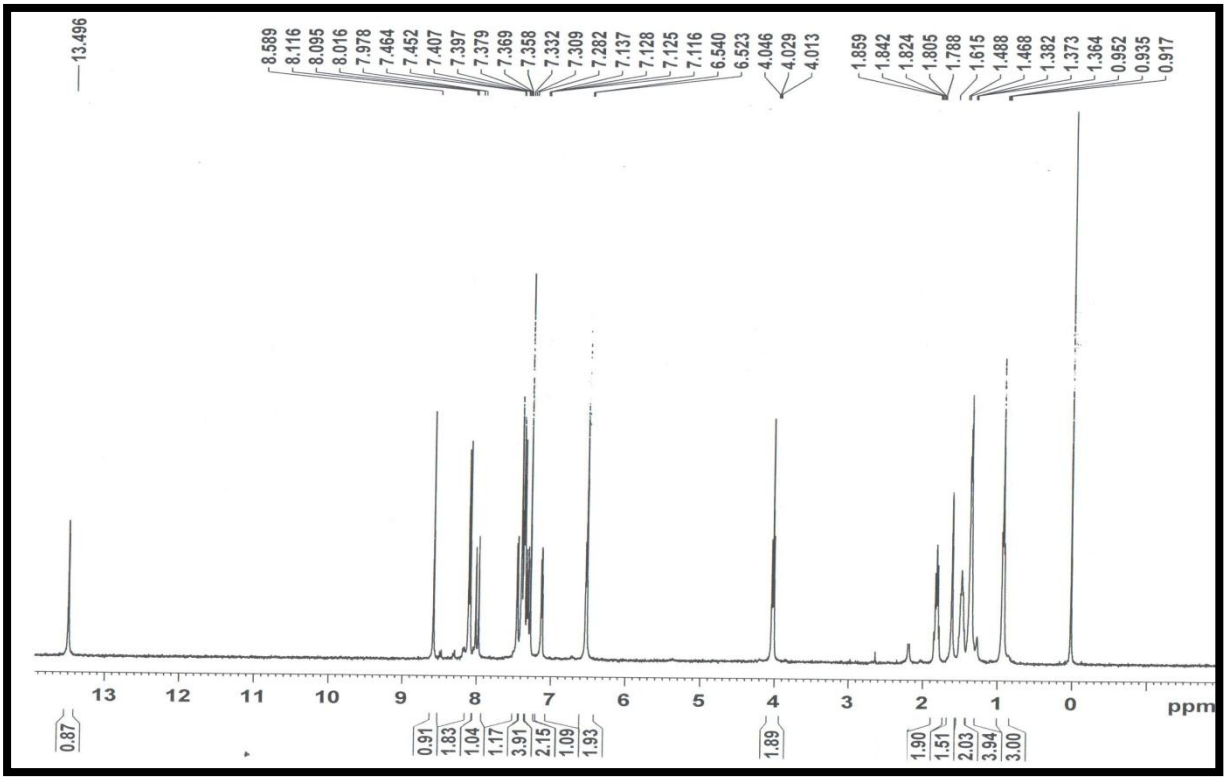

^{1}H-NMR of E6

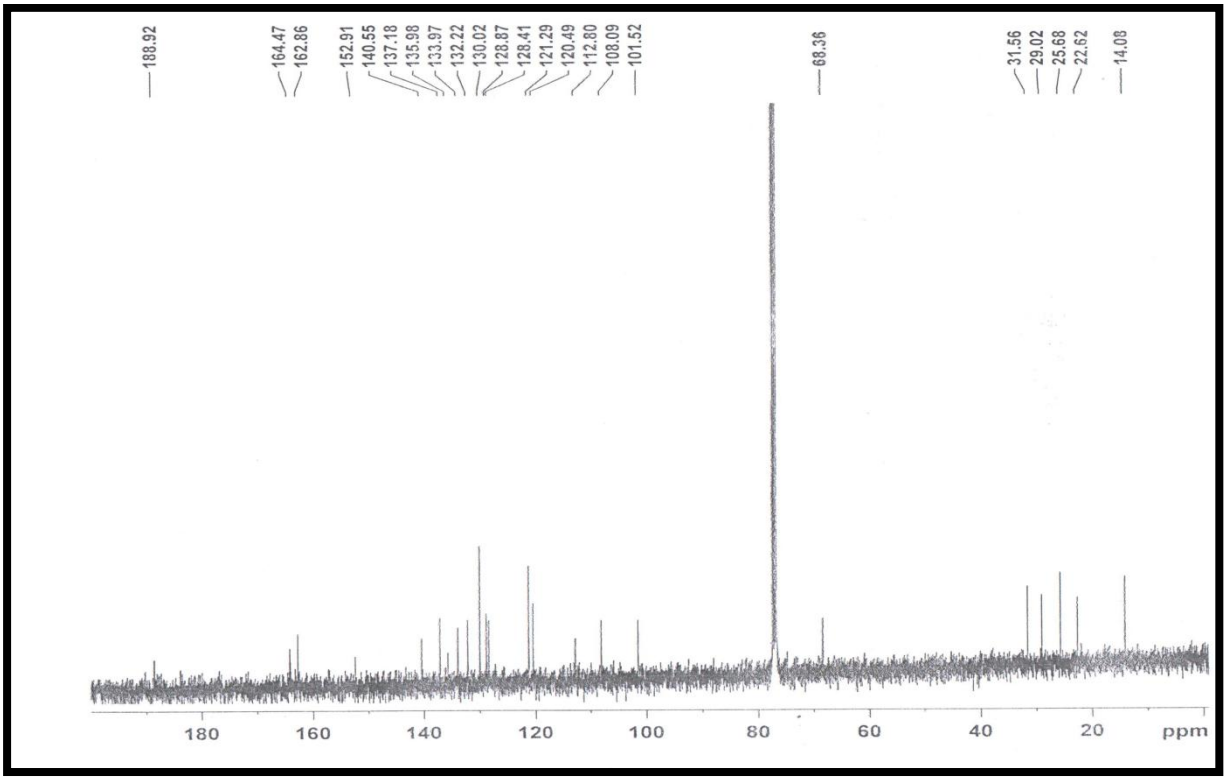

^{13}C-NMR of E6

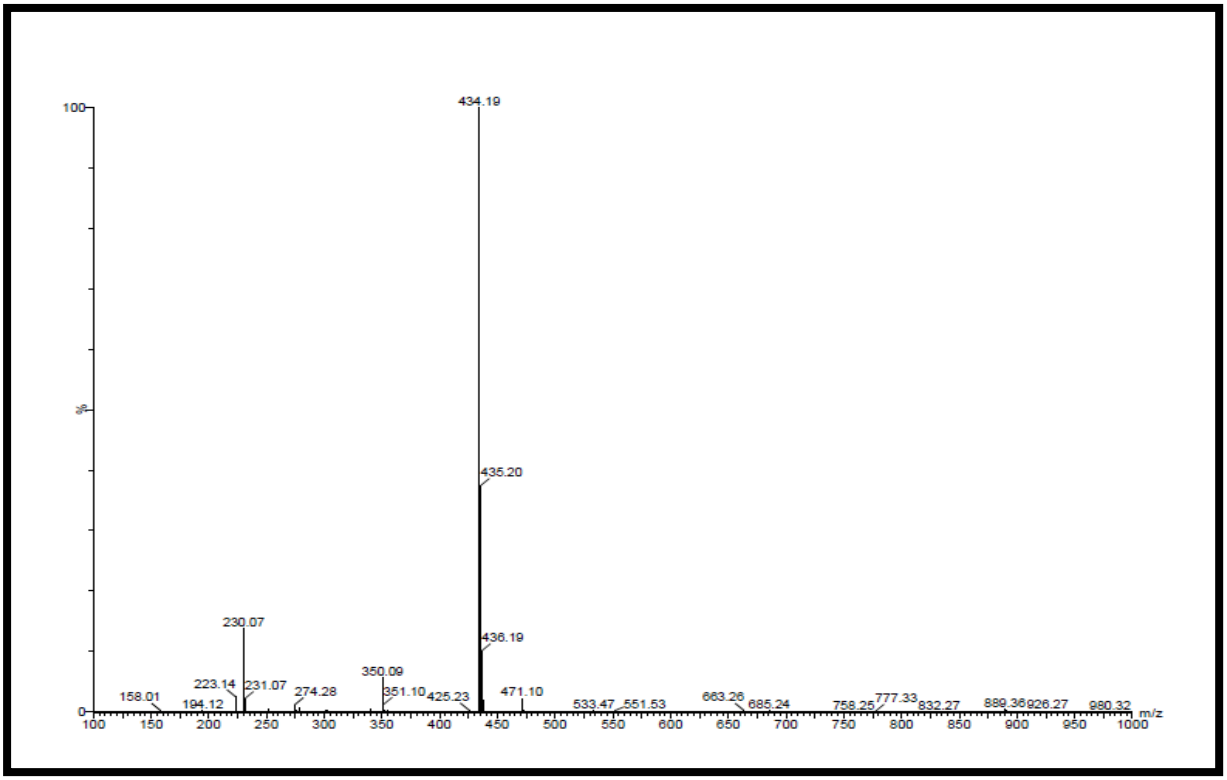

ESI-MS of E6

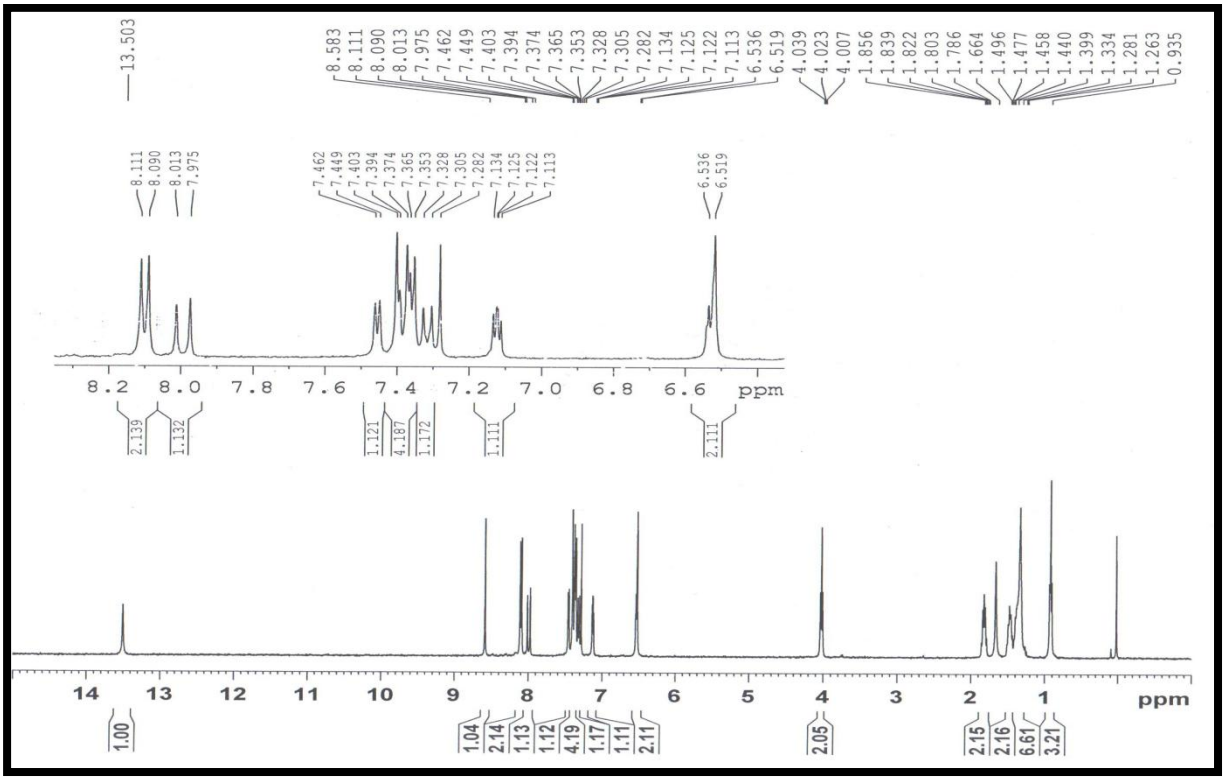

^{1}H-NMR of E7

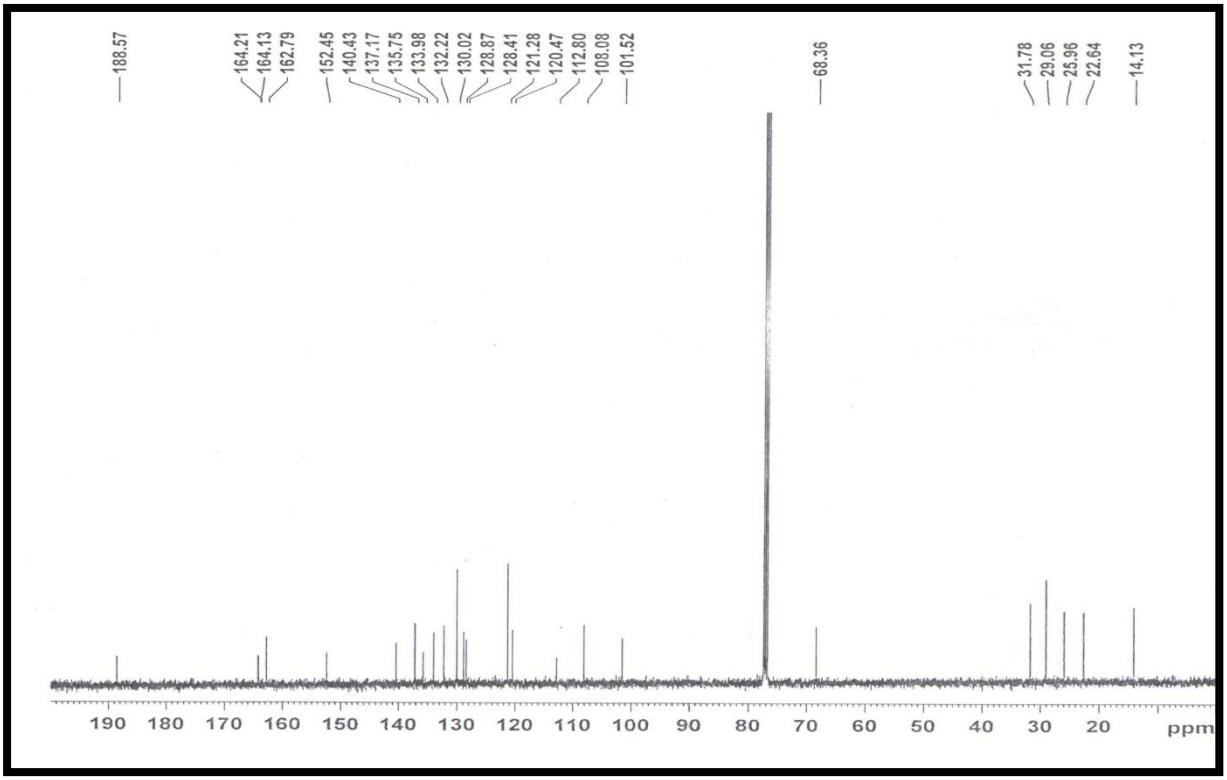

^{13}C-NMR of E7

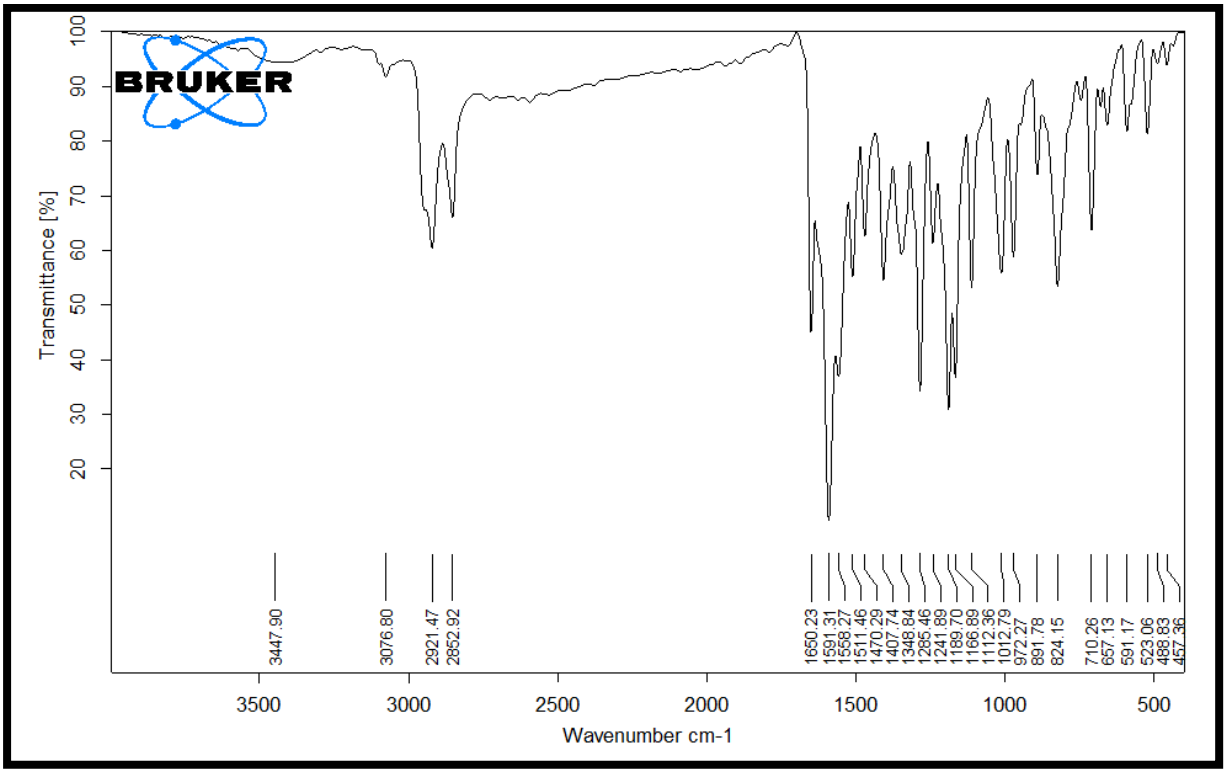

IR of E7

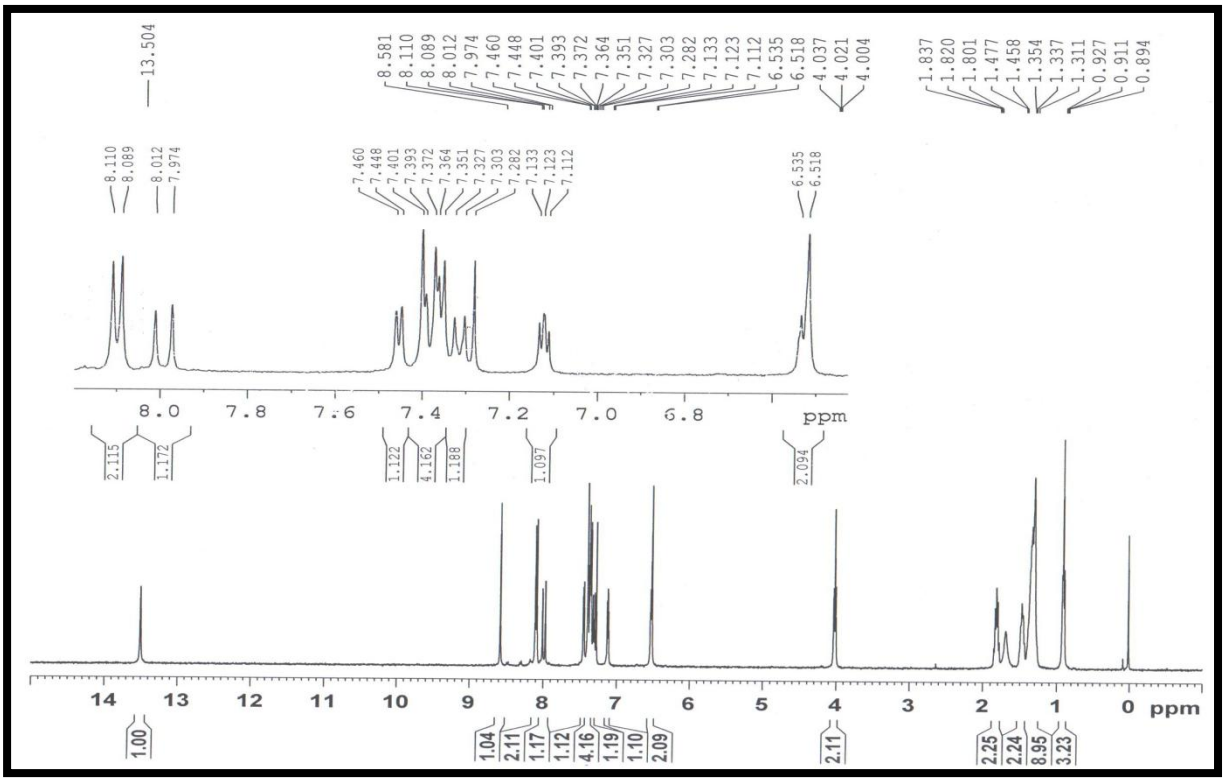

^{1}H-NMR of E8

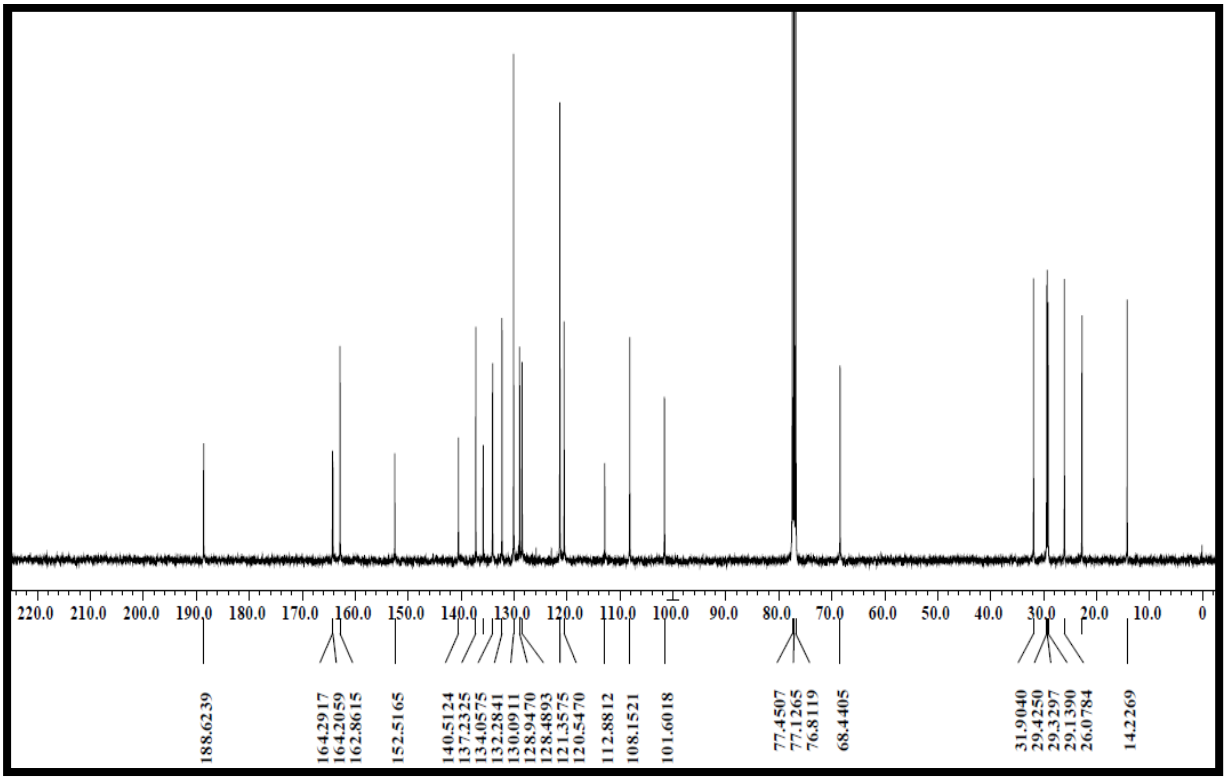

^{13}C-NMR of E8

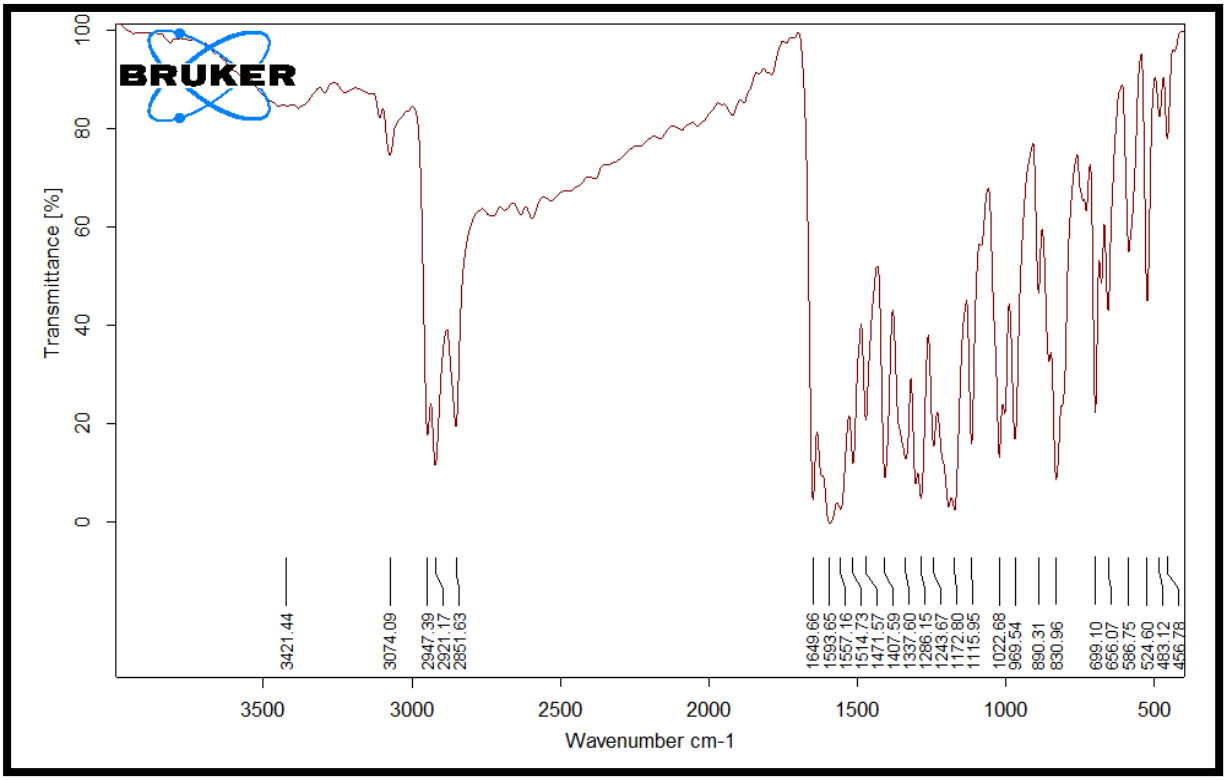

IR of E8.

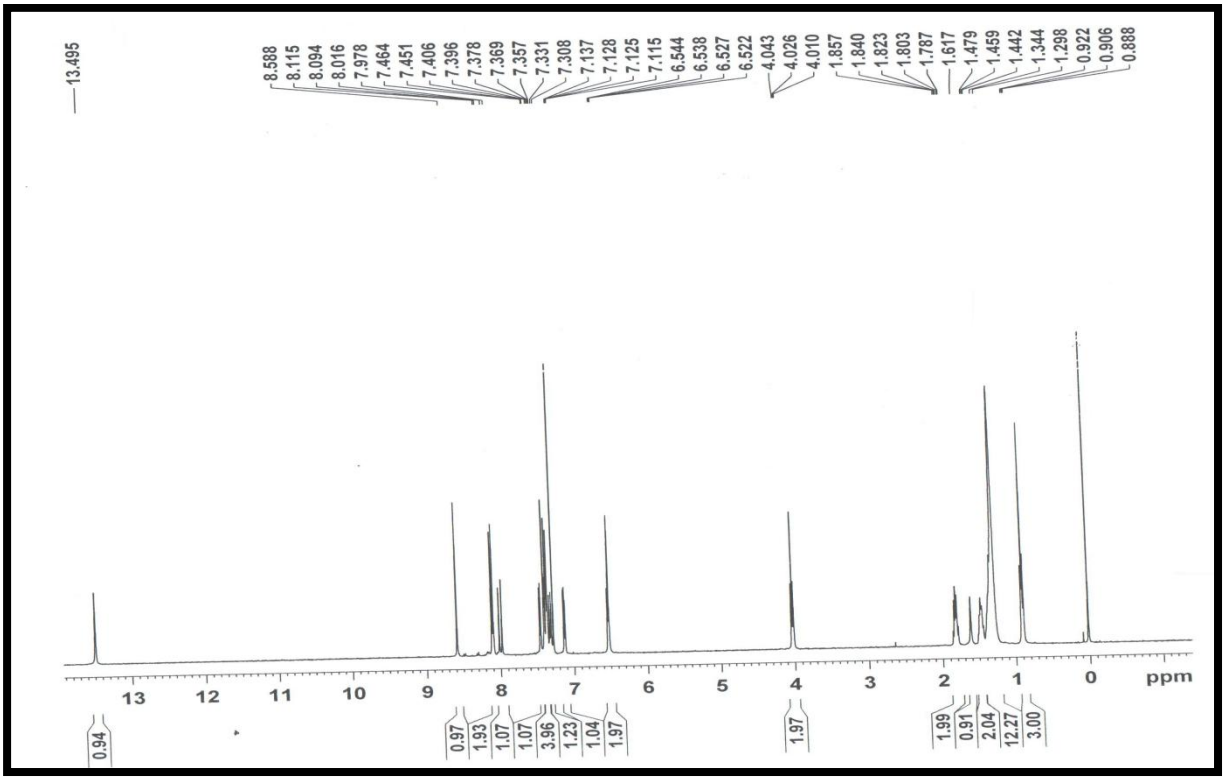

^{1}H-NMR of E10

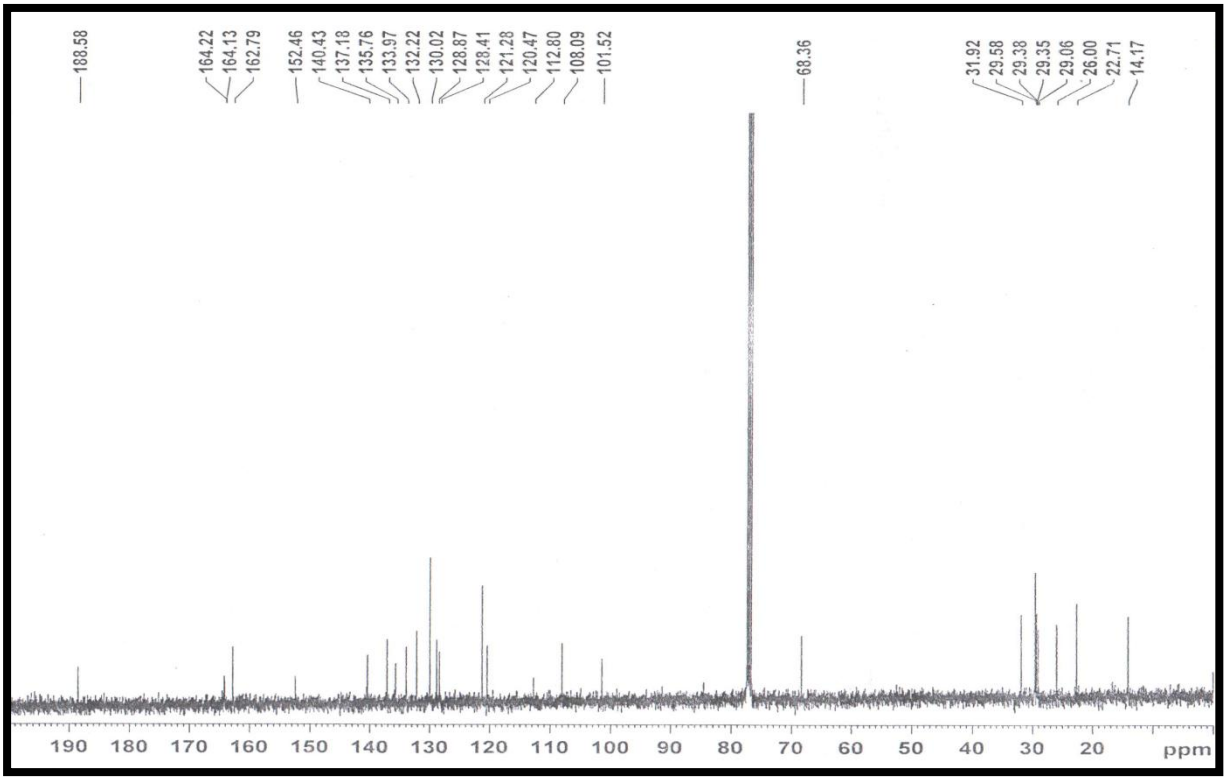

^{13}C-NMR of E10

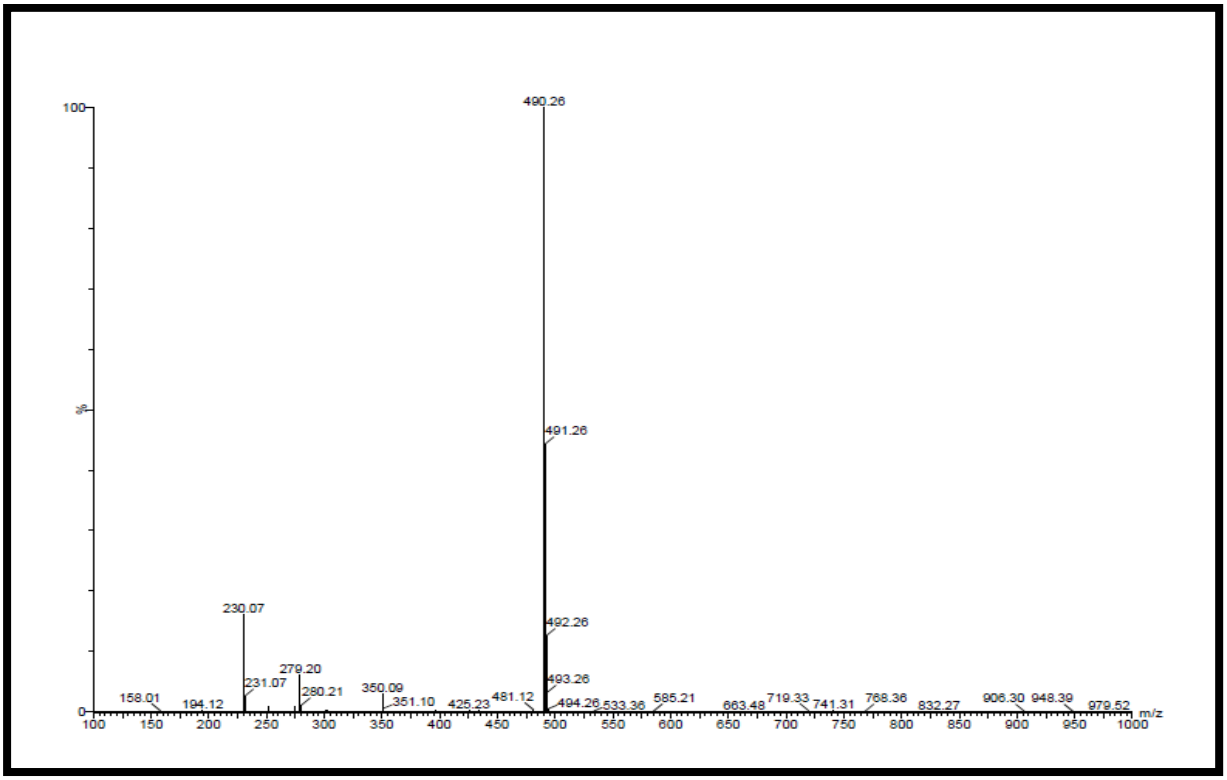

ESI-MS of E10.

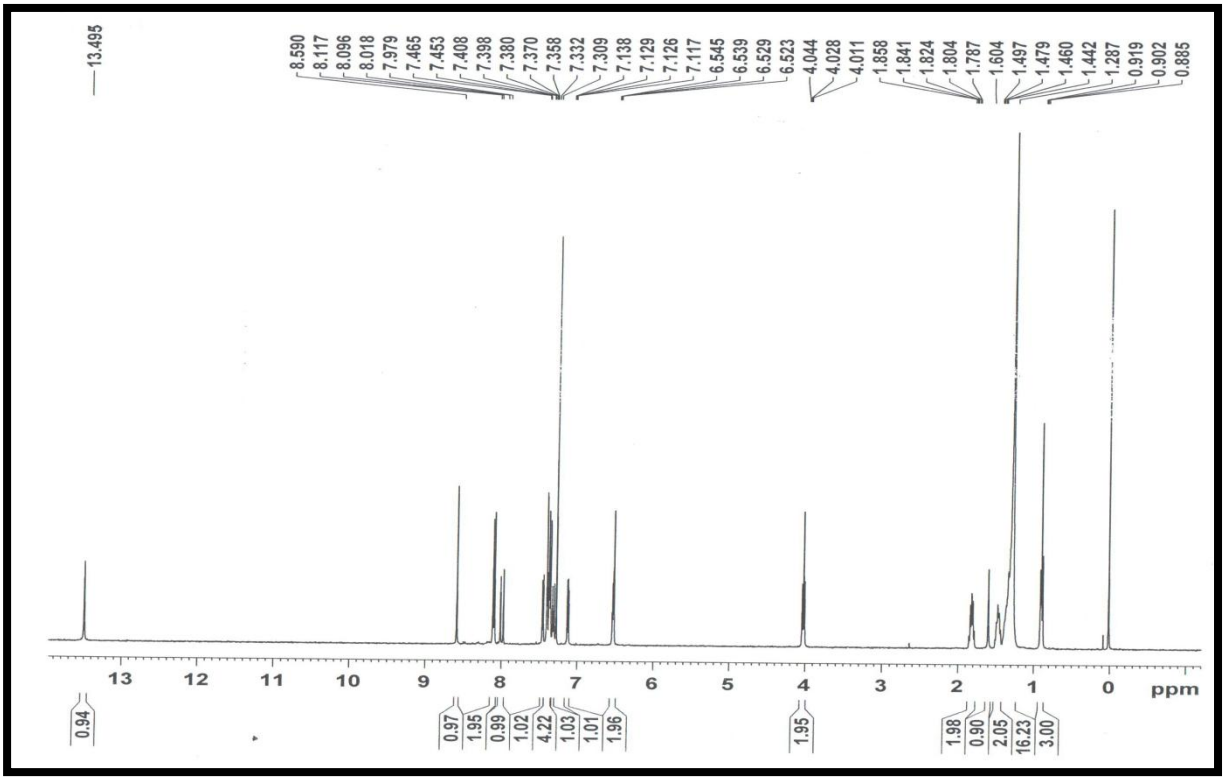

^{1}H-NMR of E12

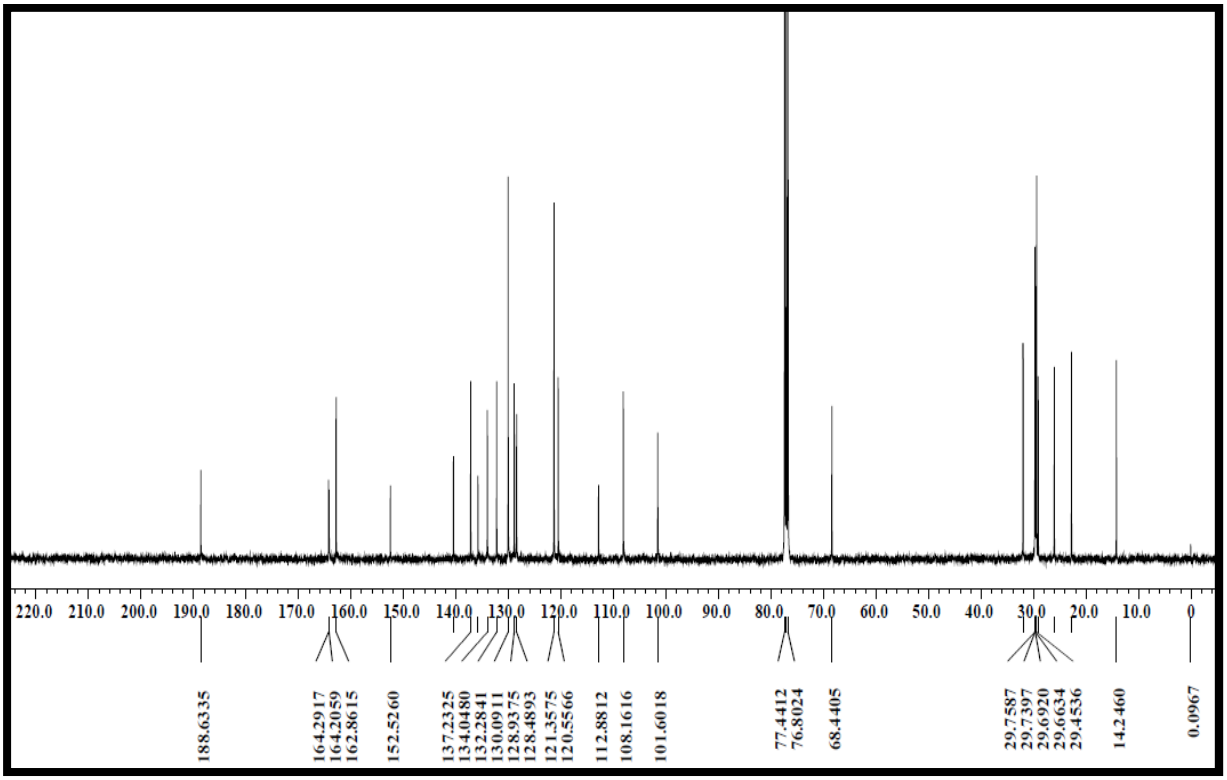

^{13}C-NMR of E12

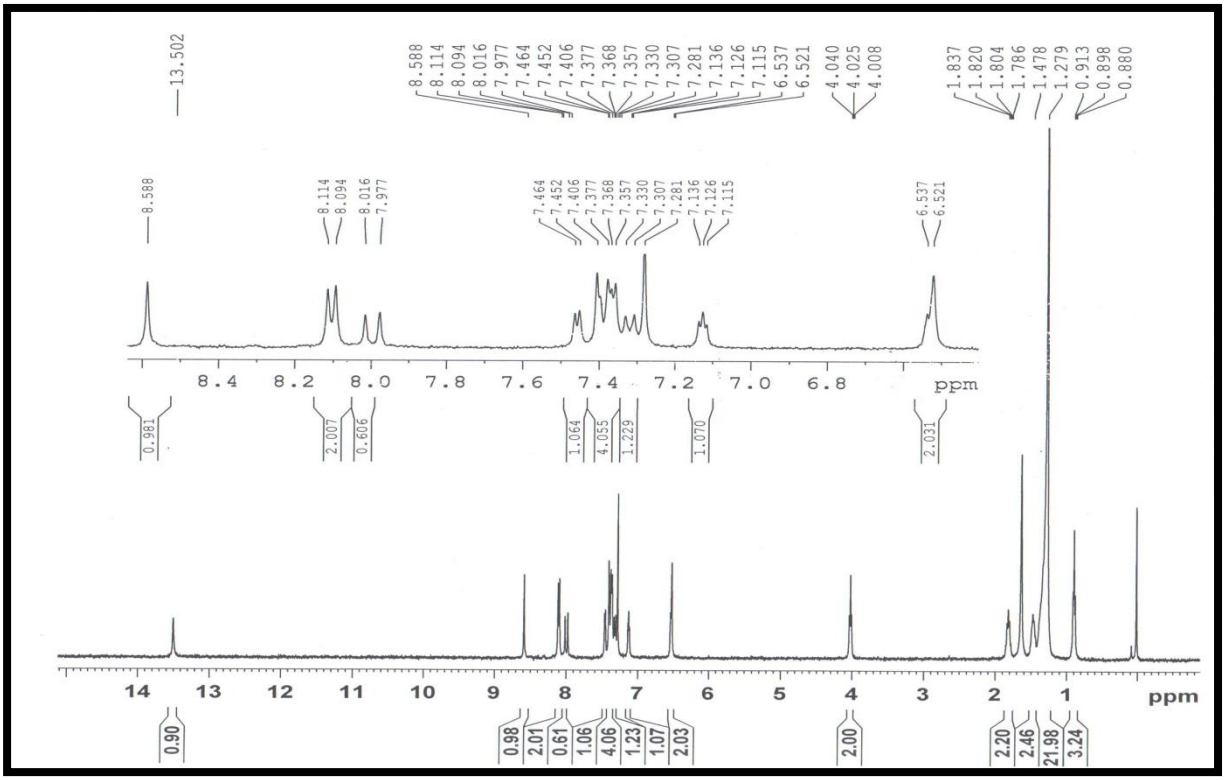

^{1}H-NMR of E14

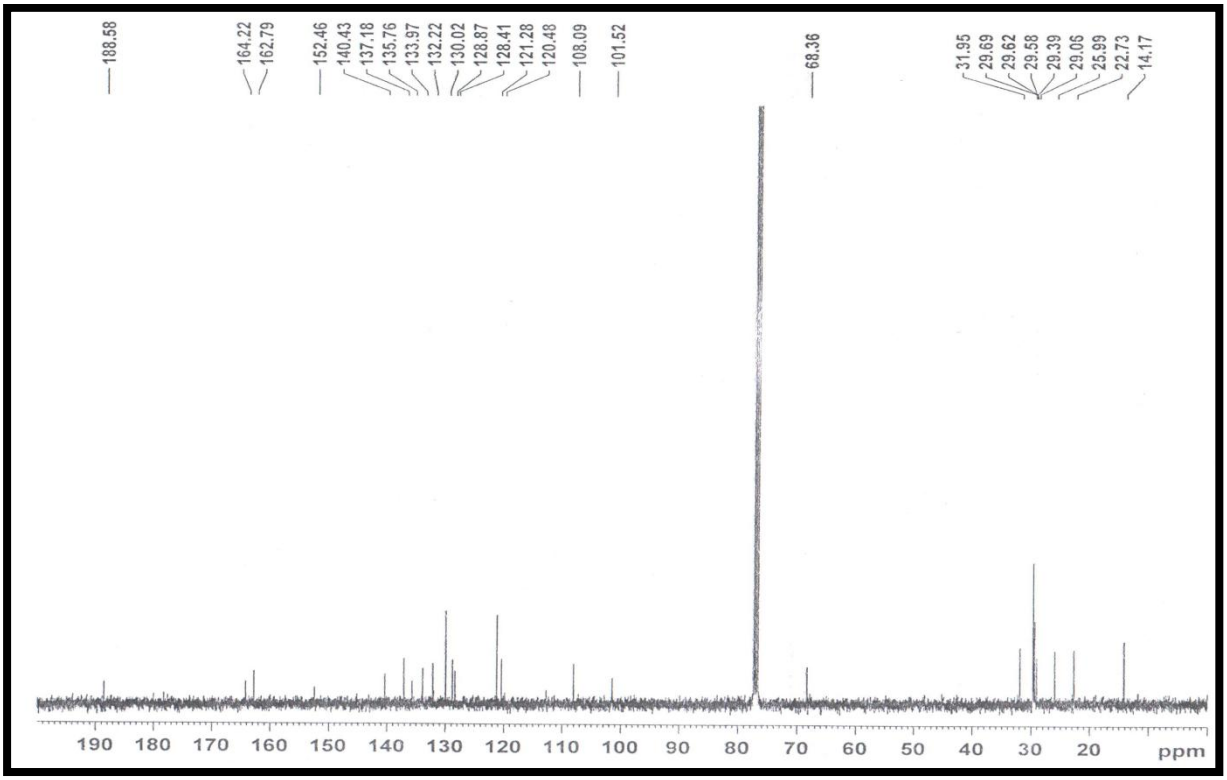

^{13}C-NMR of E14

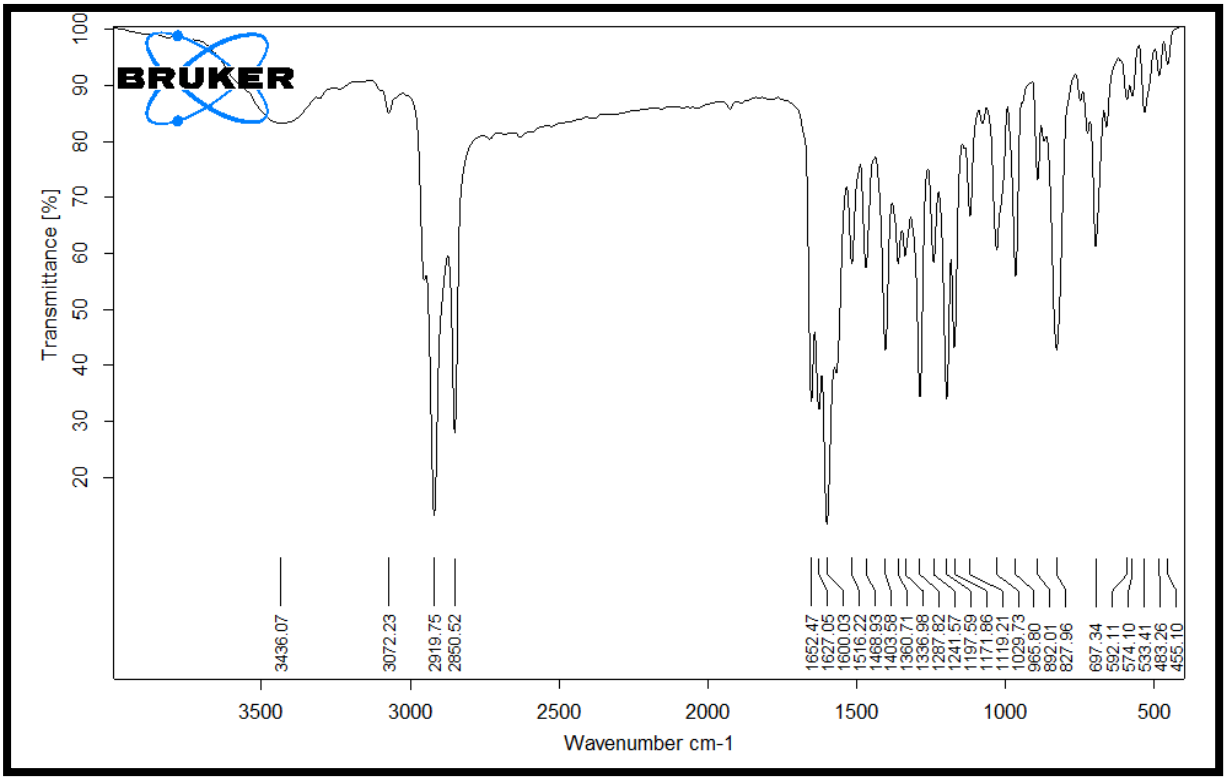

IR of E14

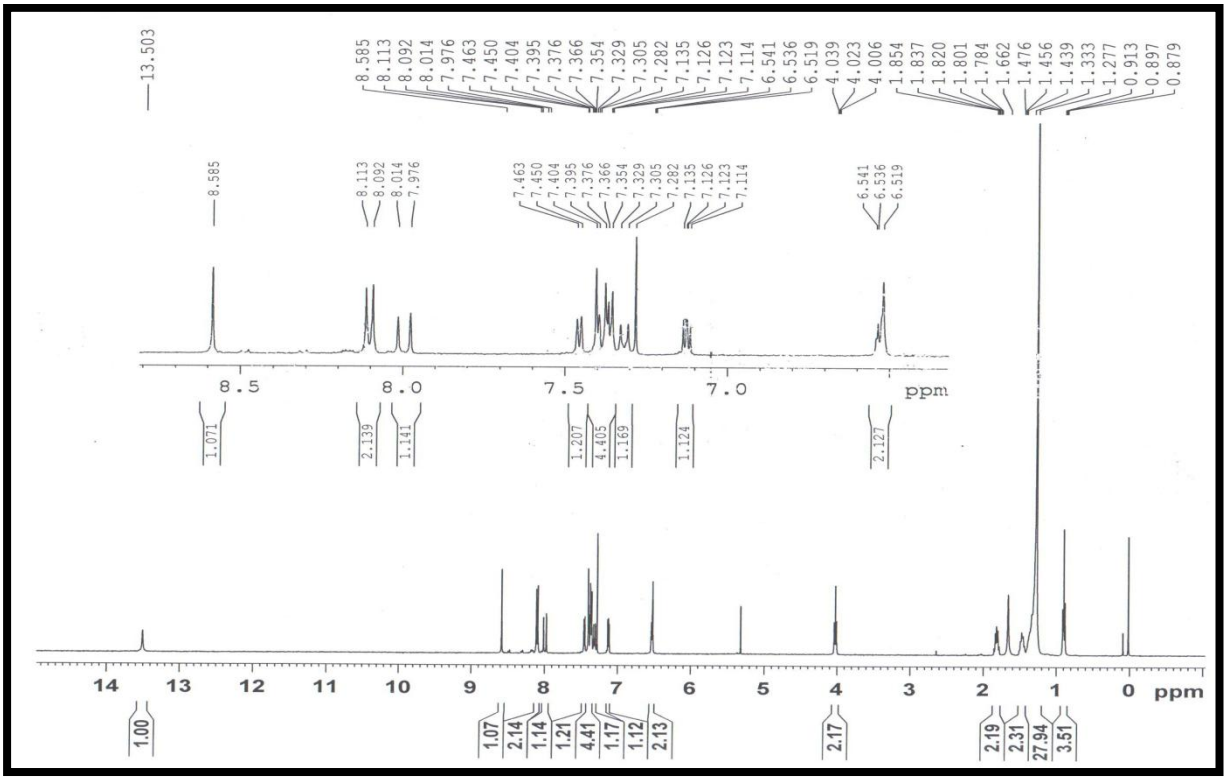

^{1}H-NMR of E16

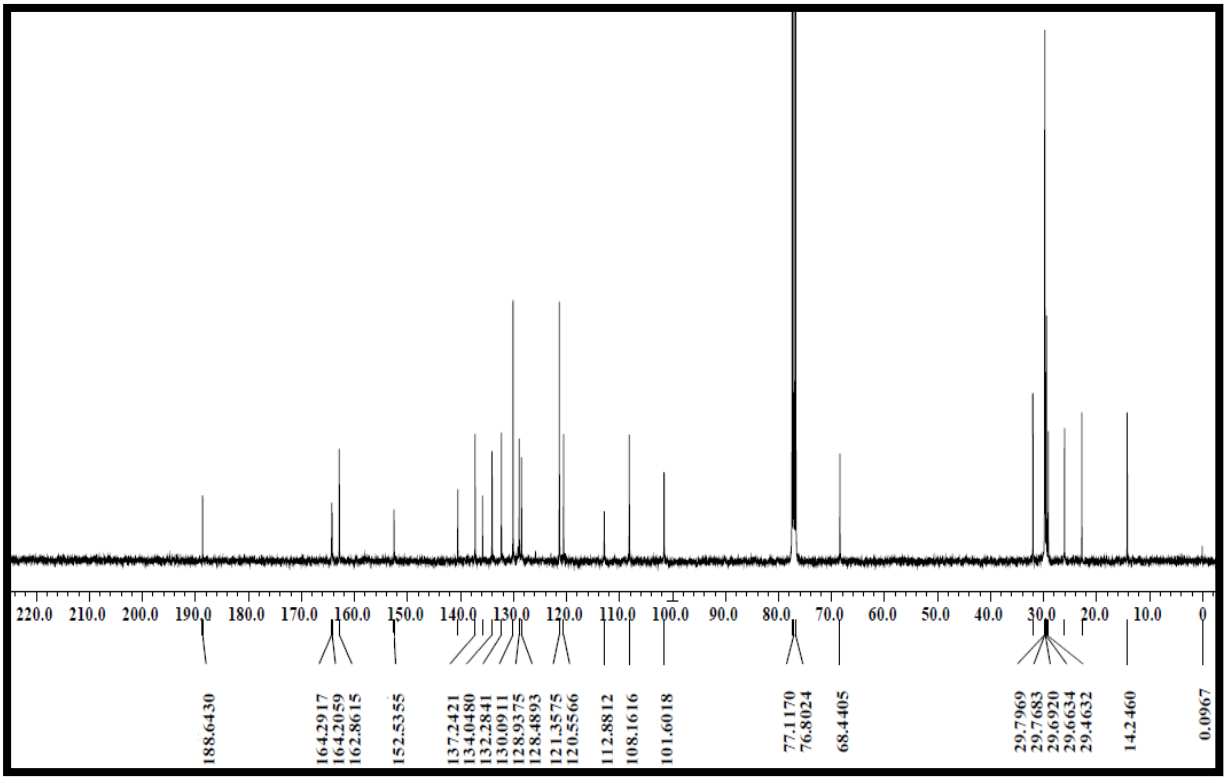

^{13}C-NMR of E16

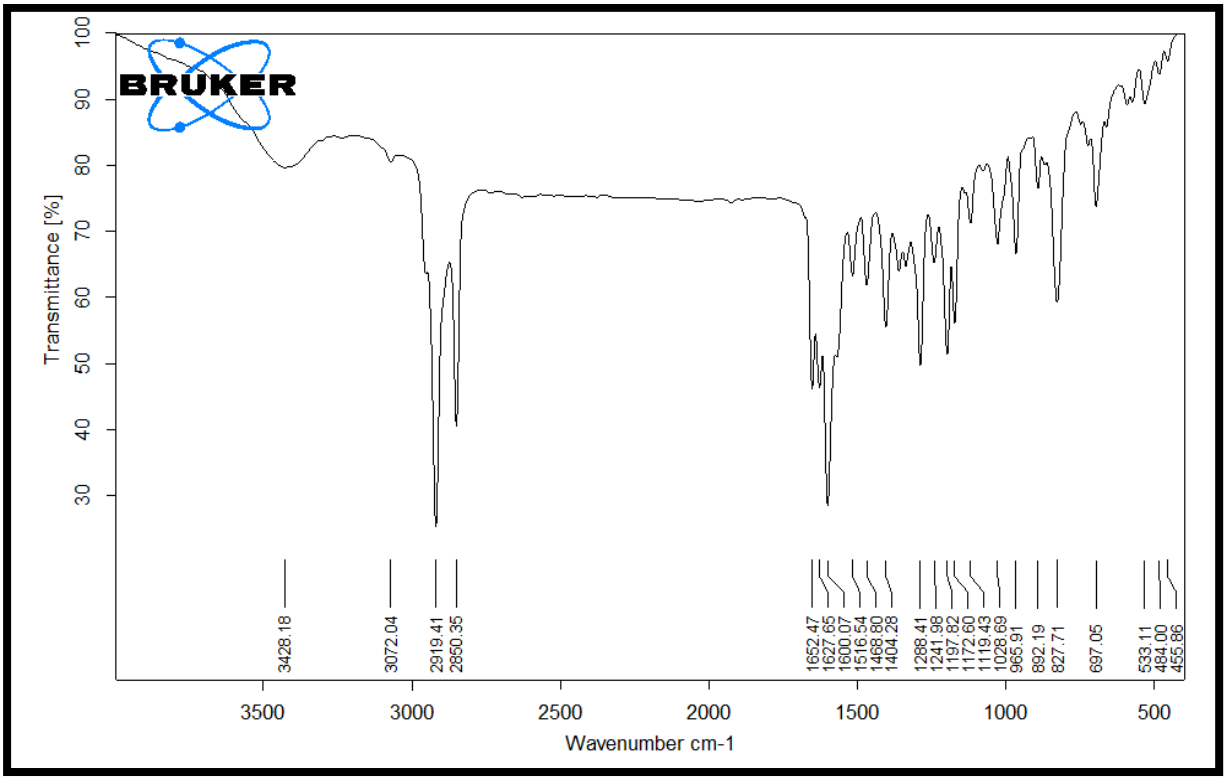

IR of E16

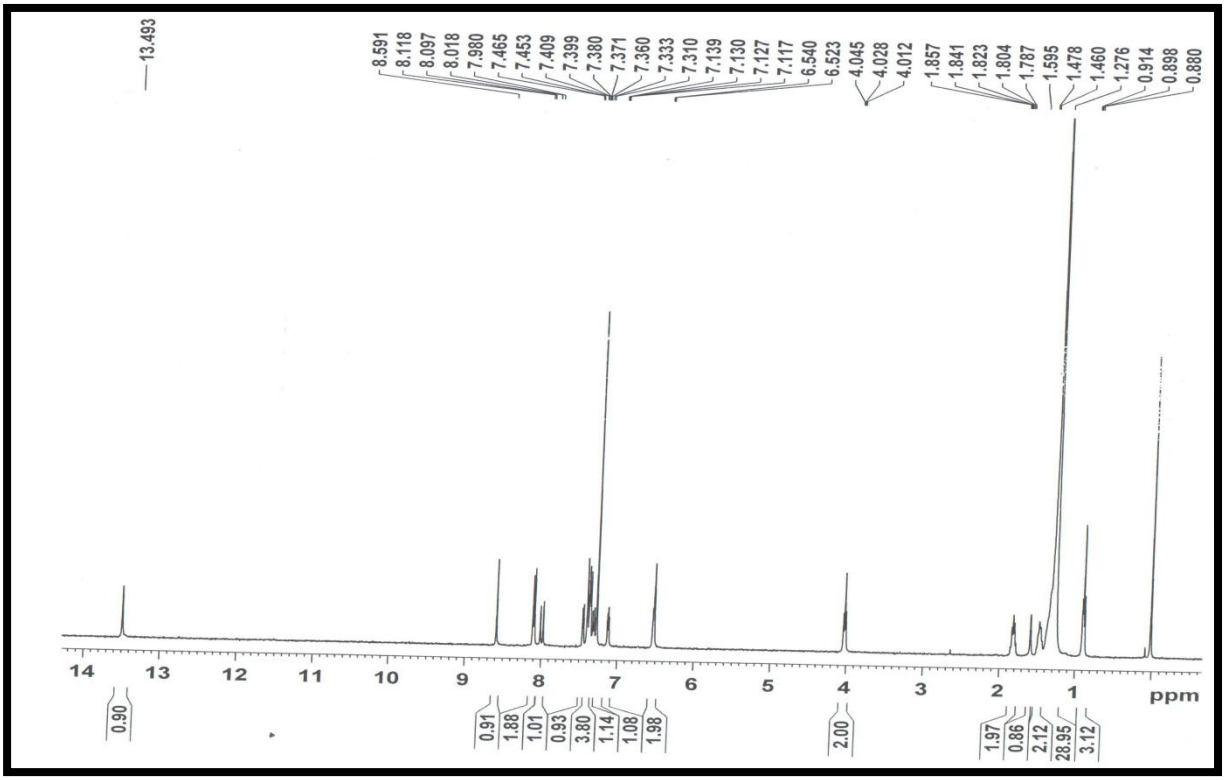

^{1}H-NMR of E18

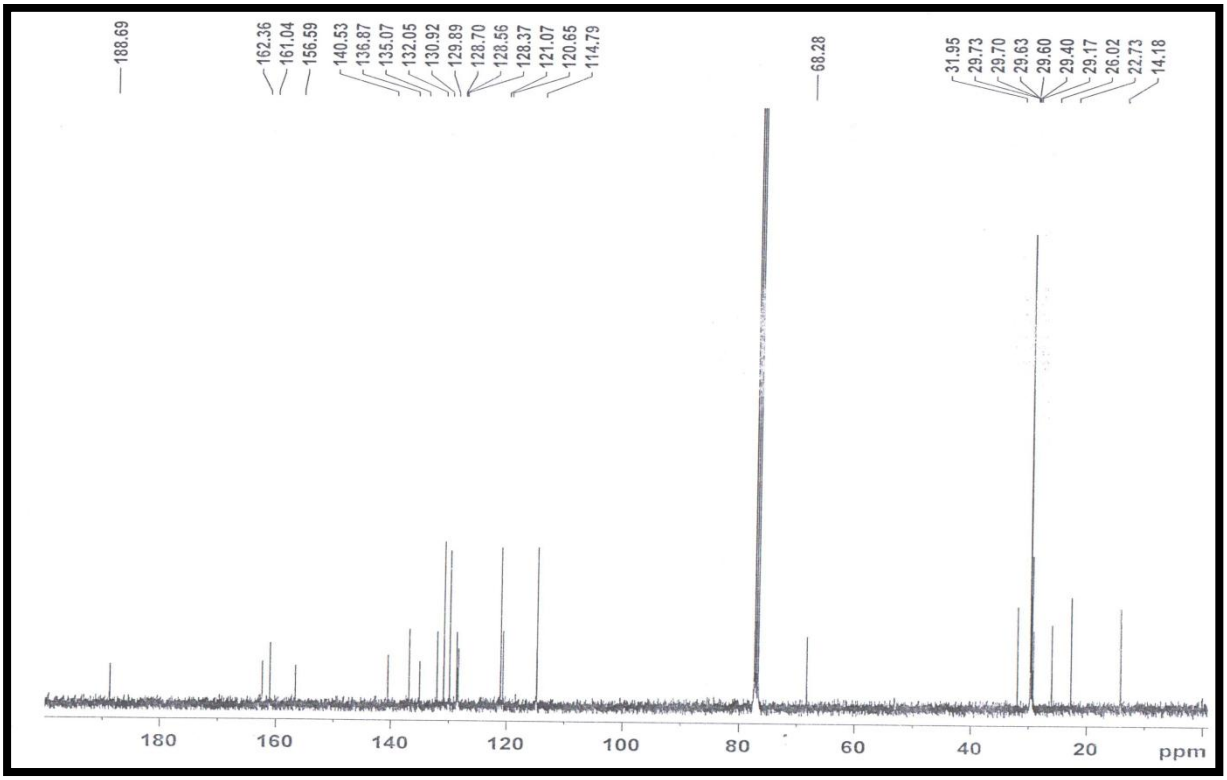

^{13}C-NMR of E18

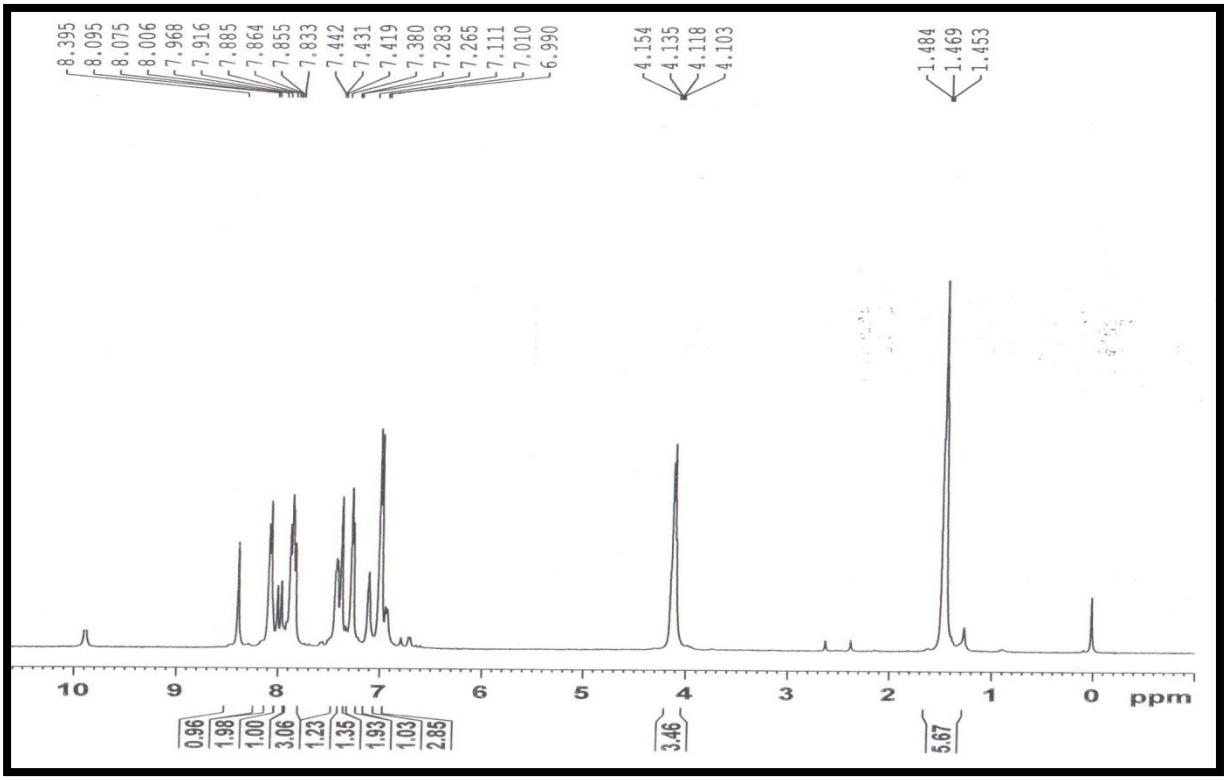

^{1}H NMR of F2

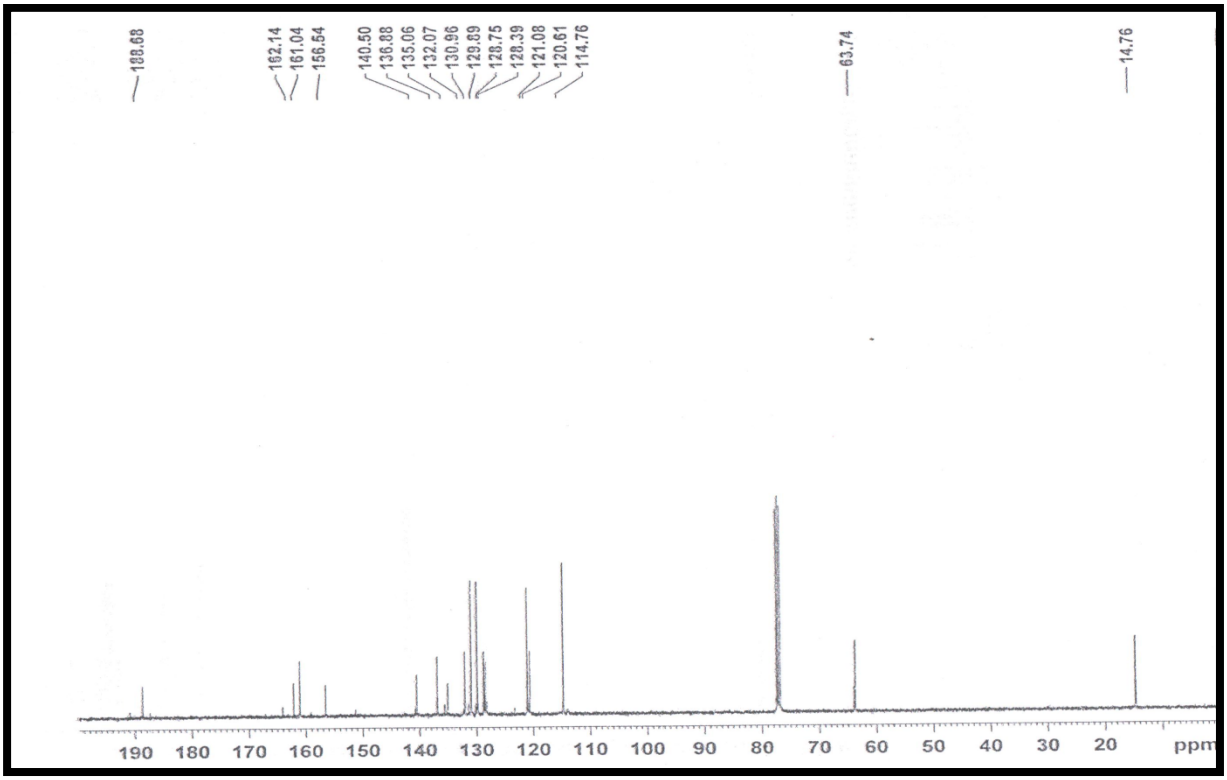

^{13}C NMR of F2

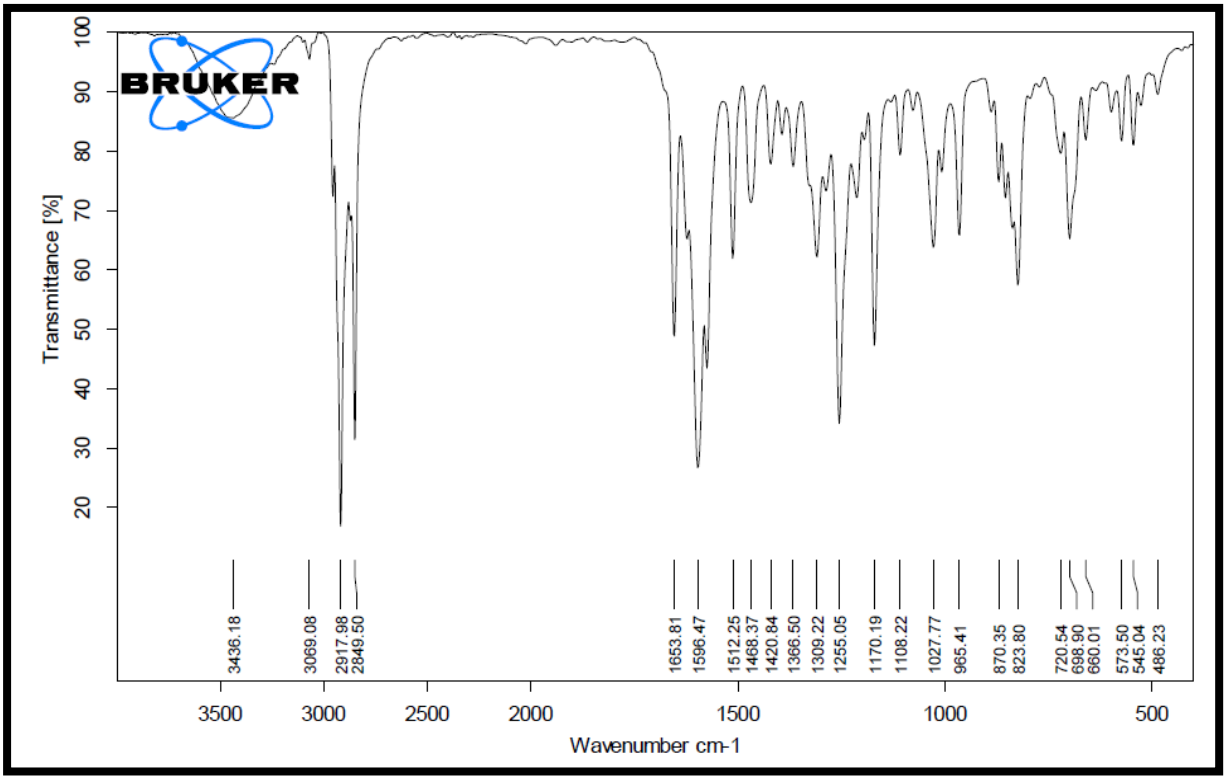

IR of F2

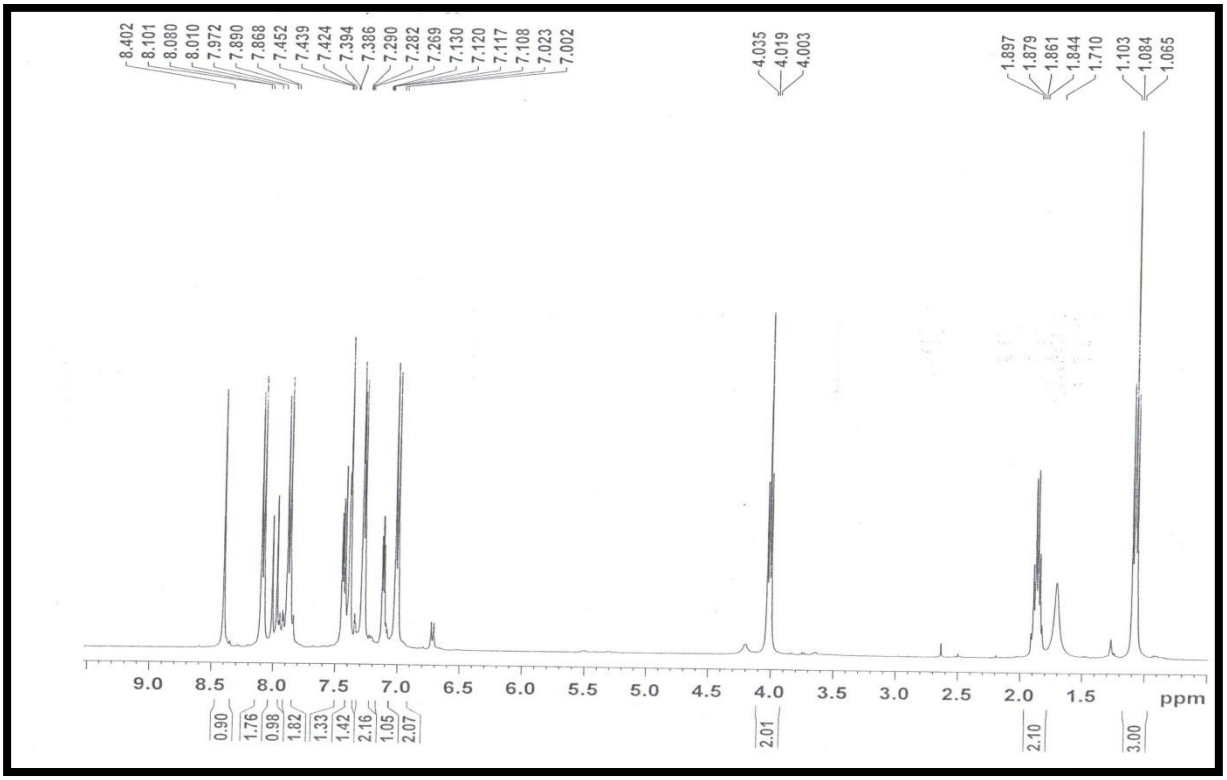

^{1}H NMR of F3

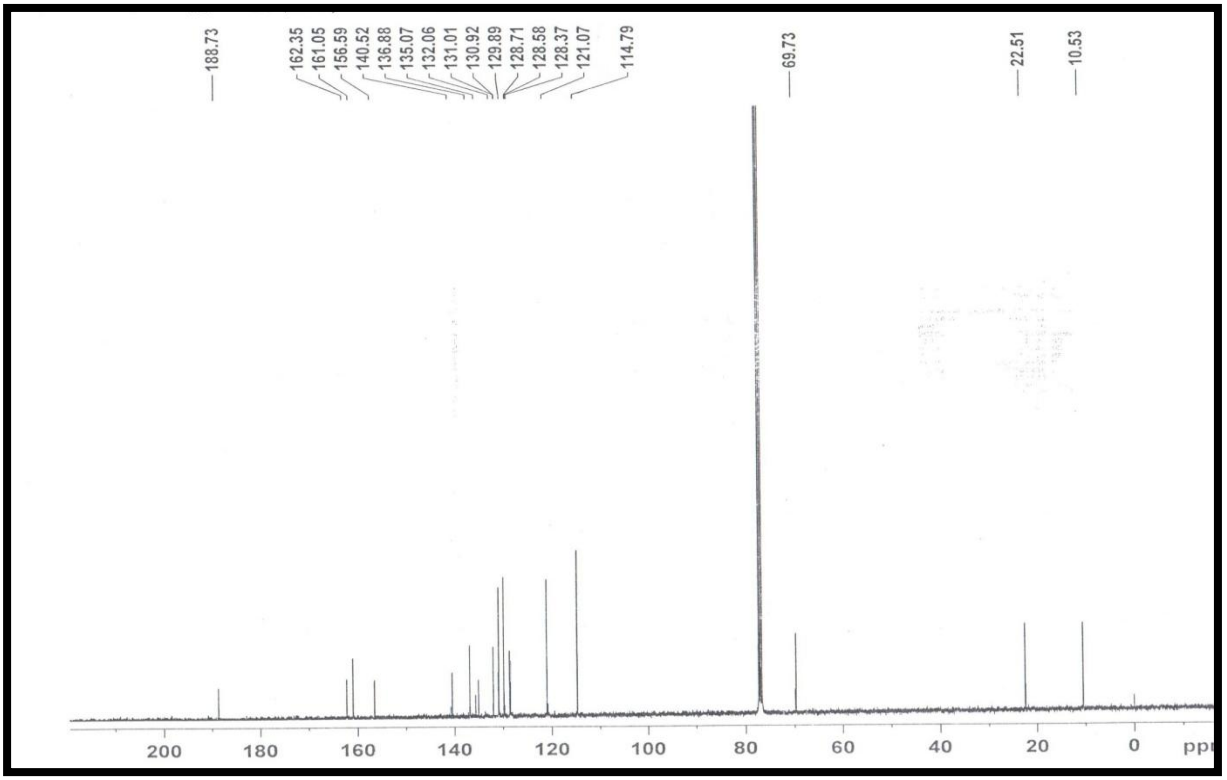

^{13}C NMR of F3

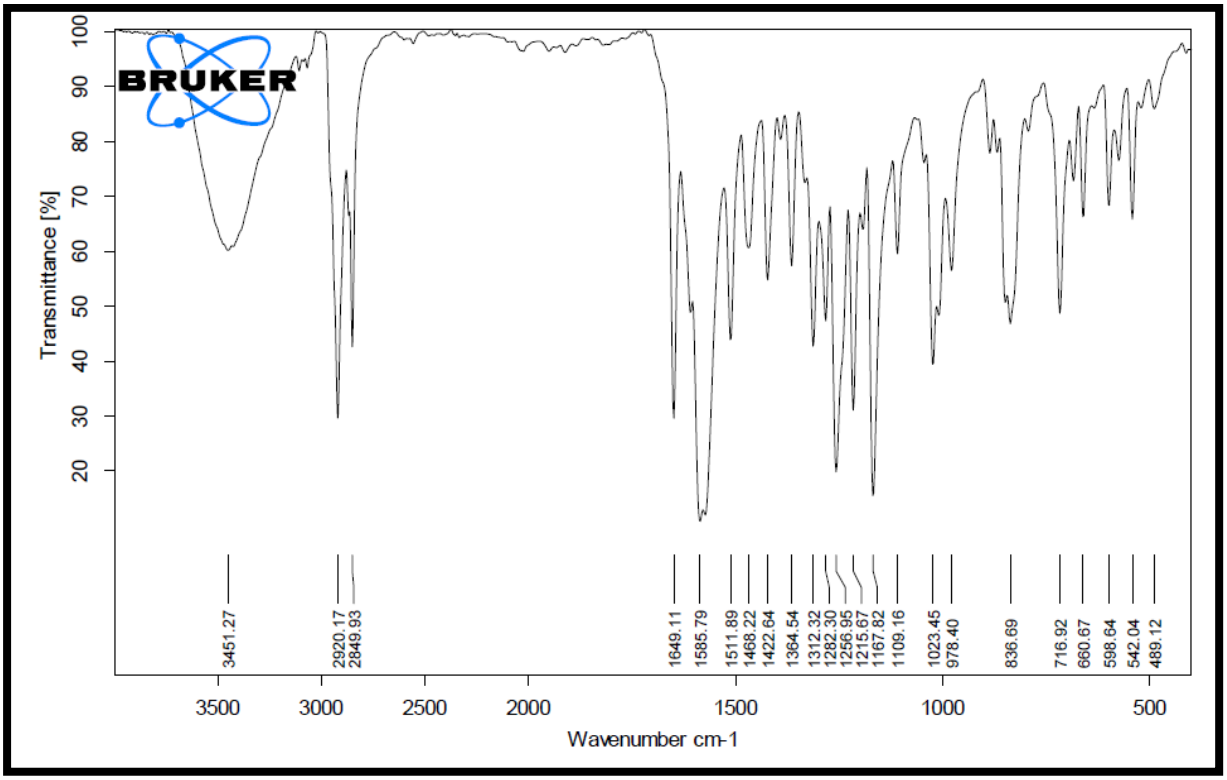

IR of F3

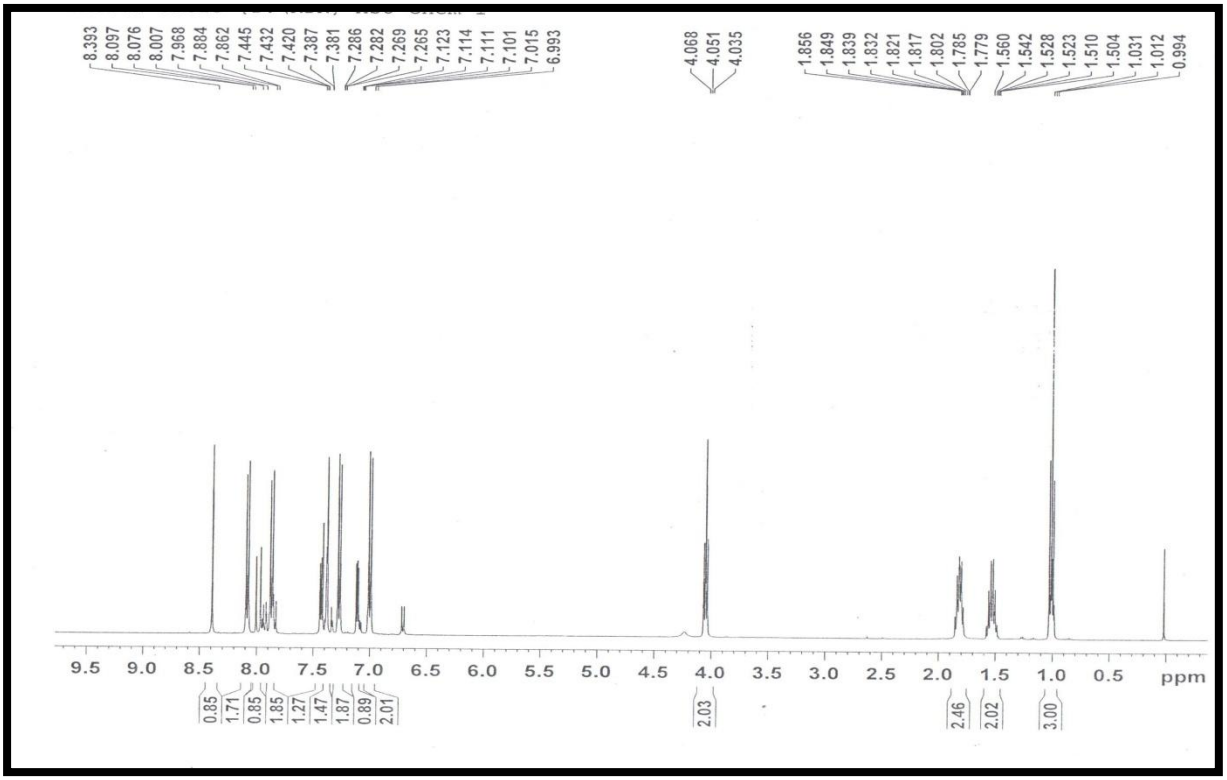

^{1}H NMR of F4

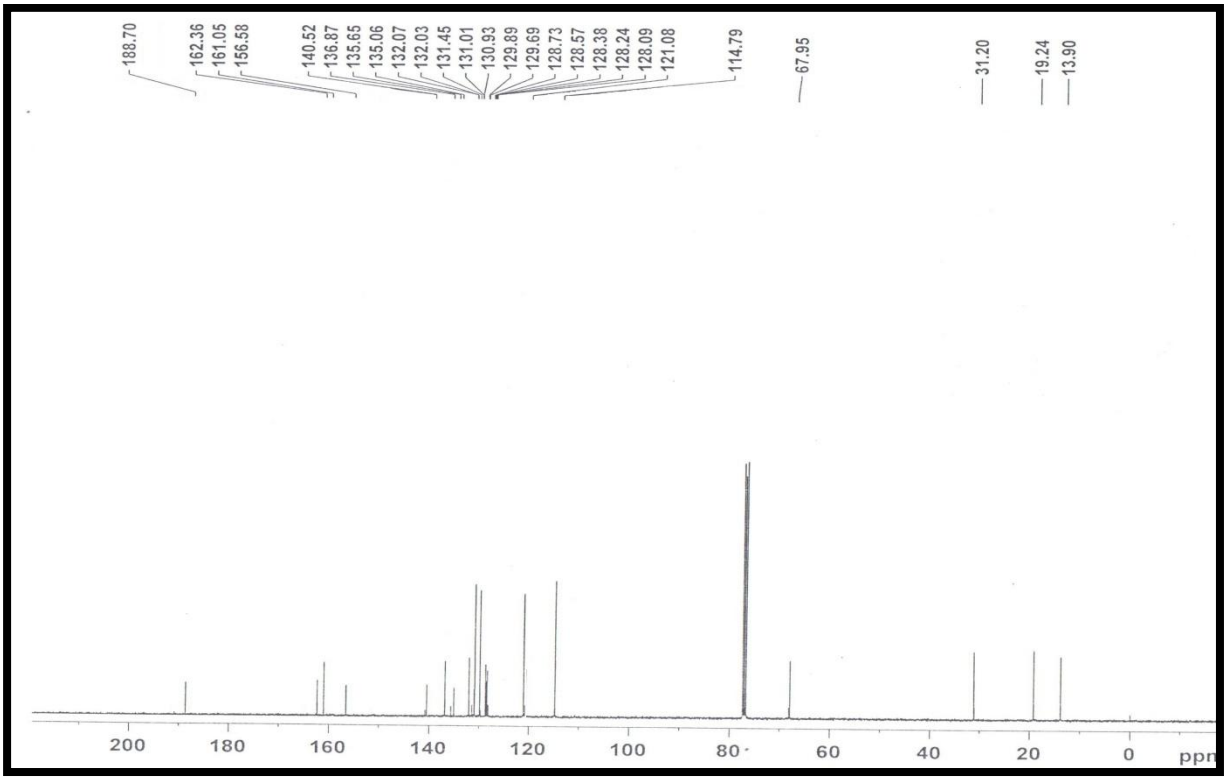

^{13}C NMR of F4

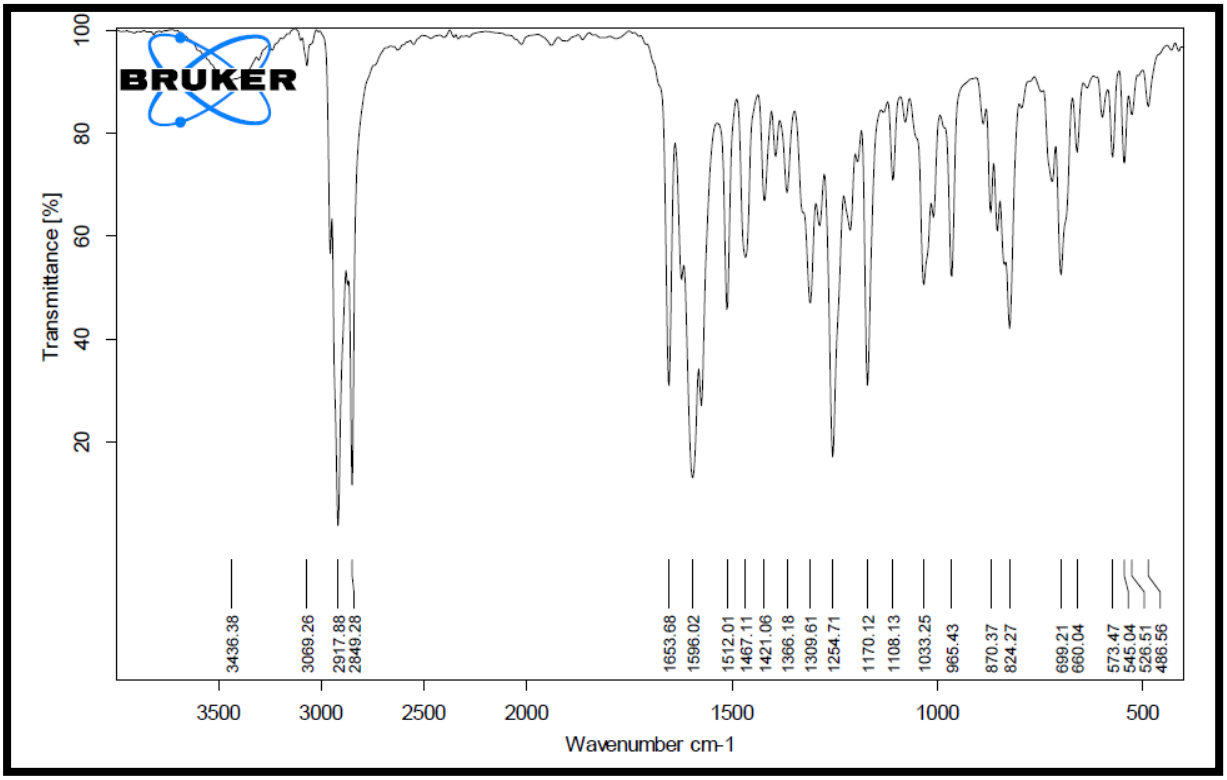

IR of F4

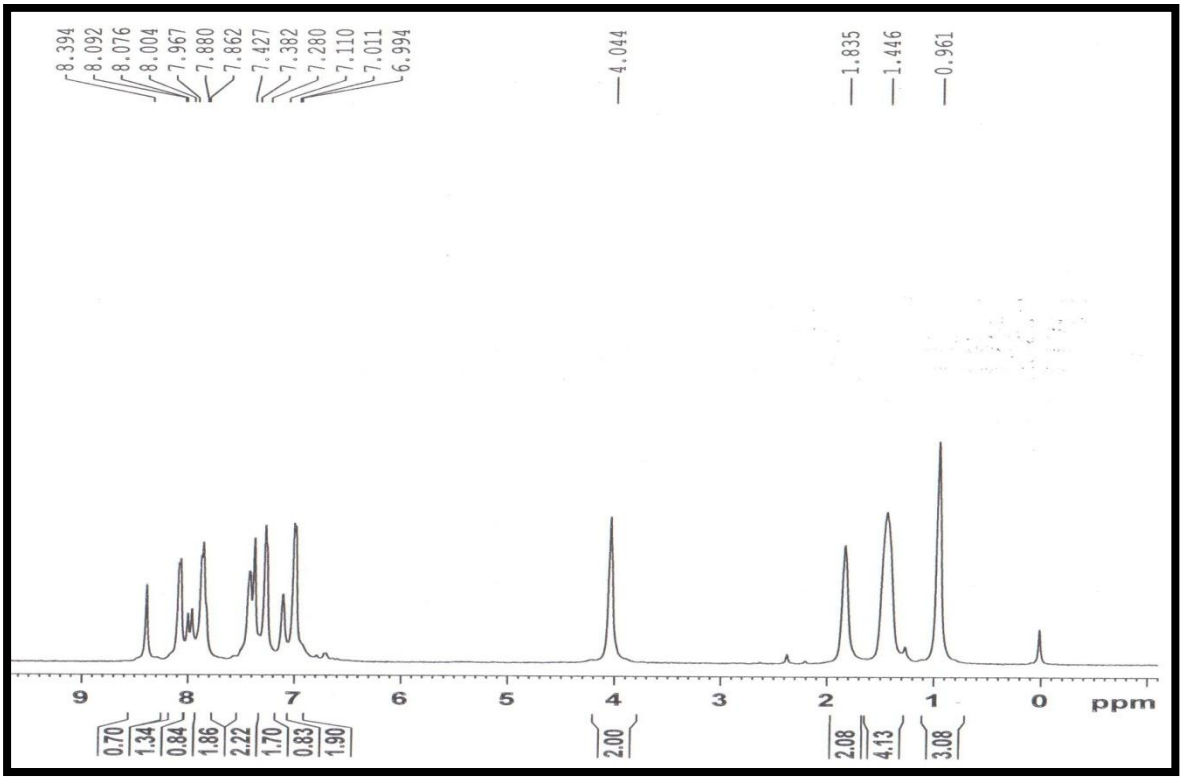

^{1}H NMR of F5

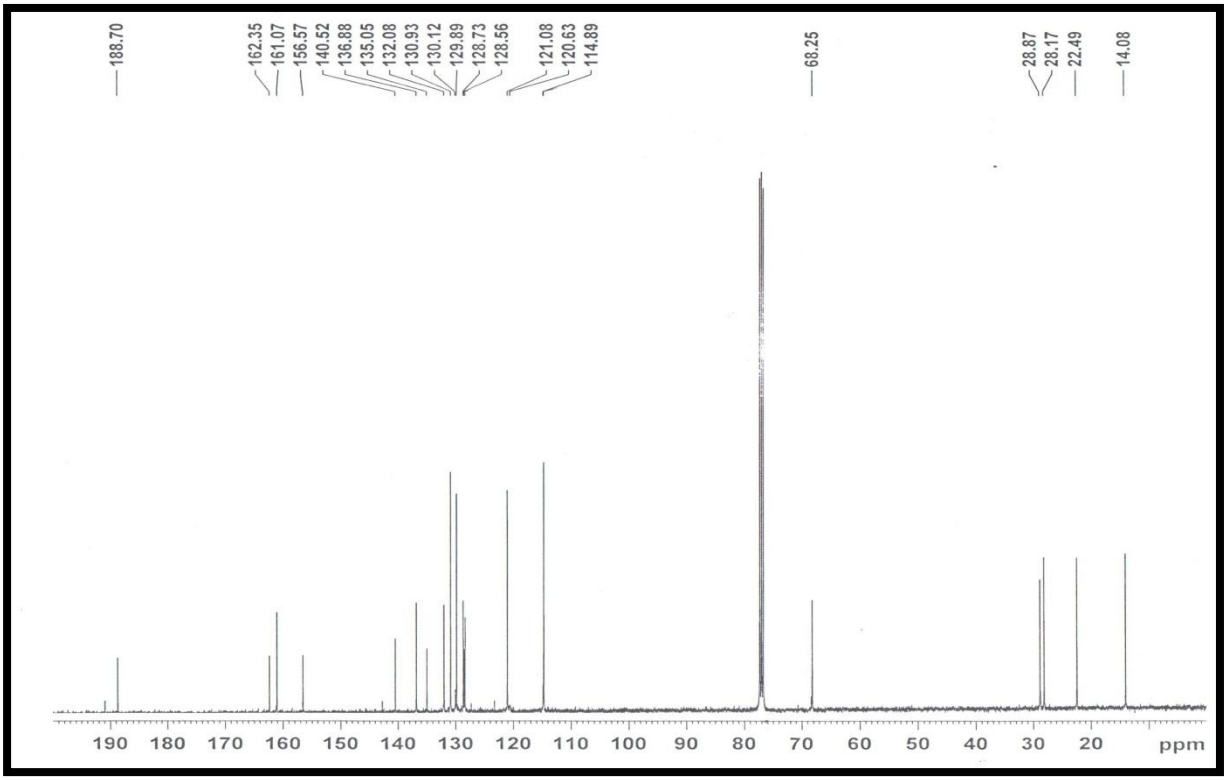

^{13}C NMR of F5

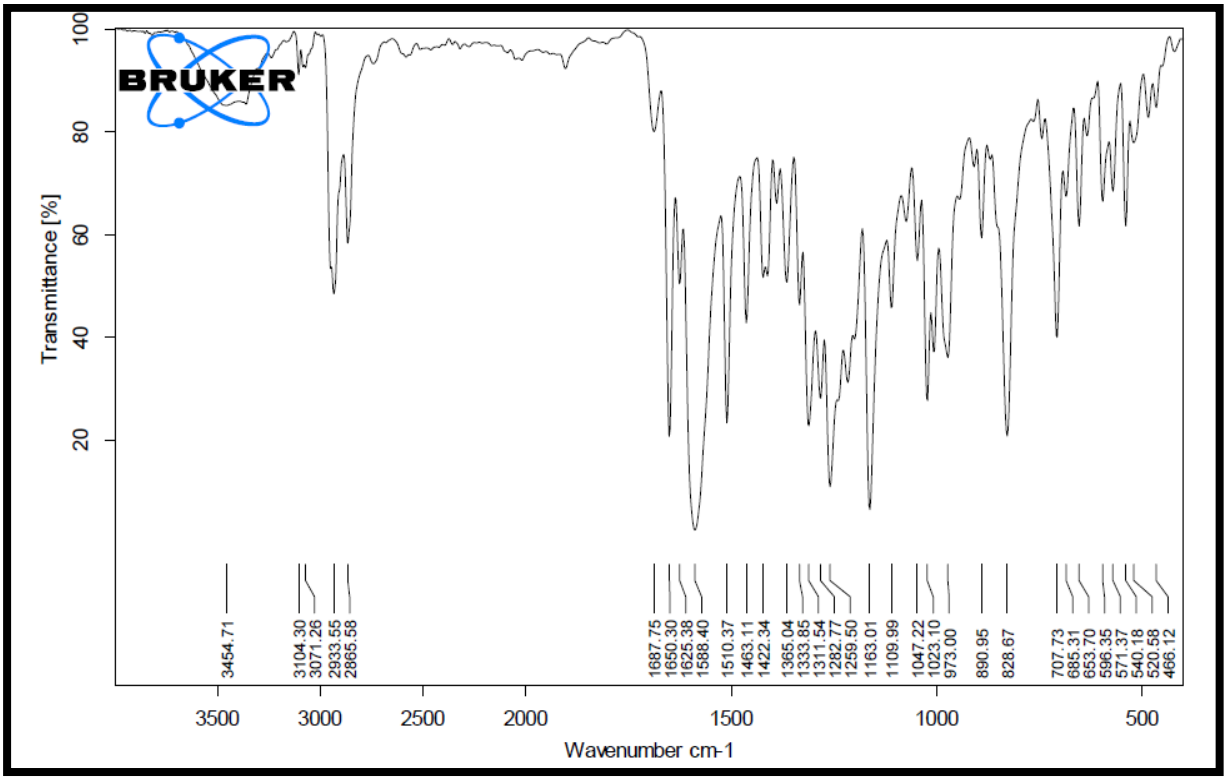

IR of F5

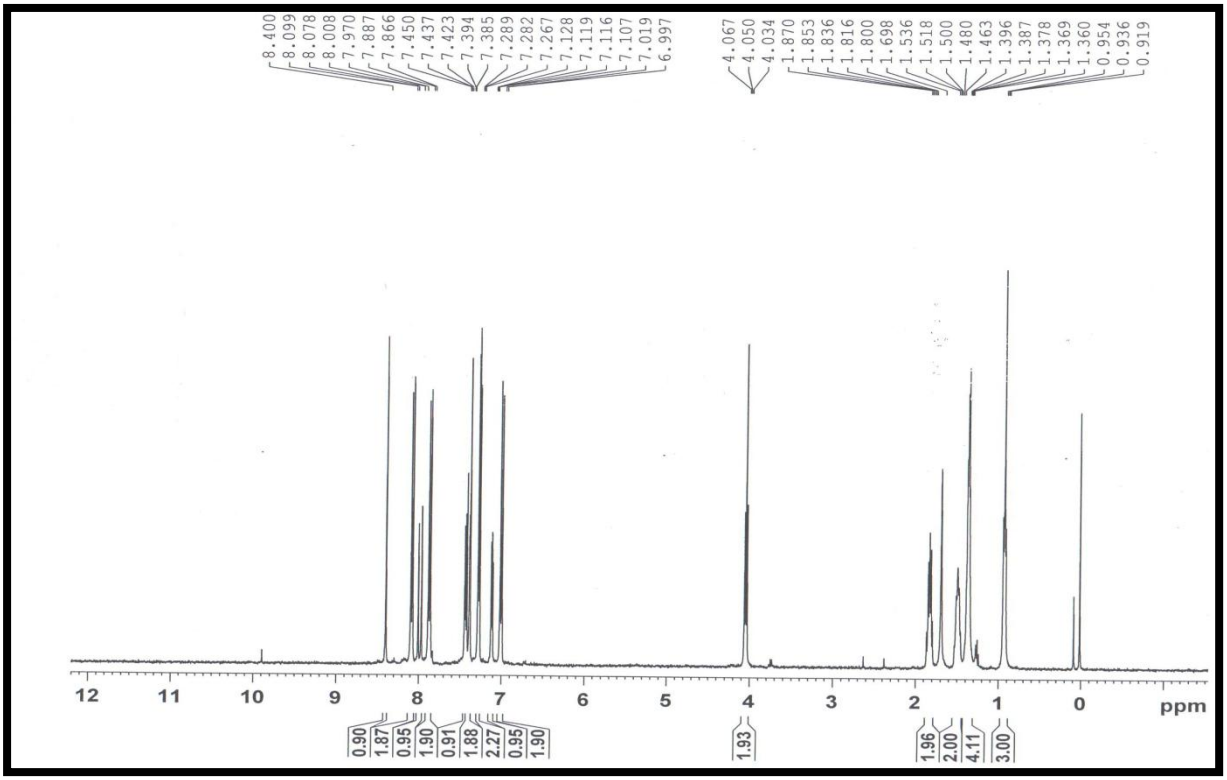

^{1}H NMR of F6

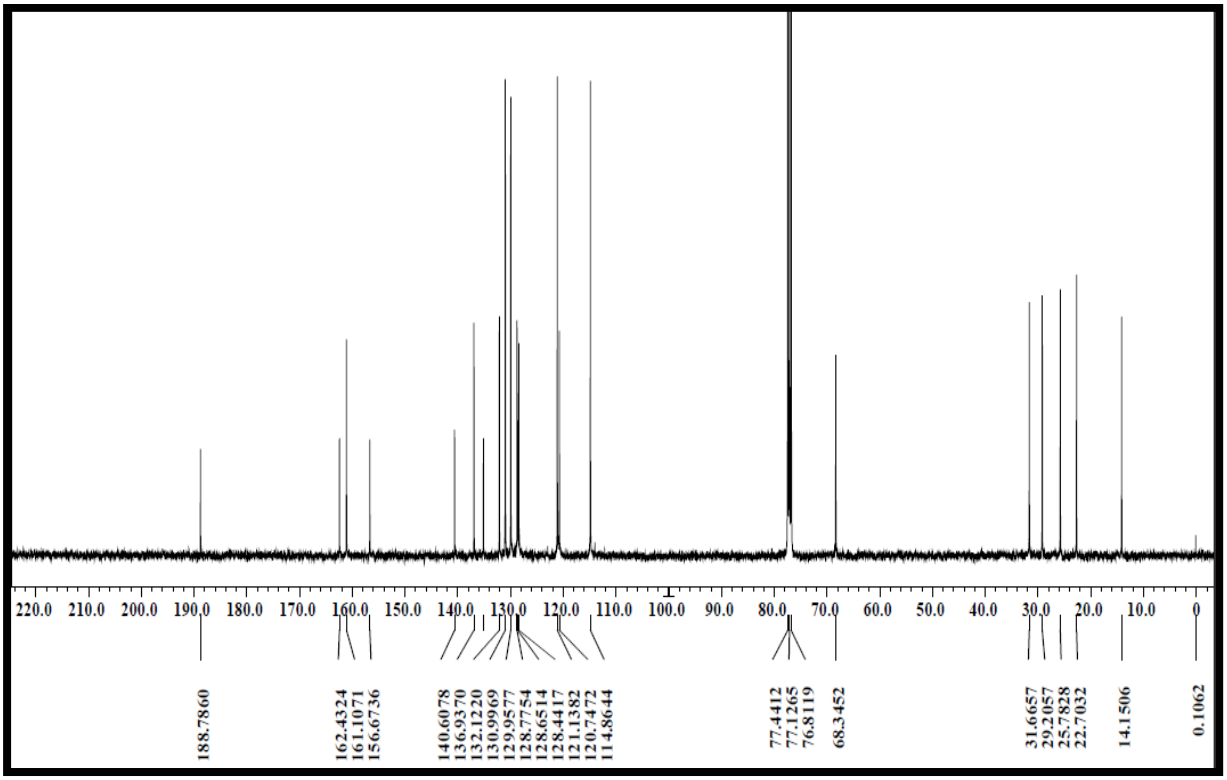

^{13}C NMR of F6

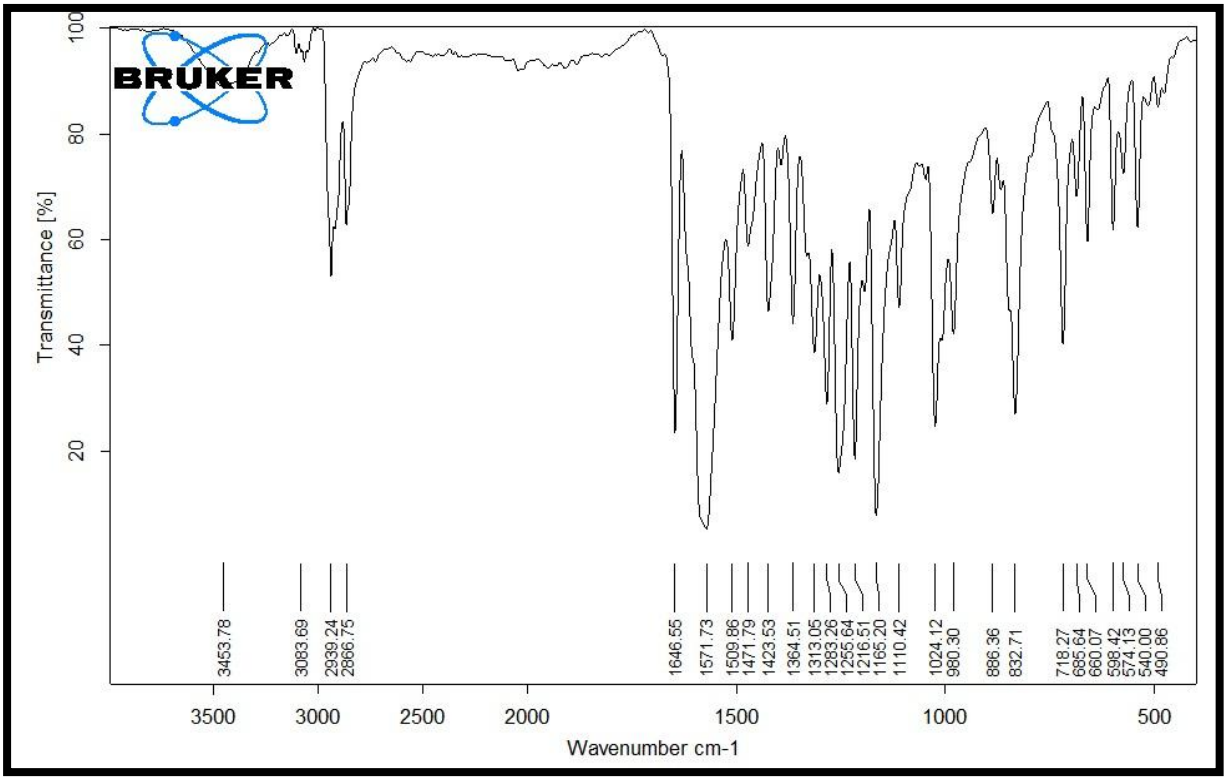

IR of F6

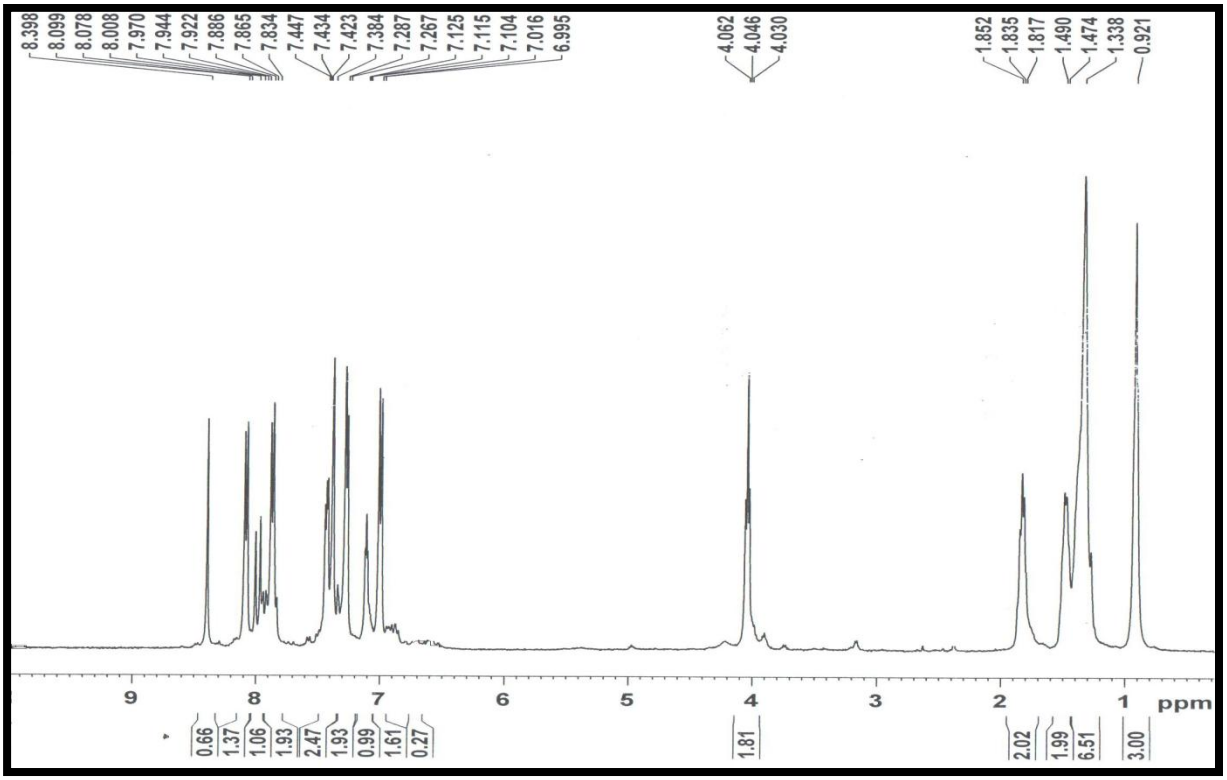

^{1}H NMR of F7

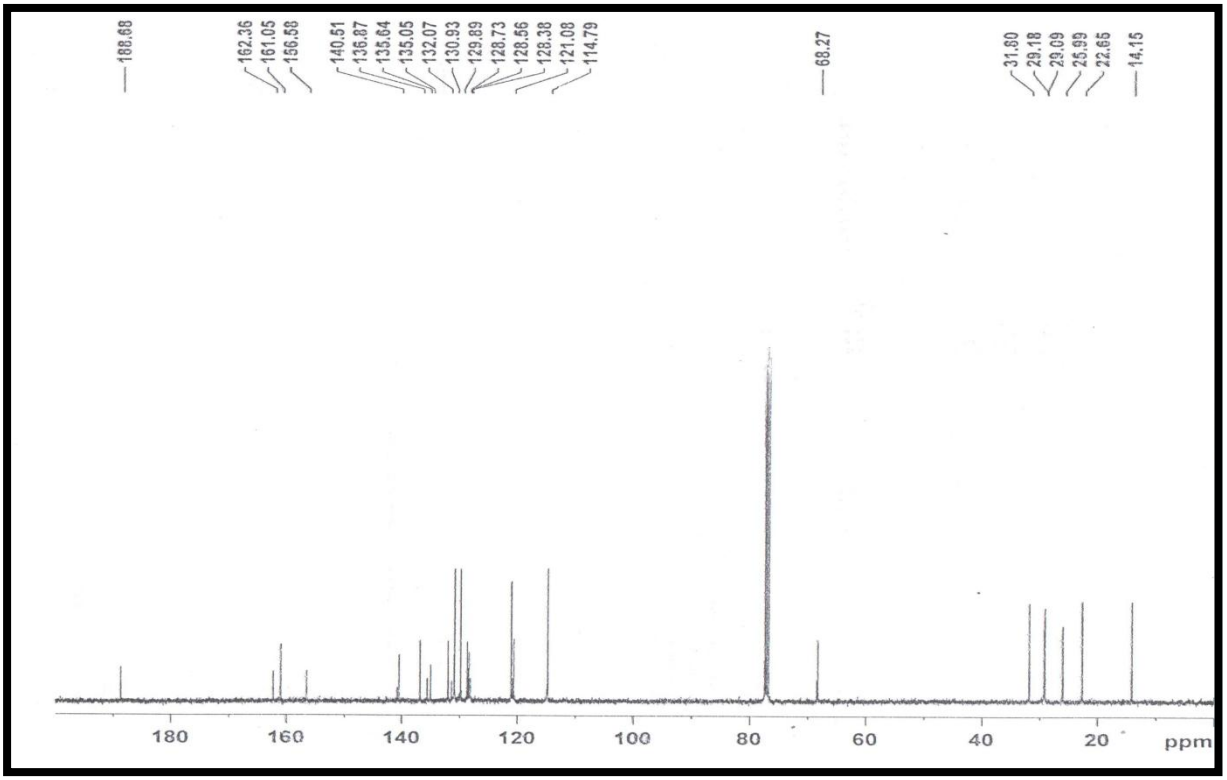

^{13}C NMR of F7

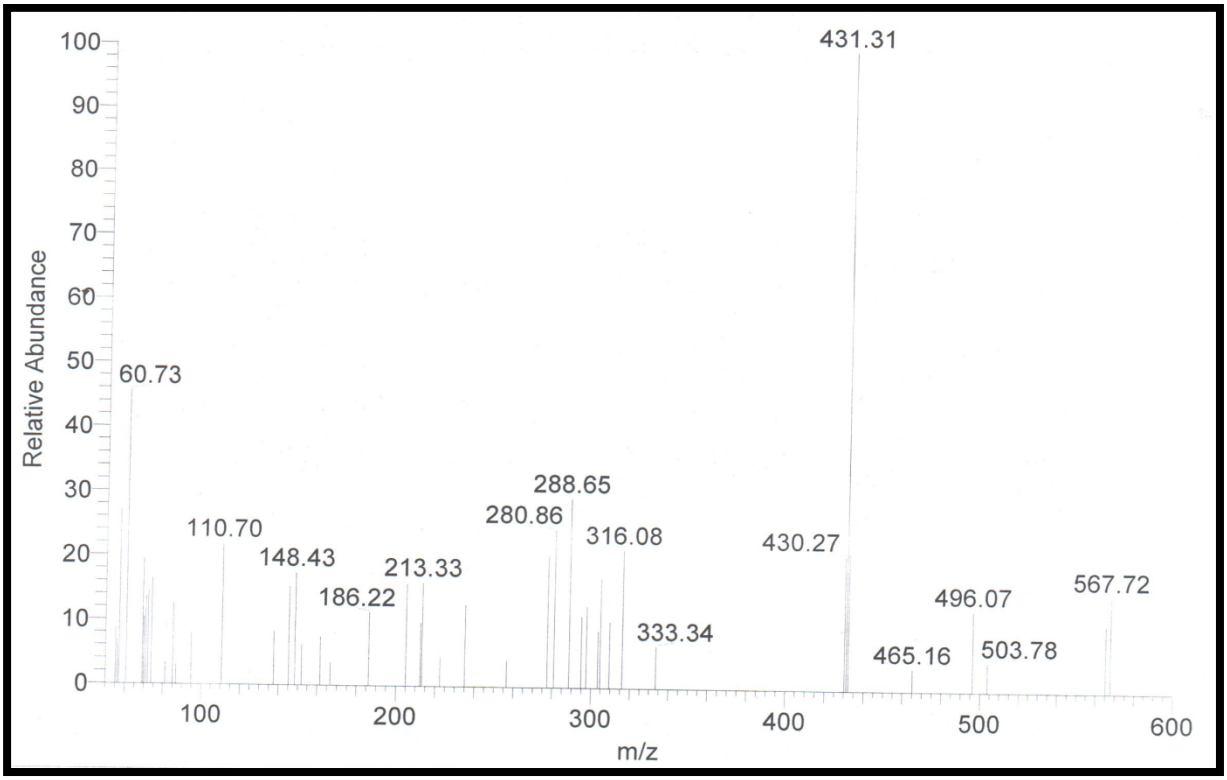

ESI-MS of F7

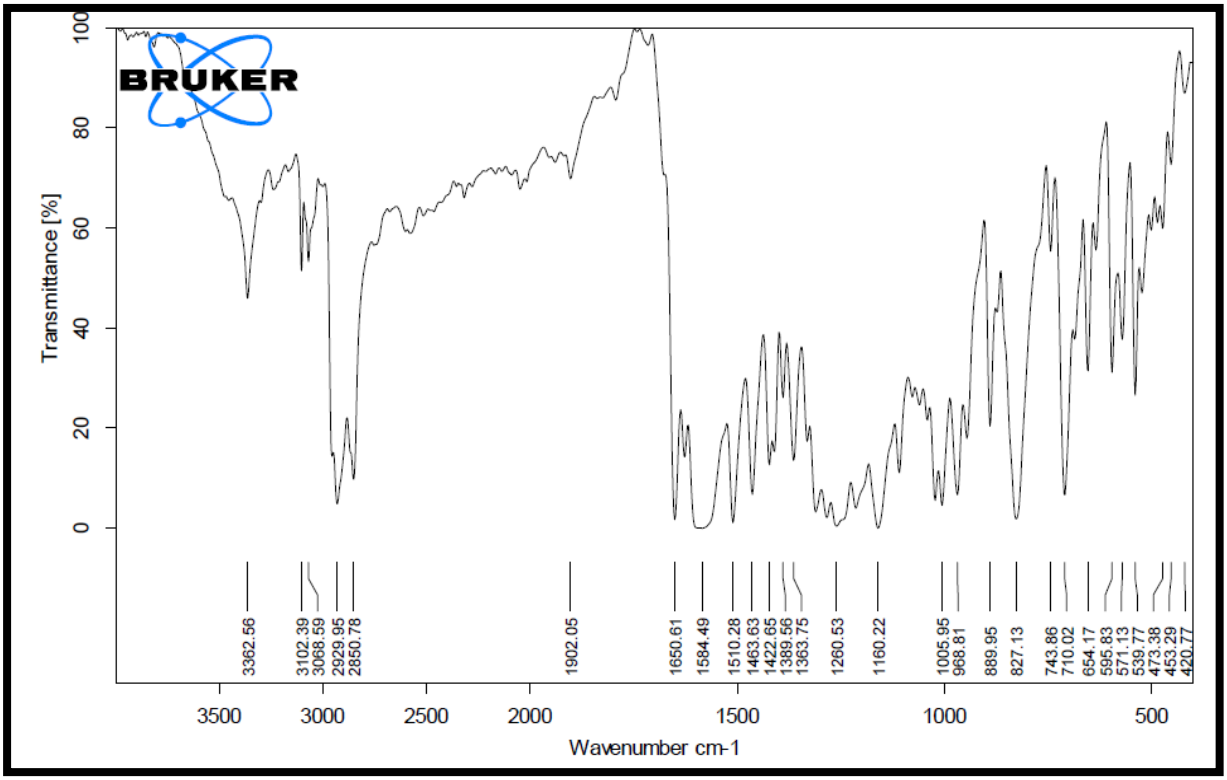

IR of F7

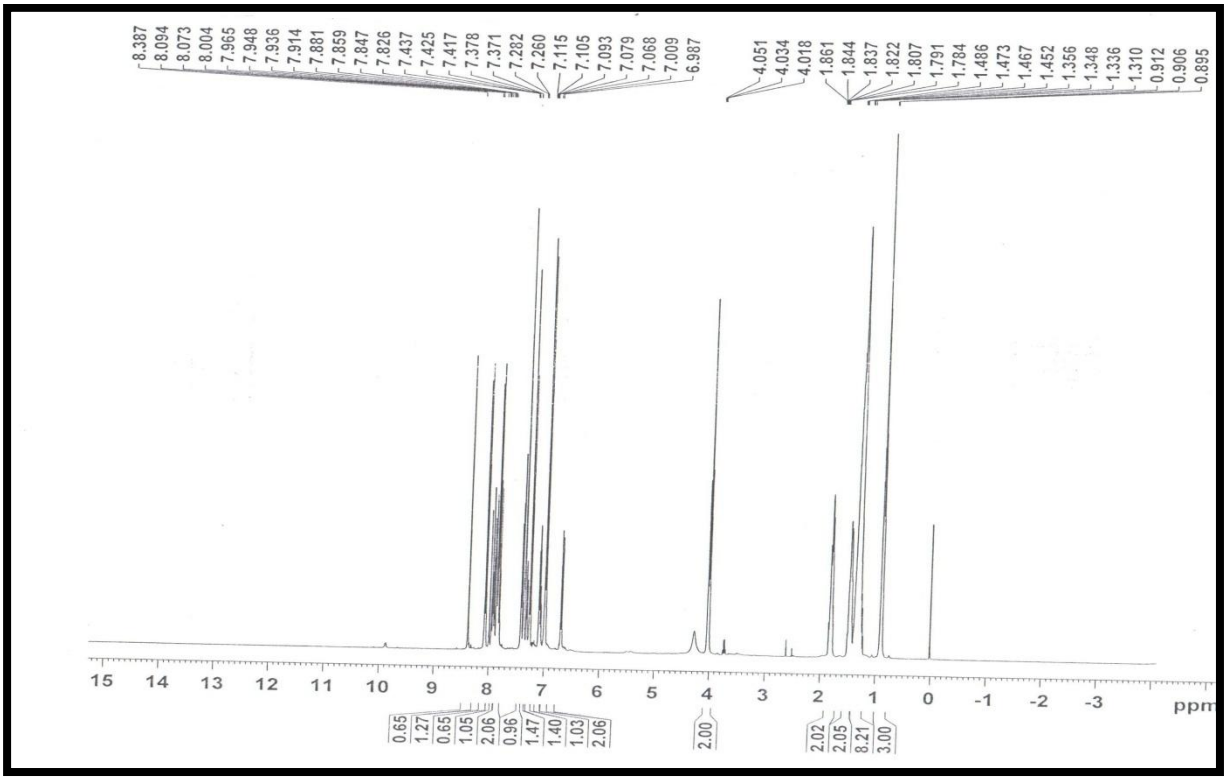

^{1}H NMR of F8

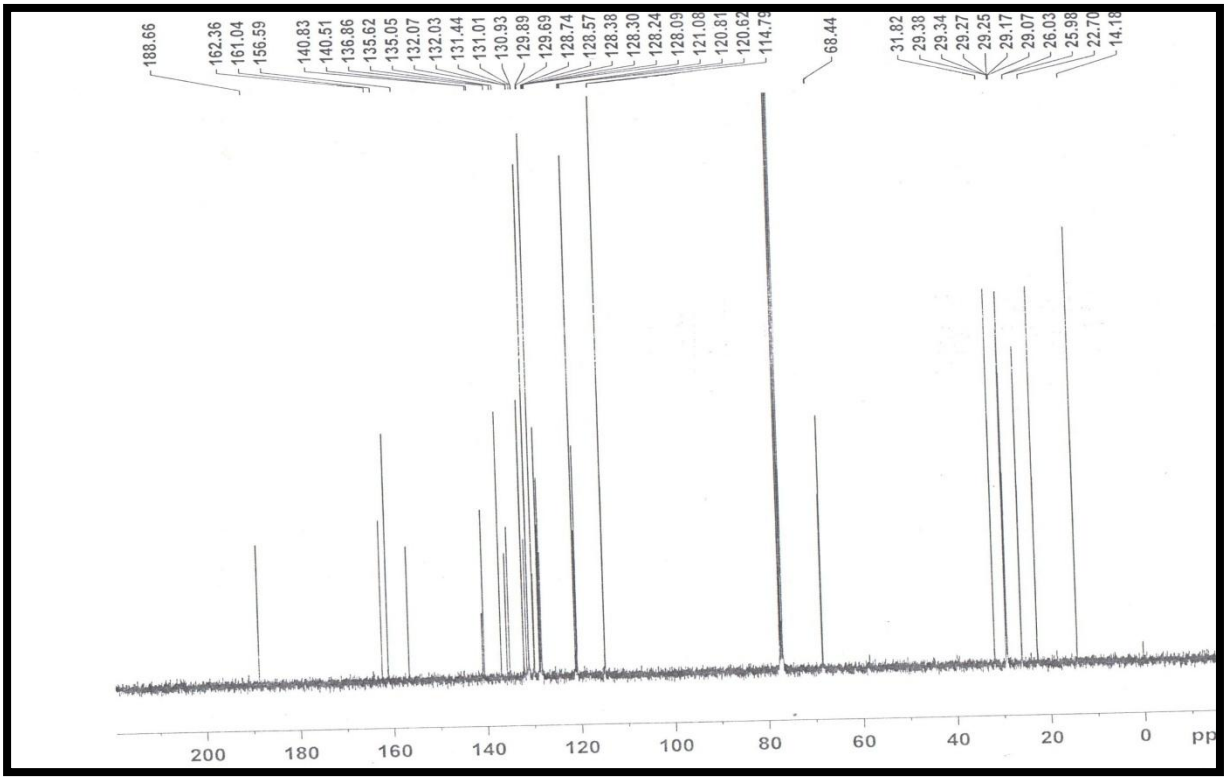

^{13}C NMR of F8

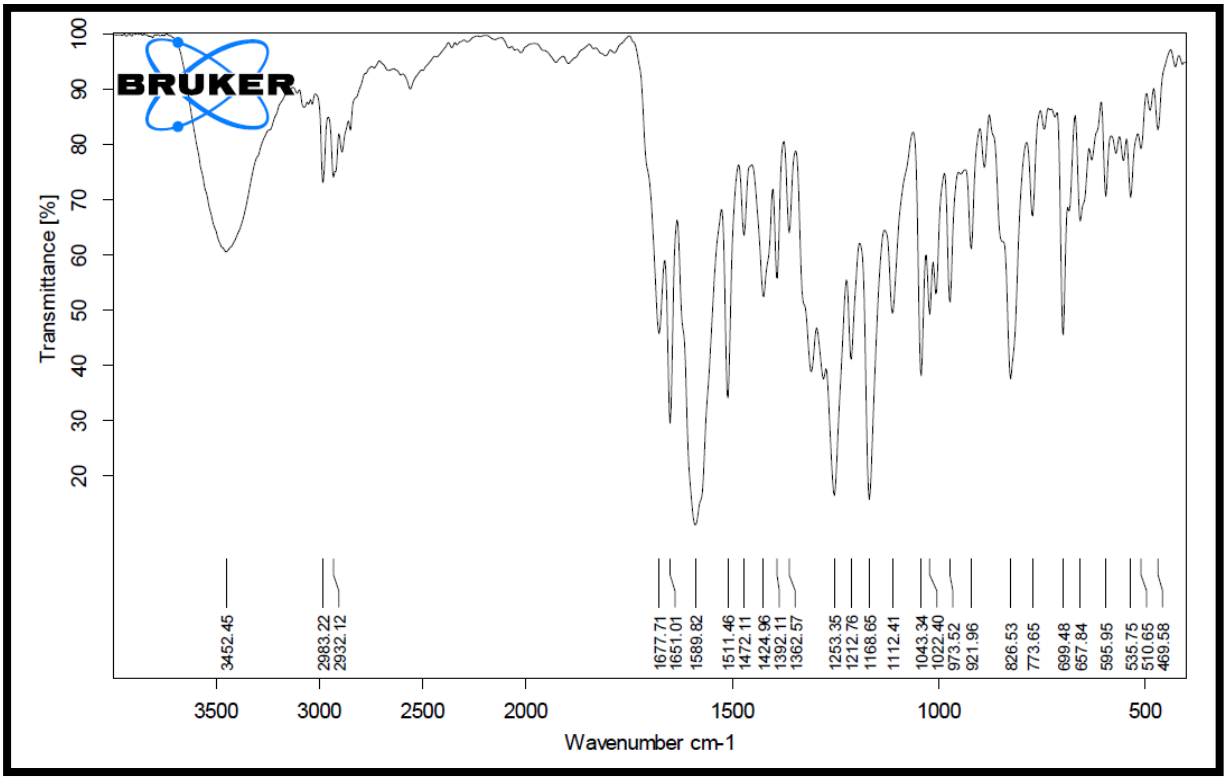

IR of F8

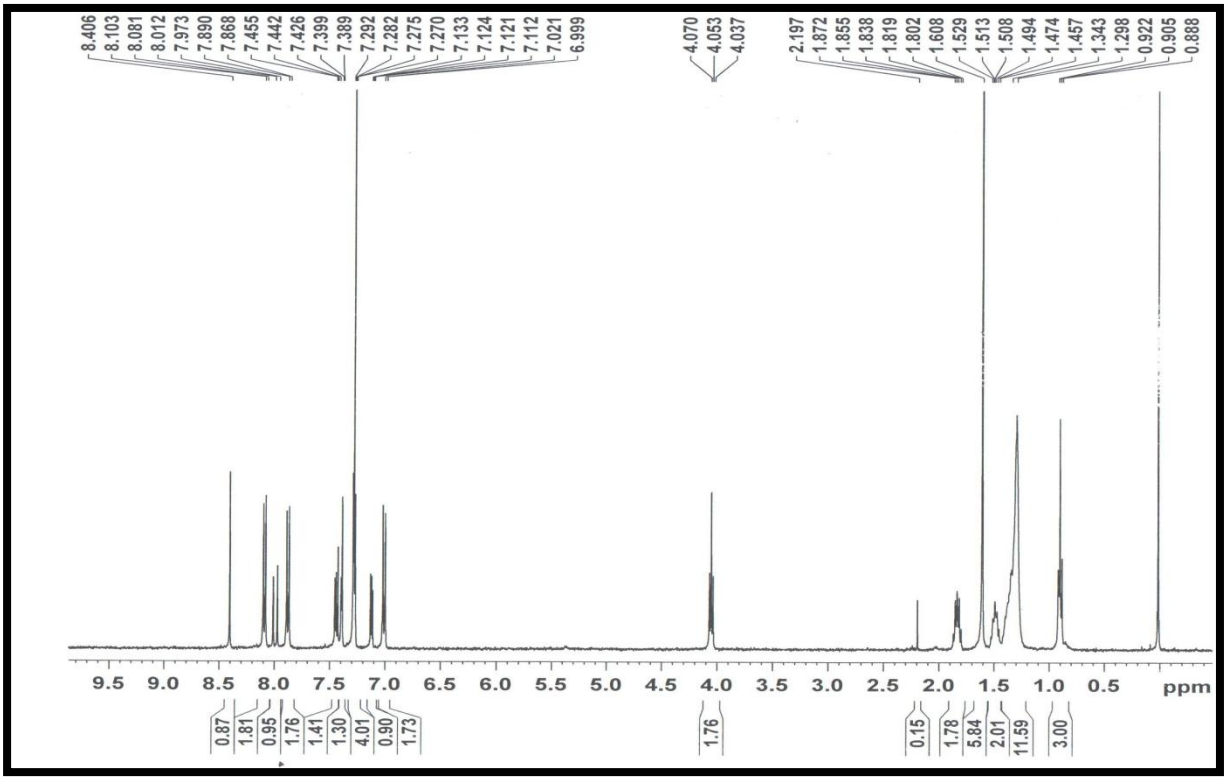

^{1}H NMR of F10

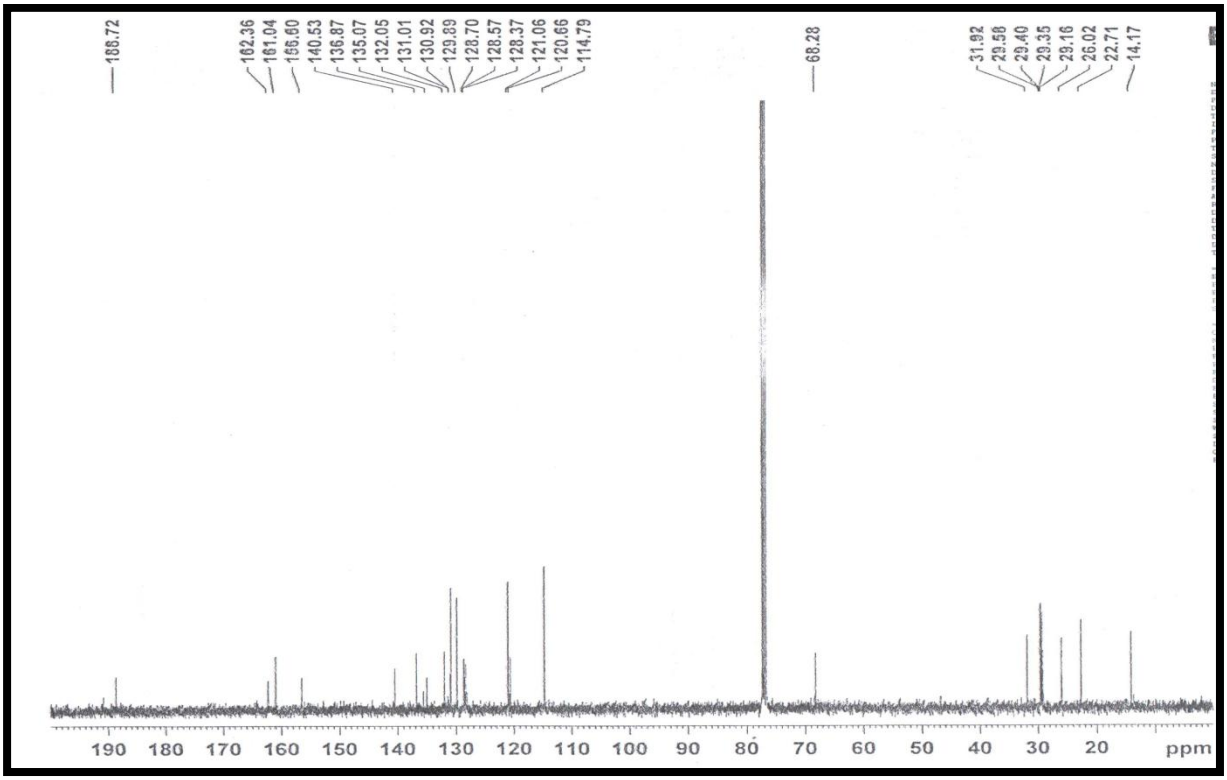

^{13}C NMR of F10

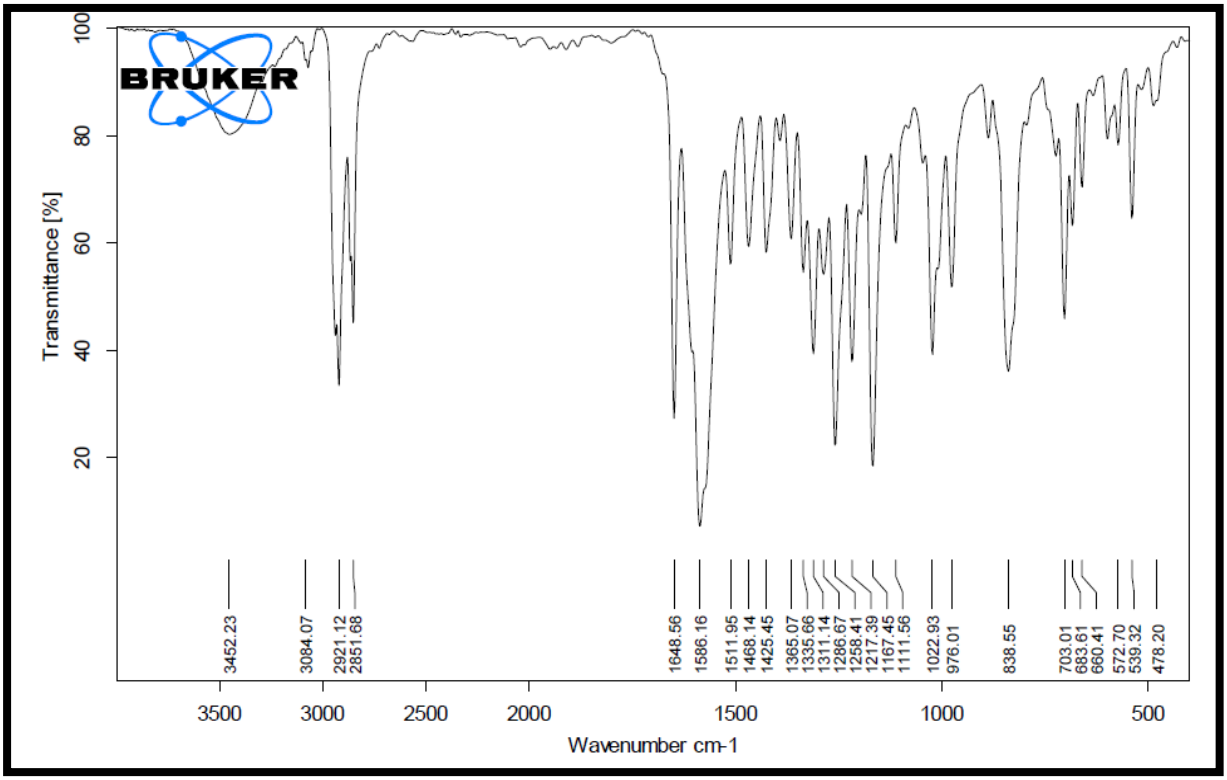

IR of F10

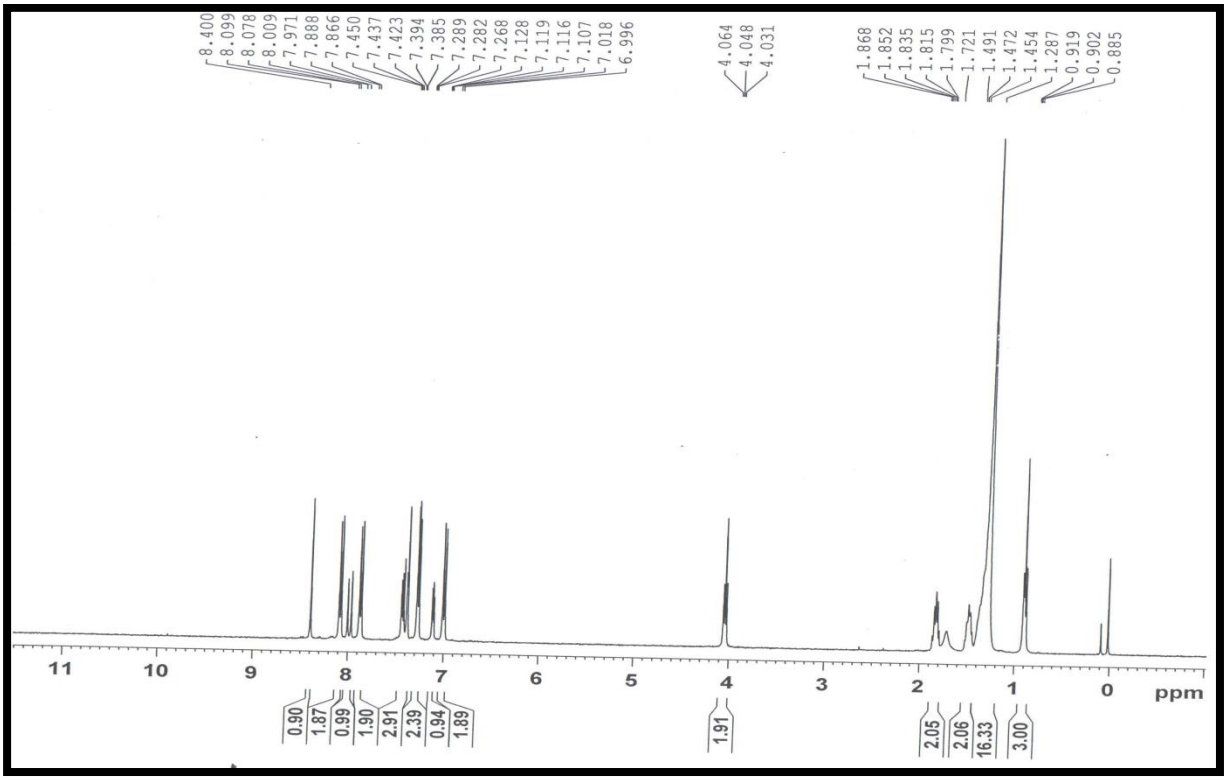

^{1}H NMR of F12

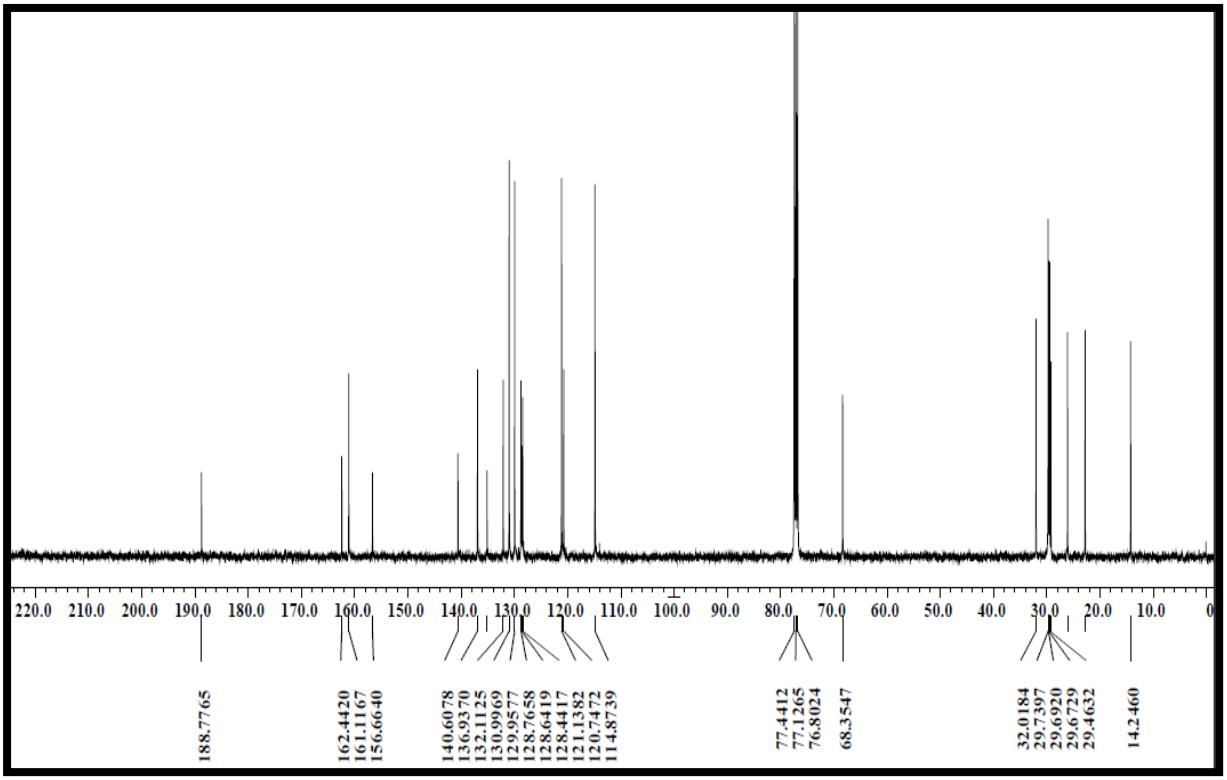

^{13}C NMR of F12

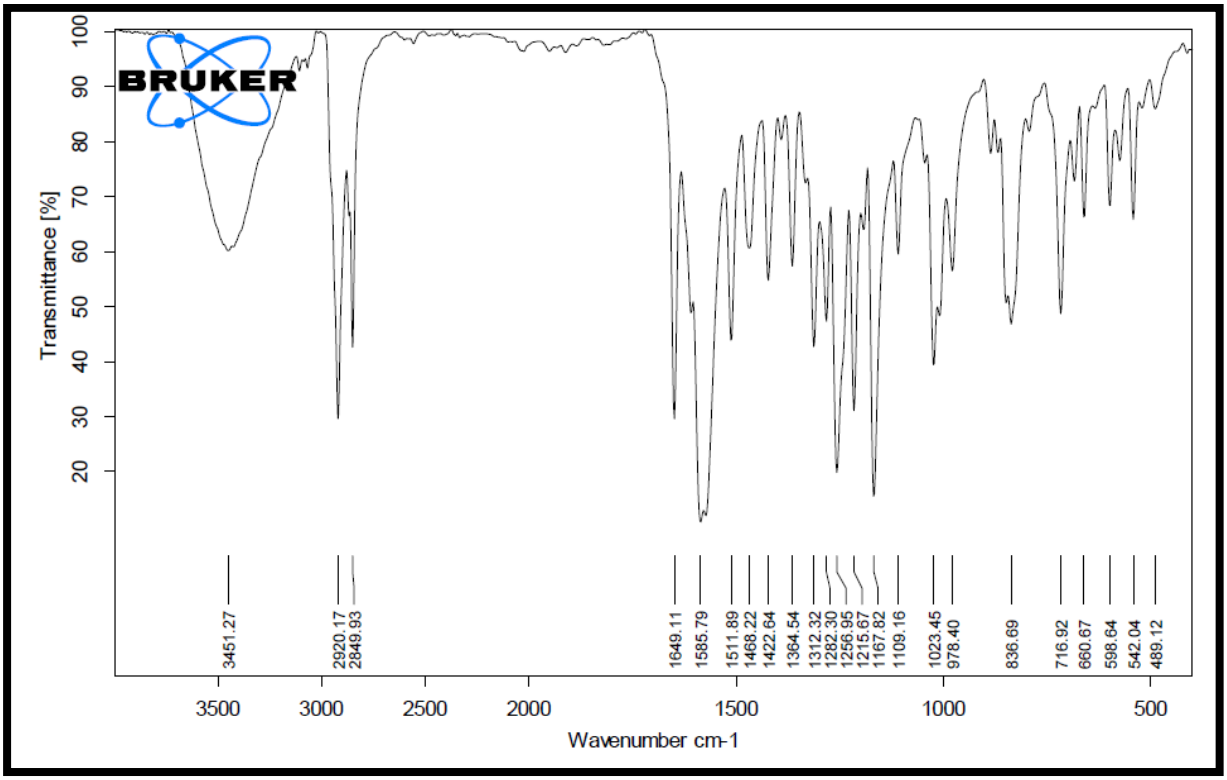

IR of F12

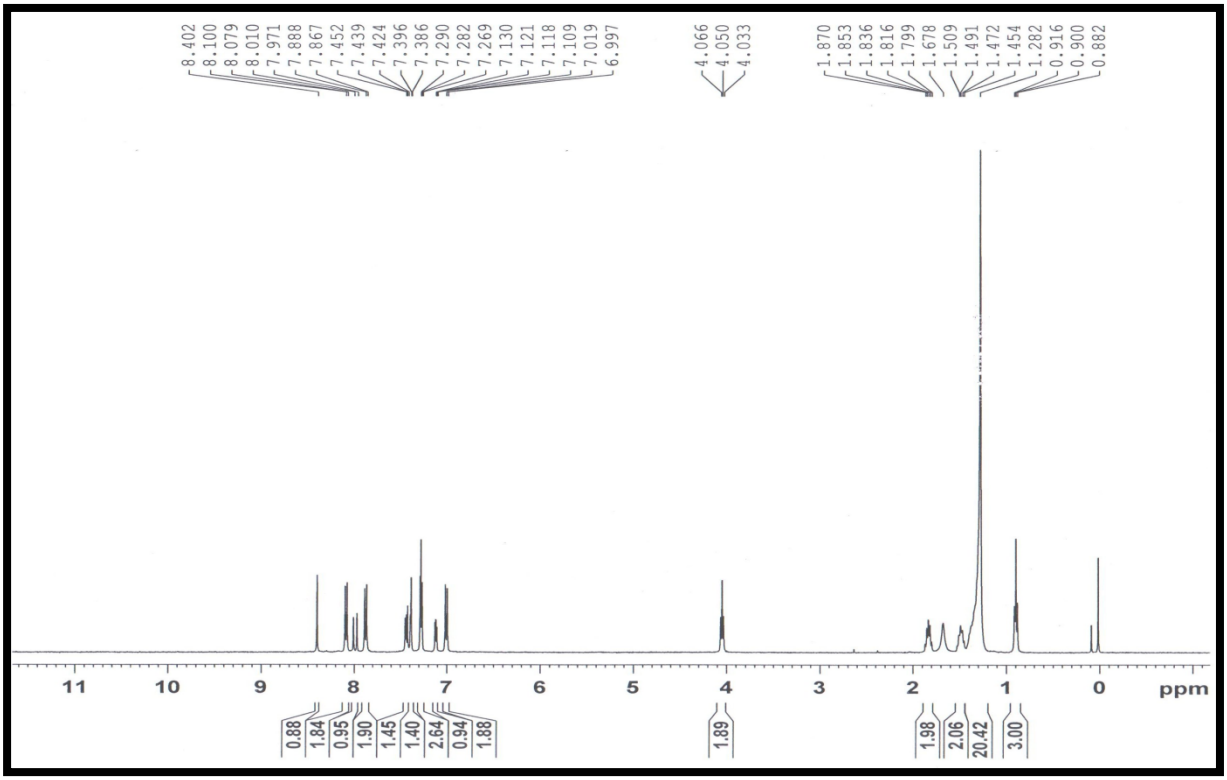

^{1}H NMR of F14

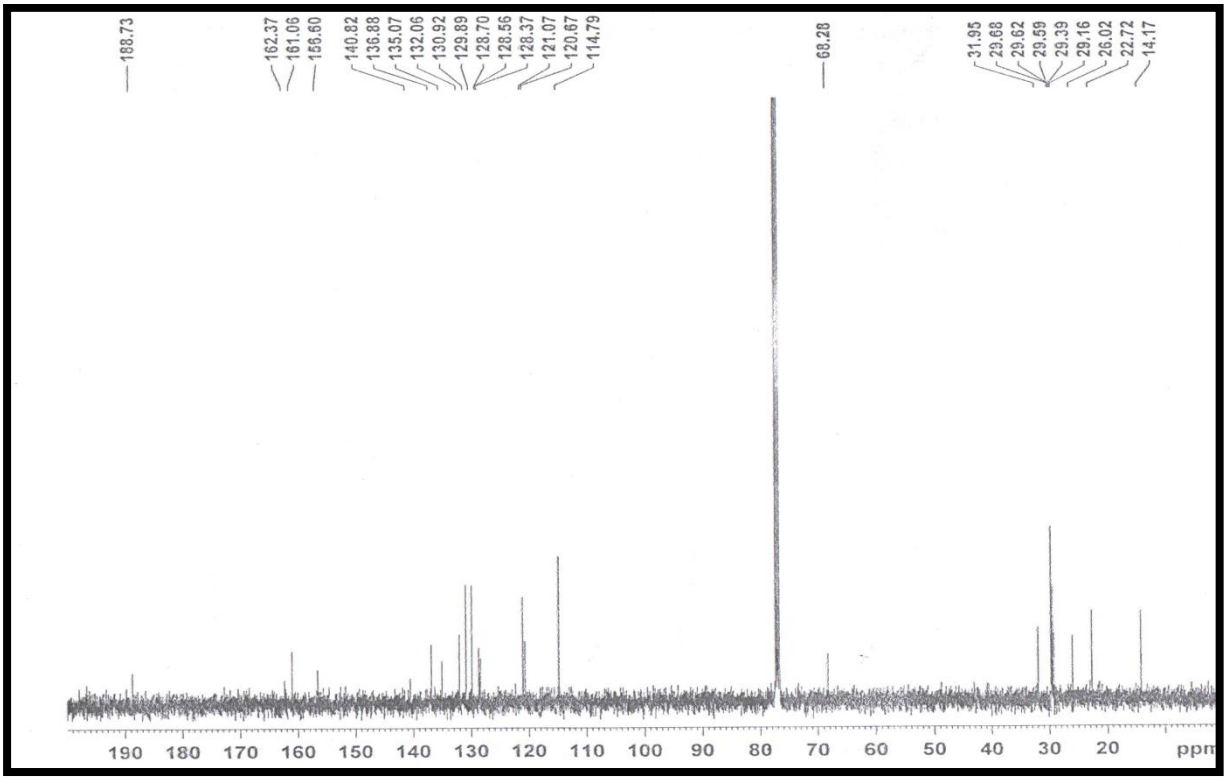

^{13}C NMR of F14

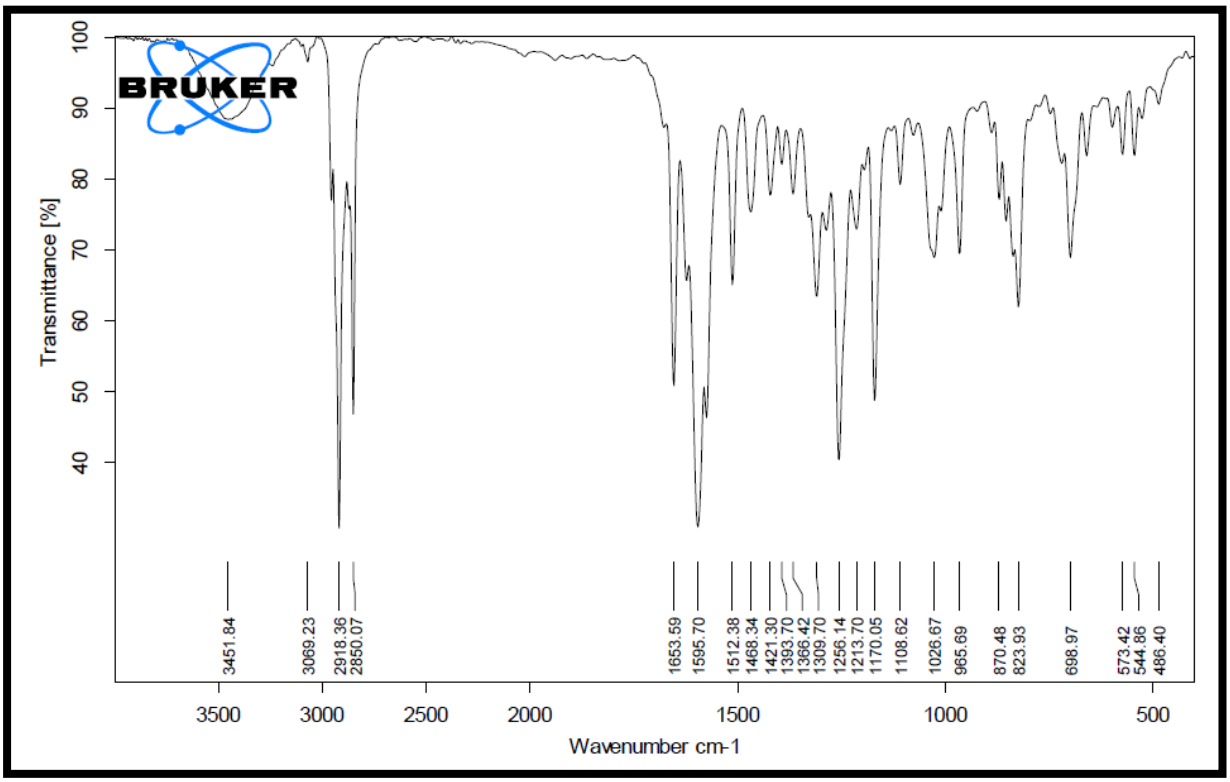

IR of F14

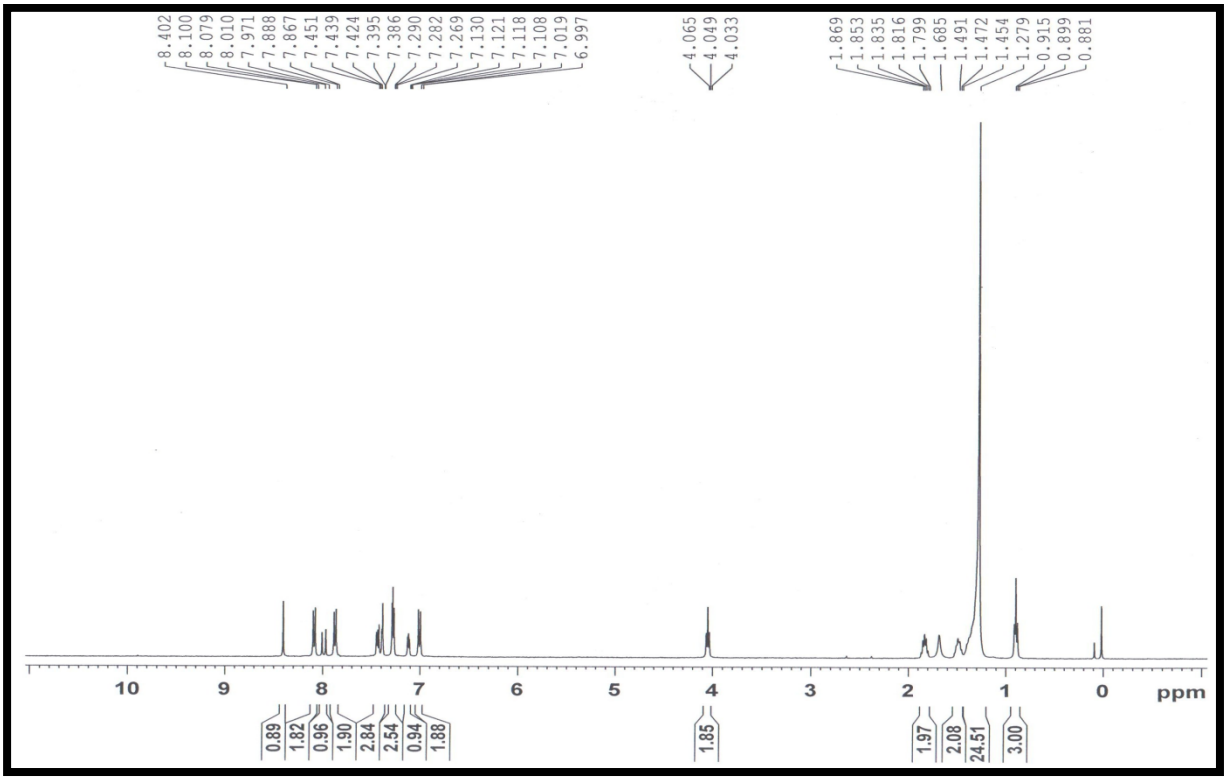

^{1}H NMR of F16

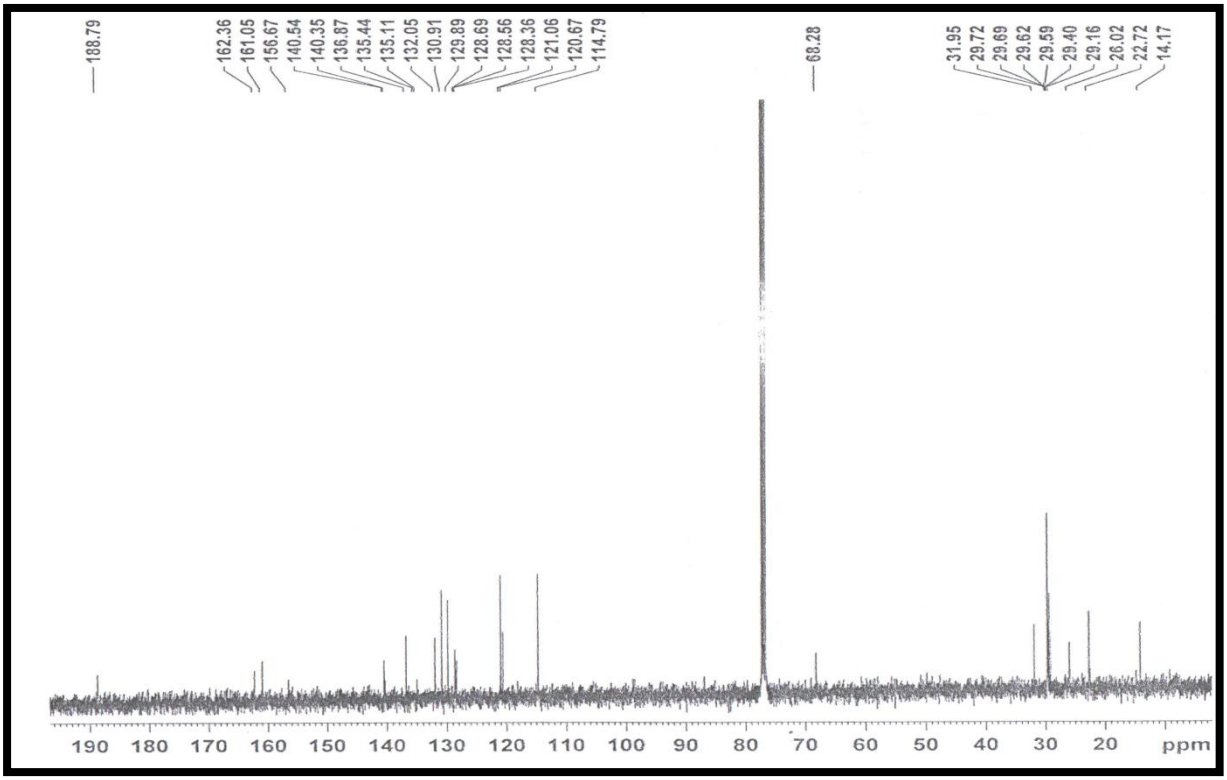

^{13}C NMR of F16

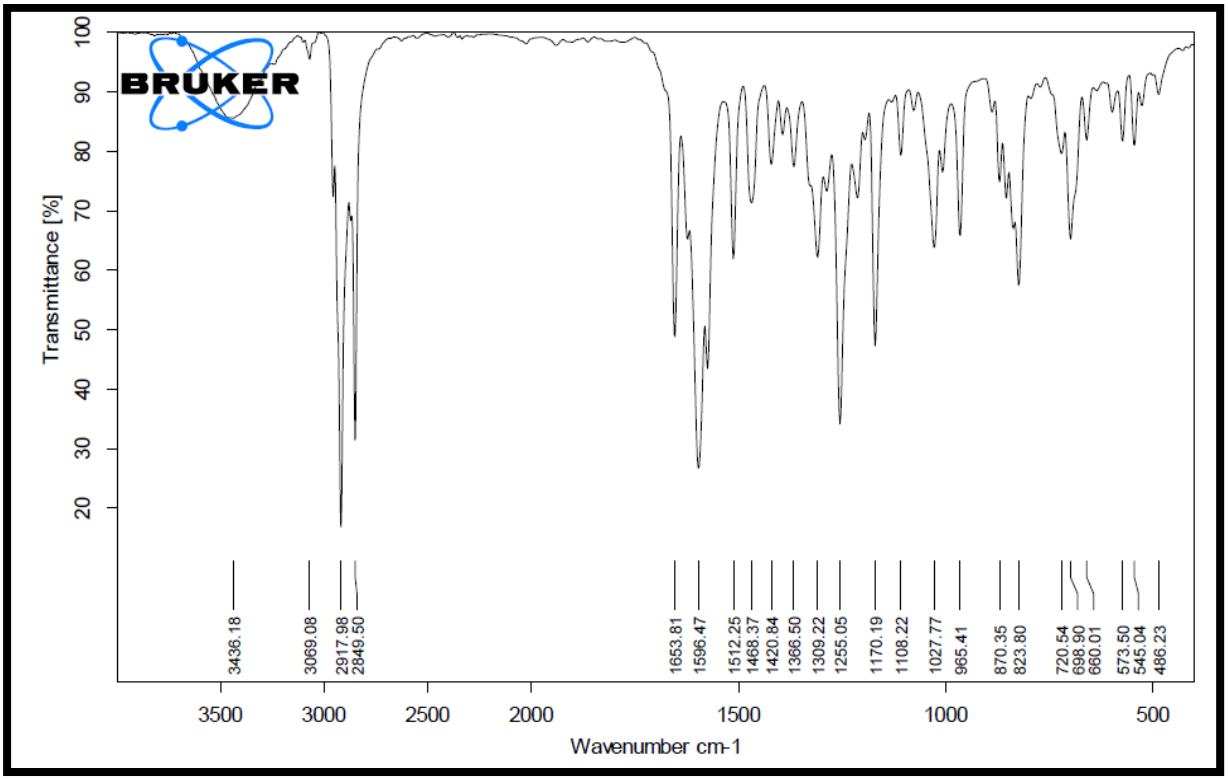

IR of F16

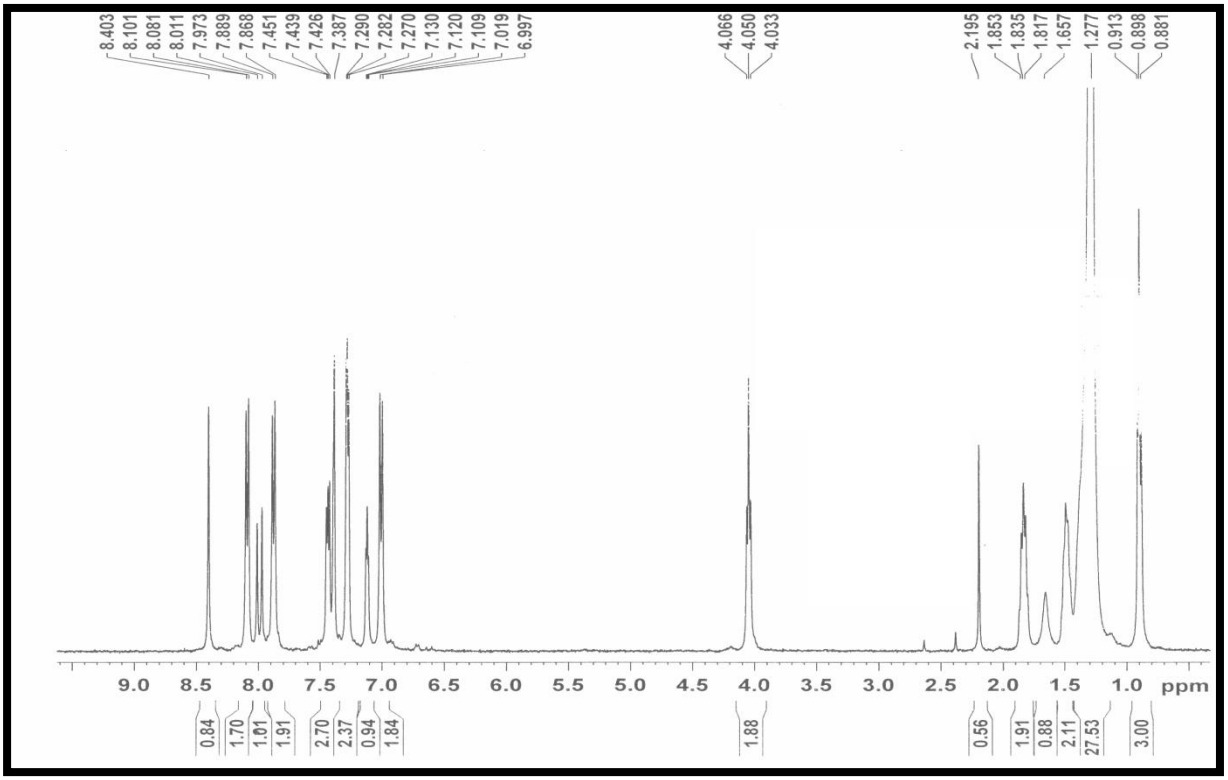

^{1}H NMR of F18

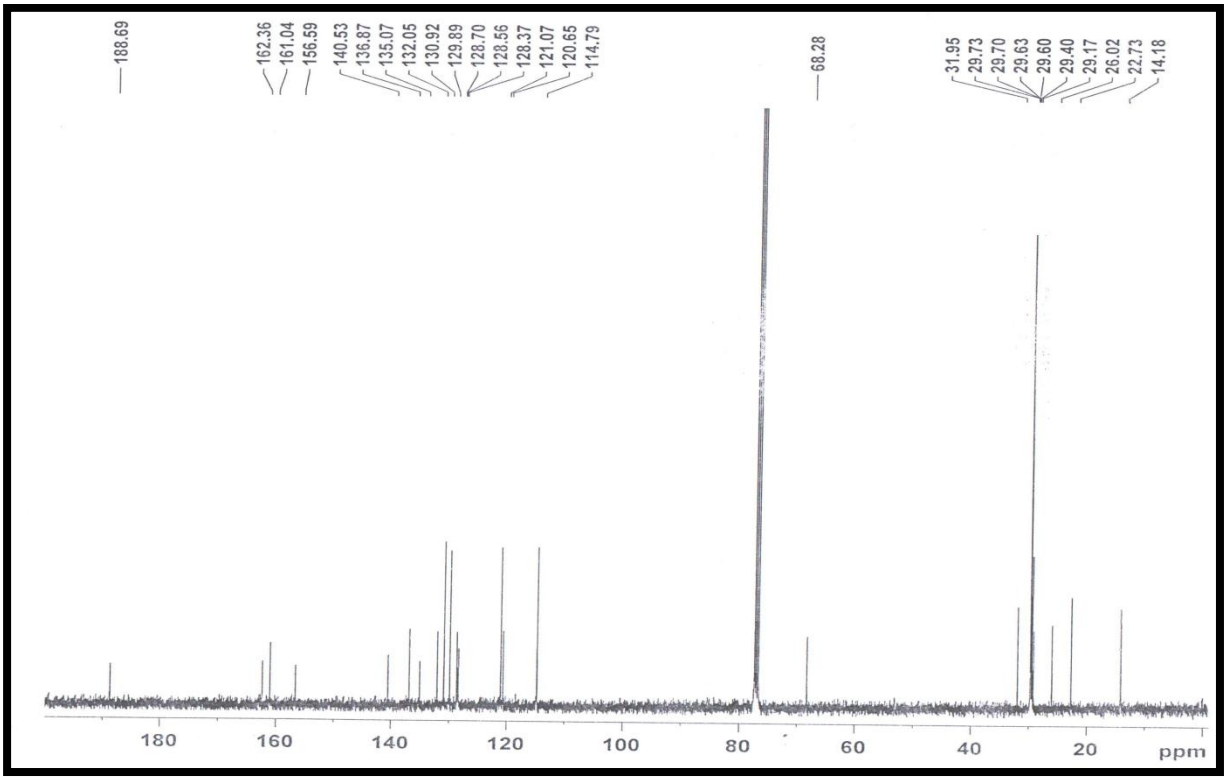

^{13}C NMR of F18

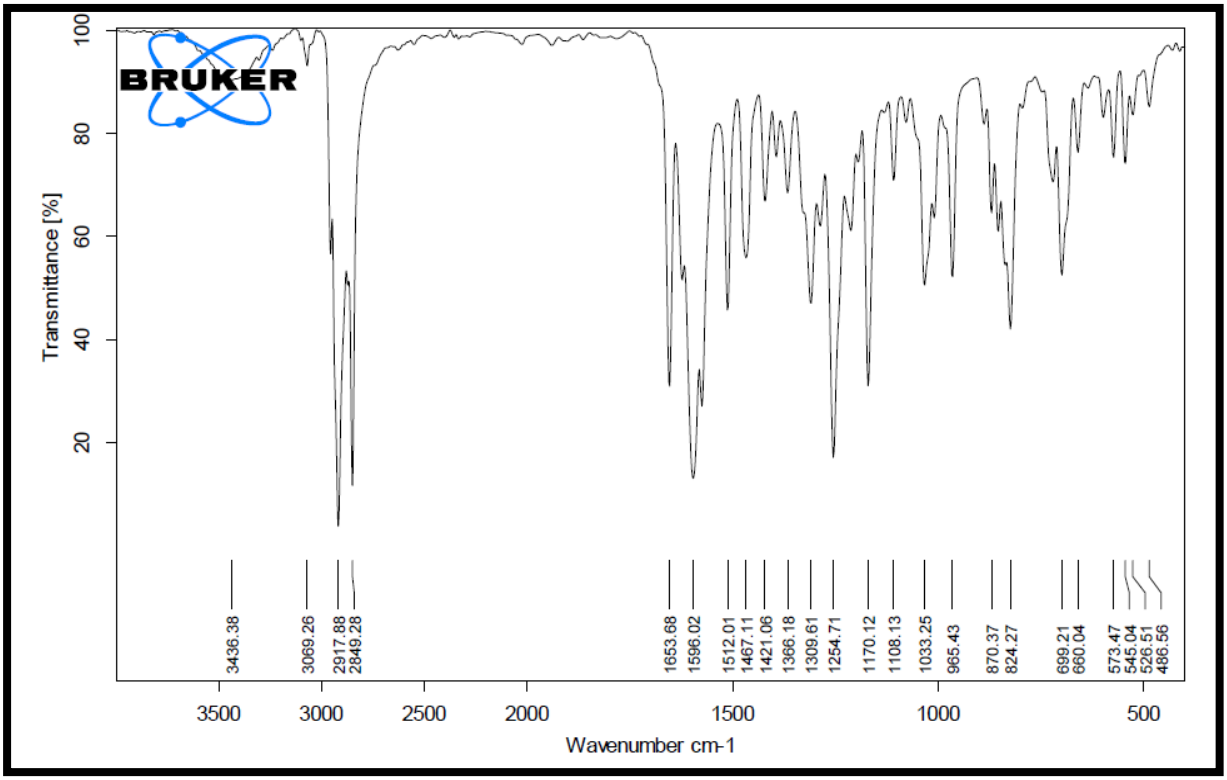

IR of F18